



ALMA MATER STUDIORUM  
UNIVERSITÀ DI BOLOGNA

## DOTTORATO DI RICERCA IN

SCIENZE BIOTECNOLOGICHE, BIOCOMPUTAZIONALI, FARMACEUTICHE E  
FARMACOLOGICHE

Ciclo 37

**Settore Concorsuale:** 06/A2 - PATOLOGIA GENERALE E PATOLOGIA CLINICA

**Settore Scientifico Disciplinare:** MED/04 - PATOLOGIA GENERALE

## TITOLO TESI

CRISPR/CAS9 METHODOLOGIES AS A TOOL FOR INVESTIGATING FANCONI ANEMIA PATHWAY IN  
CANCER: PERSPECTIVE ON PANCREATIC CANCER TREATMENT

**Presentata da:** Irene Casamassima

**Coordinatore Dottorato**

Maria Laura Bolognesi

**Supervisore**

Andrea Cavalli

**Co-Supervisore**

Fulvia Farabegoli

Esame finale anno 2025



ALMA MATER STUDIORUM  
UNIVERSITÀ DI BOLOGNA

## Ph.D. PROGRAMME IN

BIOTECHNOLOGICAL, BIOCOMPUTATIONAL, PHARMACEUTICAL AND  
PHARMACOLOGICAL SCIENCES

Cycle 37<sup>th</sup>

**Academic recruitment field:** 06/A2 – GENERAL PATHOLOGY AND CLINICAL PATHOLOGY

**Academic discipline:** MED04 – GENERAL PATHOLOGY

## THESIS TITLE

CRISPR/CAS9 METHODOLOGIES AS A TOOL FOR INVESTIGATING FANCONI ANEMIA PATHWAY IN  
CANCER: PERSPECTIVE ON PANCREATIC CANCER TREATMENT

**Ph.D. Student:** Irene Casamassima

**Coordinator of the PhD programme**

Maria Laura Bolognesi

**Supervisor**

Andrea Cavalli

**Co-Supervisor**

Fulvia Farabegoli

Final exam, 2025

# Abstract

The concept of precision medicine is advancing the discovery of new therapeutic targets for cancer treatment, offering tailored approaches based on the genetic profile of individual patients. One such approach is the paradigm of Synthetic Lethality, where cancer cells with specific genetic mutations are targeted by therapies that spare normal, healthy cells. This concept has been successfully applied in the treatment of various cancers, including ovarian, breast, and pancreatic cancers. The first synthetic lethality-based treatment to gain approval was for patients with BRCA1/2 mutations, using PARP inhibitors. These drugs disrupt the DNA repair machinery of cancer cells by inhibiting single-strand break repair, while the BRCA1/2 mutations prevent double-strand break repair. However, a major limitation of this approach is the development of resistance to PARP inhibitors, and the fact that not all cancer patients carry BRCA1/2 mutations. Therefore, there is a need to identify new synthetic lethal partners to expand the therapeutic potential of PARP inhibitors.

The Fanconi Anemia pathway is involved in DNA repair and has a well-established connection with BRCA2-mediated repair processes. This PhD thesis aims to explore and validate advanced genomic methodologies to investigate the genes involved in the FA pathway, with a particular emphasis on their relationship with PARP inhibitor treatment. The ultimate goal is to identify therapeutic targets that could improve patient stratification for personalized cancer therapies, with a specific focus on pancreatic cancer cells.

This study primarily focuses on utilizing genomic tools, specifically CRISPR-Select and CRISPR interference (CRISPRi), to investigate the Fanconi Anemia pathway and its relationship with sensitivity to the PARP inhibitor Talazoparib. The key genes explored include FANCA, FANCC, FANCD2, and FANCM. In Chapter 1, CRISPR-Select demonstrated its precision and reliability in assessing the impact of gene mutations on cell survival and drug response. It revealed that FANCA, FANCD2 and FANCM deficiencies increased Talazoparib sensitivity in a diploid normal cell model.

Given the genetic heterogeneity of pancreatic cancer patients, including mutations in Fanconi Anemia genes, Chapter 2 focused on the commercially available FANCC-deficient PANC 03.27 cell line. This model further established the association between Fanconi Anemia pathway deficiencies and heightened Talazoparib sensitivity in a pancreatic cancer context.

To expand the investigation of Fanconi Anemia genes in pancreatic cancer, Chapter 3 focused on the usage of CRISPRi to develop a platform for gene silencing. FANCD2 and FANCC were targeted to compare results from CRISPRi with those obtained using CRISPR-Select for FANCD2, and in the non-edited pancreatic cancer cell line for FANCC. HeLa cells were chosen as a control model where CRISPRi had been developed and optimized. The pancreatic cancer cell line Capan-1 (BRCA2-defective) has been chosen as a cancer cell model representing patients who already receive PARPi treatment to verify how FANCC or FANCD2 deficiency further affects drug response. The BxPC3 (BRCA2-proficient) cell line has been used to test whether FANCC and FANCD2 silencing causes Talazoparib sensitivity. However, FANCC silencing proved difficult in both Capan-1 and HeLa cells, leading to the suspension of experiments in BxPC3 until further optimization of FANCC silencing could be achieved.

On the other hand, FANCD2 silencing was successful in HeLa cells, but unexpectedly, it did not increase Talazoparib sensitivity, contrary to the results obtained with CRISPR-Select in Chapter 1. This discrepancy highlights the need for further investigations into the CRISPRi method, including its suitability as a screening tool for Fanconi Anemia gene deficiencies and the selection of HeLa cells as a model system. Additional studies will be required to refine the methodology and better assess the role of Fanconi Anemia genes in pancreatic cancer.

Overall, the CRISPR-Select technique proved to be a precise and reliable platform to investigate a gene mutation impact on cell survival and drug response, proving that FANCA, FANCD2 and FANCM are increasing the Talazoparib sensitivity treatment in a diploid normal cell context. FANCC deficiency was found to increase the sensitivity to Talazoparib treatment in the pancreatic cell line PANC 03.27. Further studies need to be done to find suitable cell models to translate this study into a pancreatic cancer cell line using the CRISPRi method.

# Contents

<b>Abstract</b>	I
<b>List of Figures</b>	VI
<b>List of Abbreviations</b>	VIII
<b>Introduction</b>	1
0.1 Fanconi Anemia Pathway . . . . .	1
0.1.1 Interstrand Cross Link recognition by FANCM . . . . .	2
0.1.2 Core complex formation and FANCD2-FANCI ubiquitination . . . . .	3
0.1.3 Unhooking, TLS and HR steps . . . . .	4
0.2 Synthetic Lethality concept . . . . .	7
0.2.1 PARPi treatment . . . . .	8
0.2.2 Synthetic Lethality and FA pathway . . . . .	10
0.2.3 FA pathway and Pancreatic Cancer . . . . .	11
0.2.4 FA genes correlation with PARPi . . . . .	13
0.2.5 DNA damaging drugs . . . . .	15
0.3 Aim of the thesis . . . . .	17
<b>1 Detection of Synthetic Letality between FANCA, FANCD2, FANCM and the PARPi Talazoparib in MCF10A cells by CRISPR-Select</b>	19
1.1 CRISPR-Select . . . . .	20
1.1.1 Overview of the CRISPR-Select technique . . . . .	20
1.1.2 CRISPR-Select cassette design . . . . .	22
1.1.3 CRISPR-Select cassette delivery . . . . .	26
1.1.4 Time-point collection and processing . . . . .	27
1.1.5 NGS data collection and analysis . . . . .	28
1.2 FANCA, FANCD2 and FANCM genes background . . . . .	31
1.2.1 FANCA . . . . .	31
1.2.2 FANCD2 . . . . .	32
1.2.3 FANCM . . . . .	33
1.3 Results . . . . .	34

1.3.1	BRCA2 is a control gene for the CRISPR-Select <sup>TIME</sup> assay .	34
1.3.2	FANCA, FANCD2 and FANCM are synthetic lethal partners of the PARPi Talazoparib . . . . .	36
1.4	Conclusions of Chapter 1 . . . . .	39
<b>2</b>	<b>Evaluation of the SL correlation between FANCC and Talazoparib in Pancreatic Cancer cell lines</b>	<b>40</b>
2.1	Introduction . . . . .	40
2.1.1	FANCC protein Background . . . . .	41
2.2	Results . . . . .	43
2.2.1	FANCC deficiency sensitizes cells to the PARPi Talazoparib in a PDAC cell model . . . . .	43
2.2.2	FANCC-Mediated Talazoparib Sensitivity is associated with DNA Damage cell accumulation . . . . .	45
2.3	Conclusions of Chapter 2 . . . . .	47
<b>3</b>	<b>Development of a cancer cell model to investigate the relationship between FA gene deficiency and Talazoparib effects</b>	<b>48</b>
3.1	Introduction . . . . .	48
3.2	CRISPR-interference . . . . .	50
3.2.1	Overview of the CRISPR-interference . . . . .	50
3.2.2	sgRNA design . . . . .	51
3.3	Results . . . . .	53
3.3.1	KRAB cell line generation . . . . .	53
3.3.2	Stable sgRNA-expressing cells . . . . .	56
3.3.3	FANCD2 silencing is not enhancing Talazoparib sensitivity in HeLa/ KRAB cells . . . . .	60
3.3.4	3.3.3 FANCD2 gene silencing did not increase $\gamma$ H2AX levels in HeLa/KRAB cells . . . . .	62
3.4	Conclusions of Chapter 3 . . . . .	64
	<b>Discussions, conclusions and Future perspective</b>	<b>65</b>
<b>4</b>	<b>Material and Methods</b>	<b>70</b>
	<b>Material and Methods</b>	<b>70</b>
4.1	Cell Culture . . . . .	70
4.1.1	iCas9-MCF10A . . . . .	70
4.1.2	PANC-1 . . . . .	70
4.1.3	PANC-03.27 . . . . .	70
4.1.4	HEK-293T . . . . .	71
4.1.5	HeLa-KRAB . . . . .	71
4.1.6	Capan-1 . . . . .	71

4.2	CRISPR-Select Assay . . . . .	71
4.2.1	gRNA, donors and primers design . . . . .	71
4.2.2	Cell transfection . . . . .	73
4.2.3	DNA extraction . . . . .	74
4.2.4	1 <sup>st</sup> and 2 <sup>nd</sup> PCR . . . . .	74
4.2.5	NGS . . . . .	75
4.3	Cell Viability Assay . . . . .	76
4.4	Western Blot . . . . .	76
4.5	Stable dCas9-KRAB cell line production . . . . .	77
4.5.1	PB-TRE-dCas9-KRAB plasmid generation . . . . .	77
4.5.2	PiggyBac Transposition . . . . .	77
4.5.3	LentiGuide cloning . . . . .	77
4.5.4	sgRNAs design . . . . .	78
4.5.5	Lentiviral production and sgRNA delivery . . . . .	79
4.6	Evaluation of gene expression levels . . . . .	80
4.6.1	Total RNA extraction . . . . .	80
4.6.2	mRNA retrotranscription . . . . .	80
4.6.3	RT-qPCR . . . . .	80
	<b>Bibliography</b>	<b>82</b>
	<b>Acknowledgements</b>	<b>103</b>

# List of Figures

1	FANCM recruitment at ICL site. . . . .	2
2	Core complex formation and D2-I complex ubiquitination. . . . .	4
3	Unhooking, TLS and HR steps for ICL repair. . . . .	5
4	FA pathway overview. . . . .	6
5	Sythetic Lethality. . . . .	8
6	PARP inhibitors pharmacological profile. . . . .	9
7	Timeline of PARPi approved by FDA. . . . .	10
8	Exocrine Pancreatic Cancers Pie Chart. . . . .	12
9	Main features of CRISPR/Cas9, CRISPRi and CRISPR-Select. . . . .	14
1.1	CRISPR/Cas9 Cassette. . . . .	20
1.2	Most frequent CRISPR-Select <sup>TIME</sup> editing outcomes . . . . .	21
1.3	Benchling website. . . . .	22
1.4	Gene sequence in Benchling. . . . .	23
1.5	CRISPOR website. . . . .	24
1.6	gRNA selection in CRISPOR. . . . .	25
1.7	Codon usage table. . . . .	26
1.8	CRISPR-Select <sup>TIME</sup> experiment . . . . .	27
1.9	Alignment statistics to the amplicons . . . . .	28
1.10	Allele assignment . . . . .	29
1.11	Global frameshift analysis . . . . .	29
1.12	Allele plot . . . . .	30
1.13	FANCA gene, domains and sites . . . . .	31
1.14	FANCD2 gene domains . . . . .	32
1.15	FANCM gene domains . . . . .	33
1.16	BRCA2 control mutations. . . . .	35
1.17	. . . . .	37
1.17	CRISPR-Select <sup>TIME</sup> and Fanconi Anemia genes . . . . .	38
2.1	FANCC exons in PANC 03.27 cells. . . . .	41
2.2	UCSC data for FANCC isoforms expression. . . . .	42
2.3	Dose response curve for MMC and Talazoparib in PANC-1 and PANC 03.27 cells. . . . .	43

2.4	Cell Viability Assay for FANCC. . . . .	44
2.5	Western Blot for $\gamma$ H2AX expression levels. . . . .	46
3.1	CRISPRi components. . . . .	50
3.2	CRISPick website, general settings. . . . .	51
3.3	CRISPick website, sgRNA selection. . . . .	52
3.4	dCas9/KRAB cell line generation. . . . .	53
3.5	dCas9/KRRAB expression . . . . .	55
3.6	Stable sgRNA-expressing cells generation . . . . .	56
3.7	FANCD2 expression in HeLa/KRAB cells . . . . .	58
3.8	FANCC expression in HeLa/KRAB cells . . . . .	59
3.9	Dose-response curve of MMC and Talazoparib in HeLa cells. . . . .	61
3.10	Cell viability assay for FANCD2 silencing. . . . .	62
3.11	Western Blot for $\gamma$ H2AX expression levels on HeLa/KRAB cells. . . . .	63

# List of Abbreviations

- ATR: ataxia-telangiectasia and Rad3-related protein
- ATRIP: ATR-interacting protein
- BRCA1/2: breast cancer susceptibility proteins 1 and 2
- CK2: casein kinase 2
- CIS: Cisplatin
- CRISPR: Clustered Regularly Interspaced Short Palindromic Repeats
- CRISPRi: CRISPR-interference
- dCas9: dead Cas9
- DSB: Double Strand Break
- FA: Fanconi Anemia
- FDA: food and drugs administration
- gBRCAm: germline BRCA-mutated
- HR: Homologous Recombination
- ICL: Interstrand Cross Link
- ITR: Inverted Terminal Repeat
- KRAB: KRÜppel-Associated Box
- LOH: Loss of Heterozygosity
- LOF: Loss of Function
- MMC: Mitomycin C
- NER: Nuclear Excision Repair

- NGS: Next Generation Sequencing
- NT: Non Targeting
- OS: Overall Survival
- PAM: Protospacer Adjacent Motif
- PARP: poly-ADP ribose polymerase
- PARPi: Poly ADP-Ribose Polymerase inhibitor
- PB: PiggyBac
- PC: Pancreatic Cancer
- PDAC: Pancreatic Ductal Adeno Carcinoma
- PNET: pancreatic neuroendocrine tumor
- RNAi: RNA interference
- shRNA: short hairpin RNA
- siRNA: small interfering RNA
- SL: Synthetic Lethality
- SSB: Single Strand Break
- ssODN: Single-stranded oligodeoxy nucleotide
- TALA: Talazoparib
- TLS: Translesion Synthesis
- TNBC: Triple Negative Breast Cancer
- TRC: Transcription-Replication Conflicts

# Introduction

## 0.1 Fanconi Anemia Pathway

Cells are constantly exposed to DNA damage from both internal (alkylation, mismatch of DNA bases, hydrolysis) [1] [2] and external sources (UV radiations, chemical agents) [2][3]. To protect their genomic integrity, cells have developed specific DNA repair mechanisms to detect and fix specific types of damage [4]. This step is crucial, as errors can lead to genomic instability, which contributes to cancer development and progression [5]. With respect to normal cells, cancer cells often adapt by altering their DNA repair processes, allowing them to survive, resist chemotherapy and continue growing [6][7]. This cancer cell plasticity presents opportunities for targeted therapies. It is possible to identify a tumor-specific target that, in combination with at least one oncogenic or non-oncogenic mutation, induces selective tumor cell death, a phenomenon known as synthetic lethality (SL) [8][9]. Recent advancements in understanding complex DNA repair pathways, such as the Fanconi Anemia (FA) pathway, have paved the way for SL approaches [10][11][12]. These strategies aim to target and disrupt the altered DNA repair mechanisms in cancer cells, making them more susceptible to treatment, particularly in cases where they are resistant to standard therapies [9][13].

To better understand the relationship between the FA pathway, DNA repair mechanisms, SL, and the potential for targeting this pathway in cancer therapy, it is essential to first examine the FA pathway in detail. The FA pathway is a DNA repair mechanism [14][15]. Up to date, 27 proteins have been found to act in this pathway at different steps of the DNA repair [16], including the FA-associated proteins (FAAPs). This pathway is responsible for maintaining genomic stability by repairing interstrand crosslinks (ICLs), which are highly toxic DNA lesions. ICLs covalently link the two strands of the DNA double helix, preventing strand separation, thereby blocking essential processes such as replication and transcription [17]. The FA pathway orchestrates a complex, multi-step repair process that involves the recognition of ICLs, recruitment of repair proteins, DNA incision, translesion synthesis, and homologous recombination (HR) to restore DNA integrity.

### 0.1.1 Interstrand Cross Link recognition by FANCM

FA was first described in 1927 by the paediatrician Guido Fanconi as an autosomal recessive disease [18][19]. Over the years, different proteins have been associated with FA disease and have been grouped together as part of the FA pathway, whose impairment leads to impaired DNA repair and cross-linker hypersensitivity. ICLs are highly genotoxic lesions that involve covalent bonds between both strands of the DNA helix [20][21]. When the replication machinery encounters an ICL, the FA pathway is activated to coordinate DNA repair in the S-phase of the cell cycle [20][22]. The first step of the pathway begins with the recognition and binding of DNA damage by the ATP-dependent DNA translocase FANCM, a protein with distinct roles in cell-cycle checkpoint activation, chromatin remodelling, and ICL repair [17][23].

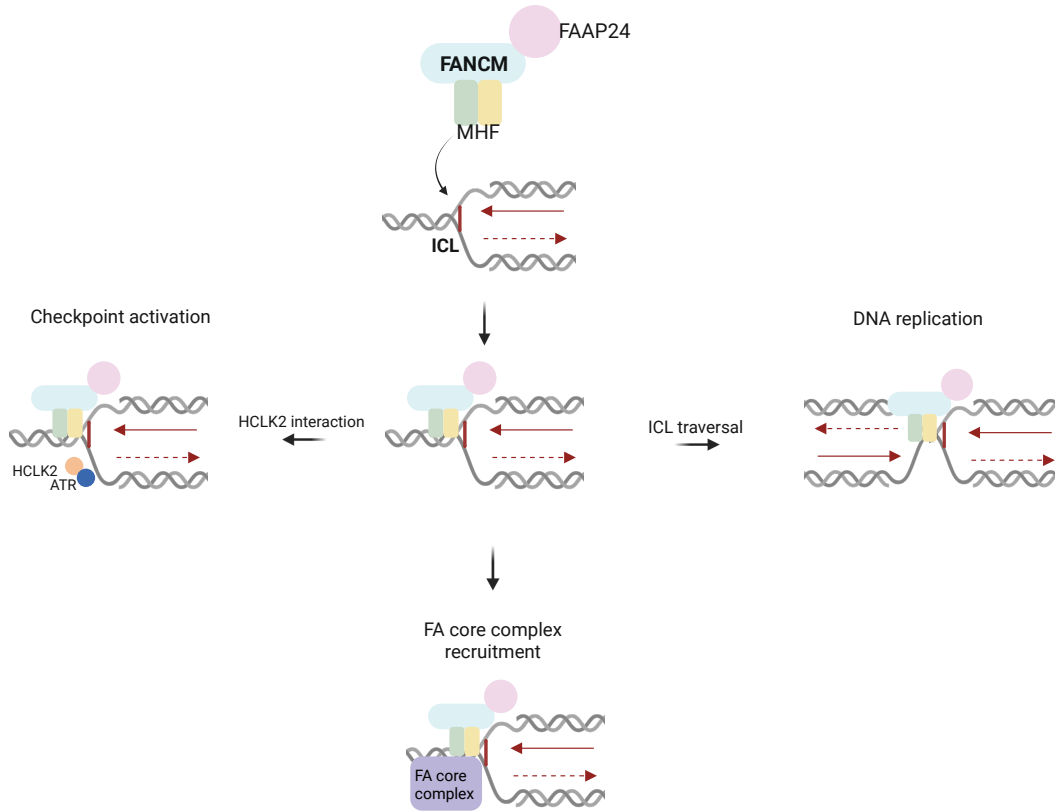


Figure 1: **FANCM recruitment at ICL site.** A schematic view of the different roles of FANCM recruitment at ICL. FANCM interacts with FAAP24, MHF1 and MHF2 forming a complex that is located next to the ICL. When interacting with HCLK2, the checkpoint regulation is activated to guarantee the proper timing of DNA repair and replication. The ICL traversal is another path by which cells can continue the replication. The interaction of the complex with the DNA is finally recruiting the FA core complex to the DNA, initiating the FA repair pathway.

Specifically, FANCM forms a complex with the histone-fold MHF complex (composed of MHF1, MHF2) [24] and FAAP24 [25] which is a protein that shares similarities with the C-terminus of FANCM and contains an endonuclease-like domain. This FANCM-MHF-FAAP24 complex locates the ICL to start the repair process. The interaction between FANCM and the MHF complex facilitates the traversal of the ICL, allowing the replication machinery to bypass the damage site and continue replication [26][24]. Additionally, the FANCM-FAAP24 complex interacts with HCLK2, activating ATR-mediated checkpoint signalling [27]. This signalling pathway ensures the precise coordination of repair processes and stabilization of the replisome. In the context of the FA pathway, the FANCM/FAAP24/MHF complex plays a crucial role in recruiting the FA core complex, which is necessary for the monoubiquitination of FANCD2 and FANCI, a key step in the repair of ICLs [27]. Figure 1 illustrates the main FANCM role in ICL recognition and resolution. The FA core complex formation is better described in the following section.

### 0.1.2 Core complex formation and FANCD2-FANCI ubiquitination

The FA core complex functions as an E3 ubiquitin ligase and it is composed of multiple sub-complexes that interact through weak, yet coordinated, interactions [28]. The first sub-complex consists of FANCC, FANCE, and FANCF and serves as an anchor between FANCM and the substrate [29][30] (Figure 2). The second one includes FANCA, FANCG, and FAAP20. The third sub-complex comprises FANCB, FANCL, FAAP 100, and UBE2T (FANCT), which contains the catalytic domains of the ligase [30][31]. Overall, the role of the core complex consists on the coordination and regulation of the E3 ligase module to properly interact with its substrates [32]. Some studies suggest that FANCF interacts with FANCM functioning as an adaptor protein [33]. FANCA and FANCG lead to the proper nuclear localization of the FA core complex [34]. Evidence shows that FANCE is implicated in the core complex integrity by interacting with FANCC, FANCF and FANCD2 [35][36][37]. However, the exact function of each protein within the core complex remains incompletely understood, necessitating further research to fully elucidate their individual roles. Once the core complex is formed, these components drive the monoubiquitination of the downstream proteins FANCD2 and FANCI, known collectively as the D2-I complex as a consequence of the ICL formation [29](Figure 2). The first step of the ubiquitination process is the activation by the E1 activating enzyme followed by the conjugation step performed by the E2 ubiquitin-conjugating enzyme (FANCT/UBET)[38][39][40]. The final step consists of the ubiquitin transfer to the Lysine residue of the substrate (D2-I complex) by the E3 ligase, specifically the RING domain of FANCL [41]. The mono-ubiquitination of the D2-I complex is a reversible post-translational modification.

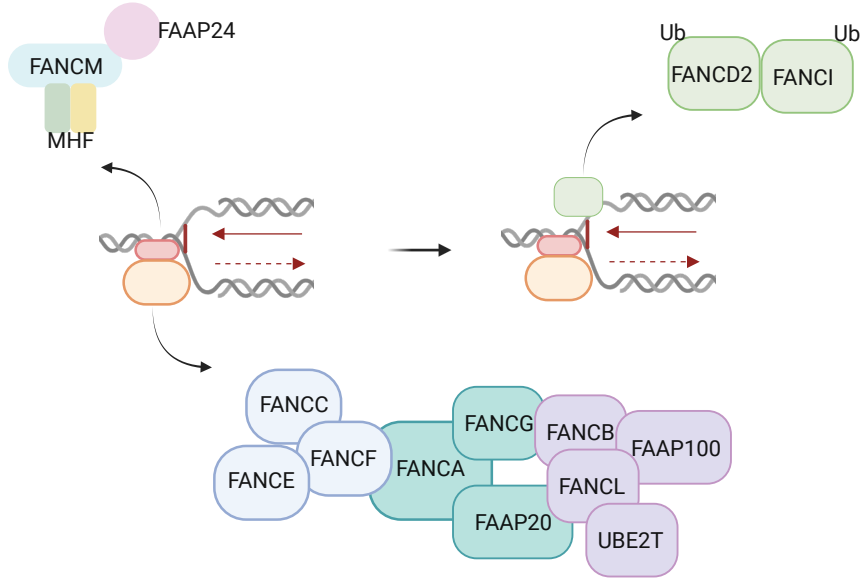


Figure 2: **Core complex formation and D2-I complex ubiquitination.** A schematic view of the core complex recruitment next to the ICL upon FANCM interaction with the DNA. The core complex is then contributing to FANCD2-FANCI monoubiquitination thanks to its E3 ubiquitin ligase activity.

The de-ubiquitination of the D2-I complex is catalyzed by the deubiquitinase USP1 and UAF1 [42][43][44][45]. This reaction is necessary for a correct ICL repair since USP1 deletion experiments suggested an increase in ICL sensitivity [46]. The de-ubiquitination of the D2-I complex must be therefore timely organized to guarantee a proper pathway functionality. To this end, FANCD2 and FANCI are being phosphorylated to properly coordinate the DNA repair [47]. Specifically, FANCI is phosphorylated by ATR-ATRIP in six sites known as the S/TQ cluster and this modification critically regulates FANCD2 (de)ubiquitination rate [47]. Conversely, CK2-mediated phosphorylation of FANCD2 prevents its monoubiquitination and loading onto the DNA in the absence of ICL [48]. All this evidence underlies how this pathway is precisely modulated by different processes avoiding further genotoxic damages.

### 0.1.3 Unhooking, TLS and HR steps

The monoubiquitinated D2-I forms a heterodimer complex which clamps the DNA near the DNA damage site [49][50][51][52][53]. This D2-I foci formation is followed by the “unhooking” step, wherein structure-specific nucleases (SSEs) are recruited to the site of damage [29] (Figure 3). This step is facilitated by SLX4 (FANCP), which is recruited by and interacts with FANCD2 and serves as a scaffold for these

nucleases [54][55]. The recruited nucleases include the XPF (FANCD1/ERCC1)-ERCC1 heterodimer, MUS81-EME1, SLX1, and FAN1 [56][57]. These nucleases cleave the DNA strands at the site of the ICL, effectively "unhooking" the lesion by generating unhooked intermediates, a single-strand region containing the ICL and a double-strand break (DSB) in the opposing strand.

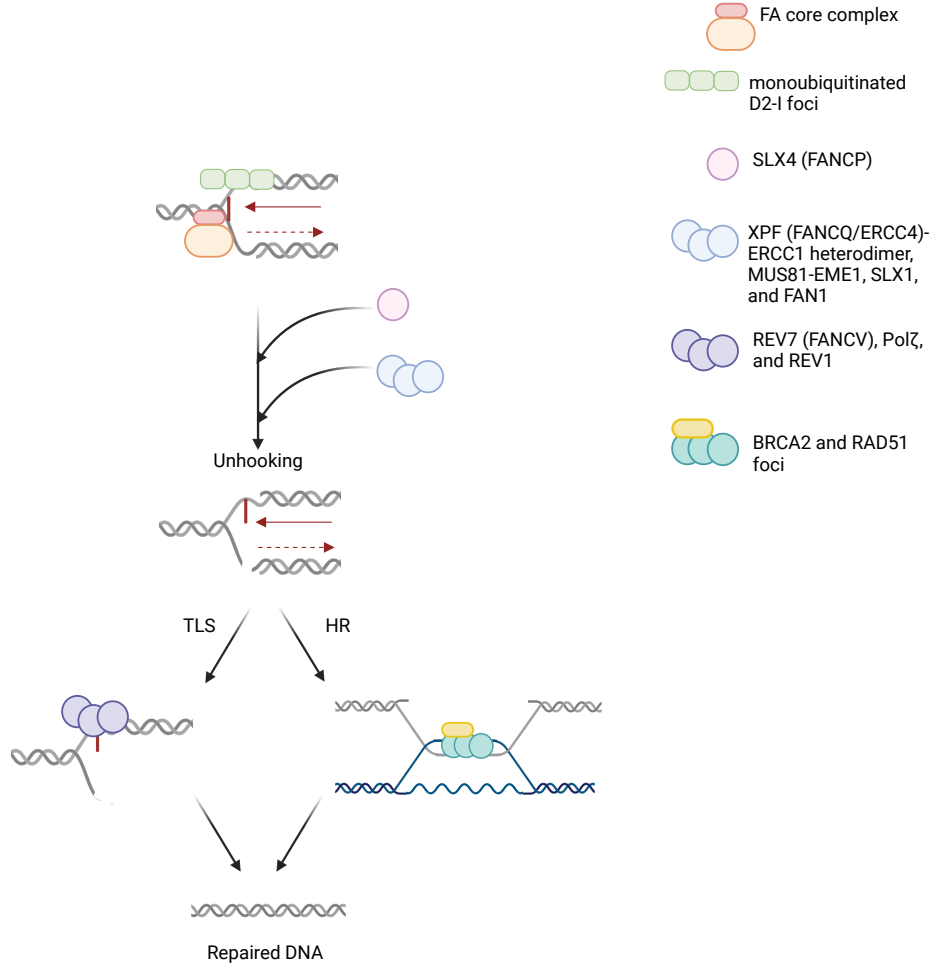


**Figure 3: Unhooking, TLS and HR steps for ICL repair.** A schematic view of the final steps of the FA pathway. The ubiquitinated D2-I complex forms a heterodimer structure which clamps the DNA near the ICL. This structure recruits specific endonucleases that cleave the DNA forming unhooked intermediates. One strand of the DNA will contain the ICL damage and will be repaired through TLS which requires specific polymerases. The other DNA strand will accommodate a DSB that will be repaired through the HR pathway involving many proteins of which only BRCA2 and RAD51 are shown. Thanks to these two combined pathways, the DNA will finally be repaired.

The unhooked ICL on the remaining DNA strand is bypassed through Translesion Synthesis (TLS), a low-fidelity DNA synthesis mechanism that allows the cell to bypass lesions and mitigate genomic toxicity (large DNA insertions and deletions) [58]. This process involves specialized polymerases, including REV7 (FANCV), Pol $\zeta$ , and REV1, which accommodate and replicate past bulky DNA lesions. Specifically, for TLS to properly occur, the integrity of the FA core complex is crucial as it interacts with REV1 [59]. The actual correlations between TLS and core complex are still unknown. Meanwhile, the DSB in the opposite DNA strand is repaired through Homologous Recombination (HR), a high-fidelity, error-free repair process [60].

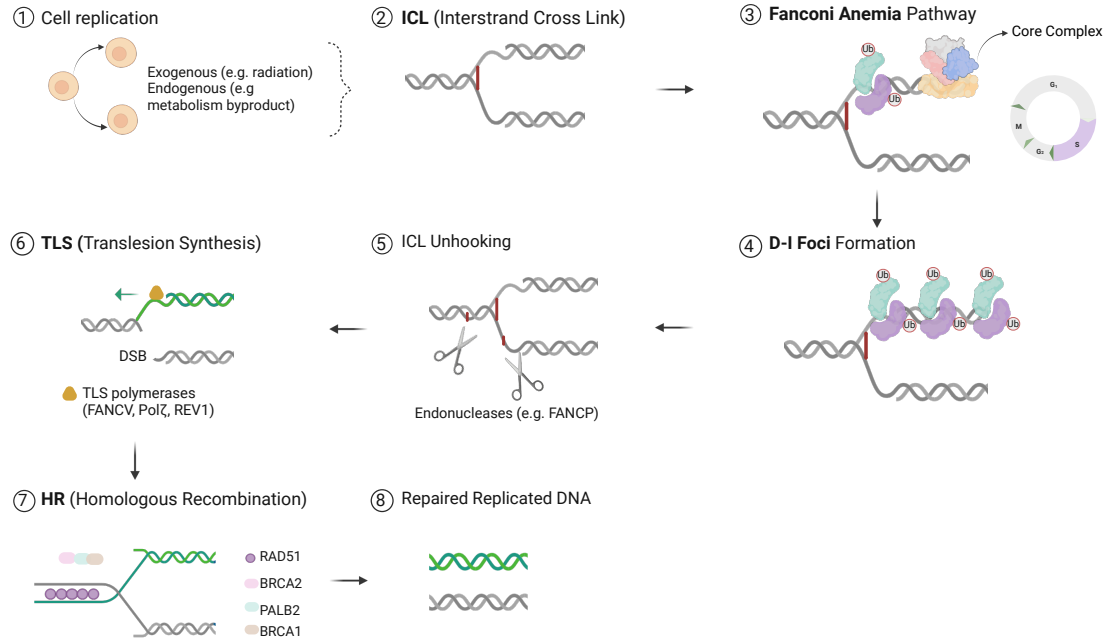


**Figure 4: FA pathway overview.** A schematic overview of the FA pathway. Endogenous and exogenous agents (1) can cause ICL (2). This will lead to the FA pathway activation (3) during the S-phase of the cell cycle. FANCM will therefore bind the DNA to initiate the FA core complex formation and the D2-I ubiquitination. The ubiquitinated D2-I complex will form foci near the damage (4) which will signal the pathway to proceed to the unhooking step (5). During the unhooking step, endonucleases will cut the DNA forming two unhooked intermediates. One will still contain the ICL and will be repaired by means of TLS (6). The other strand will harbour a DSB that will be repaired through HR (7). The DNA will be finally repaired (8).

HR ensures accurate restoration of the DNA sequence using a homologous template, to guide repair, thereby preserving genomic integrity. Briefly, the process

begins with the resection of DNA at the break site, generating single-stranded DNA (ssDNA) overhangs. These ssDNA regions are quickly coated by the protein RAD51, which forms nucleoprotein filaments. RAD51, in conjunction with BRCA2 and other mediator proteins, facilitates the search for a homologous DNA sequence, typically the sister chromatid. Once a homologous sequence is identified, the RAD51 filament invades the intact DNA duplex, forming a displacement loop (D-loop) [61]. This structure allows DNA synthesis, using the undamaged strand as a template to accurately copy the missing genetic information. After DNA synthesis, the newly synthesized strand pairs with the other broken DNA end, completing the repair process through either the synthesis-dependent strand annealing (SDSA) or double Holliday junction resolution pathway [62][63]. The latter step is crucial for maintaining genomic stability by ensuring that the repaired DNA is accurately restored to its original sequence. The damaged DNA is therefore finally repaired. Figure 3 illustrates how the unhooking, TLS and HR steps coordinate the ICL repair. Figure 4 recapitulates the FA pathway and all its steps, from the ICL formation to the DNA repair.

An important consideration, is that the FA and HR pathways are interconnected in the DNA repair process starting from the ICL damage. One of the critical points of interaction between these pathways involves the protein FANCD2 which physically interacts with RAD51. This interaction stabilizes RAD51 filaments, protects the DNA from nucleases as FAN1 and promotes the DNA strand exchange during the repair [64][65]. Moreover, FANCD2 seems to act in a parallel or compensatory way like BRCA2, which is known for stabilizing the RAD51 foci too [61]. Studies suggest that over-expression of FANCD2 might compensate for BRCA2-defectiveness [66][67]. This important correlation between the two pathways pointed out an important suggestion for developing drug treatments based on the concept of SL, which will be explored in the following section.

## 0.2 Synthetic Lethality concept

The concept of SL was first proposed in mid-90s in fruit flies [68][69] and in yeast right afterwards [70][71]. The SL is defined as a genetic interaction between two or more genes (synthetic lethal partners), whose contemporary perturbation leads to cell death [72][73][74] (Figure 4). Given the high frequency of genetic alterations in cancer cells, such as gene mutations or overexpression, targeting synthetic lethal partners of these altered genes presents an ideal therapeutic strategy [75][76]. This approach enables the selective targeting of cancer cells while sparing normal cells [76][13]. This concept opened the door for targeted therapy for oncology patients since 2014, when the Food and Drug Administration (FDA) approved this approach for ovarian cancer [77][78][79]. Specifically, the two approved synthetically lethal partners are the Poly (ADP-ribose) polymerase 1 and 2 (PARP1/2) and BRCA2

genes, which are important players in SSB (Single Strand Break) and DSB repair, respectively [80][81]. PARP function in DNA repair consists of the binding of damaged single-stranded DNA (ssDNA) or other lesions. This binding causes allosteric changes in PARP structure activating its catalytic function, which consists of adding negatively charged post-translational modifications named branched poly(ADP-ribose) (PAR) chains [82].

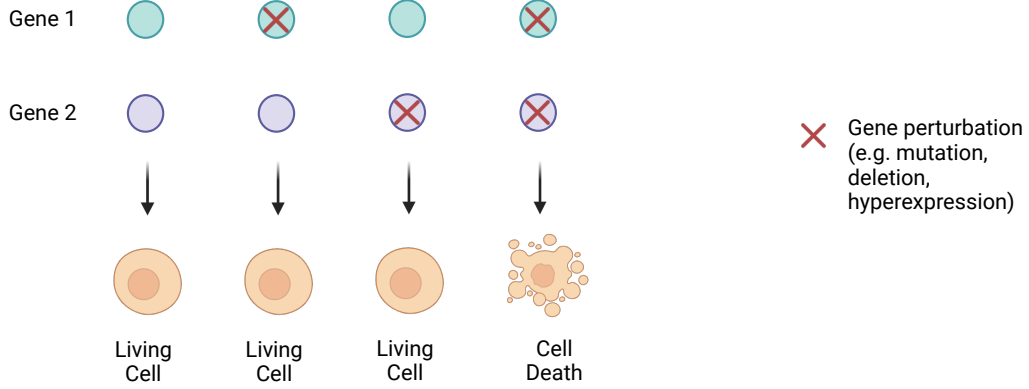


Figure 5: **Sythetic Lethality.** A schematic overview of the SL between two genes. As illustrated, the contemporary perturbation of both genes is necessary to induce cell death

This process is referred to as PARylation and it occurs in effector proteins such as XRCC1 that concur to chromatin remodelling and ssDNA repair [79][83]. By inhibiting this process, the SSB will accumulate causing the formation of DSB and replication fork collapse [83][84]. DSBs are mainly repaired through the HR pathway, in which BRCA1/2 are the main actors. In BRCA1/2-defective cells, the unrepaired DSB will lead to an increased accumulation of genotoxic damages that will lead to cell death [81][85]. Therefore, the contemporary perturbation of PARP1/2 and BRCA1/2 functions is lethal for cell survival. This outcome has encouraged BRCA1/2-defective cancer patients with PARP inhibitors (PARPi) as a selective treatment for cancer cells [79].

### 0.2.1 PARPi treatment

The first clinically approved PARPi is Olaparib (Lynparza) for BRCA1/2-mutated metastatic ovarian cancer treatment [77][86]. Over the years, other PARPi have been clinically approved like Rucaparib (Rubraca), Niraparib (Zejula) and Talazoparib (Talzenna) [79]. How these PARPi are causing a synthetic lethal outcome when combined with HR deficiencies is still under debate. One hypothesis is that they might act by trapping the PARP molecule on the DNA forming DNA-protein complexes and causing replication fork collapse [78][79][87]. However, recent studies advanced the hypothesis that PARP inhibition blocks the replisome to prevent

transcription-replication conflicts (TRC) and therefore form transcription elongation complexes [88].

Drug	IC <sub>50</sub> (nM)	Trapping ability <sup>29,237</sup>	P-glycoprotein substrate <sup>237-241</sup>	Targets <sup>242</sup>	CNS pene- tration <sup>243-246</sup>	T <sub>1/2</sub> (hours) <sup>237,238, 241,247,248</sup>	Bioavail- ability <sup>62,238-241</sup>	Known off-target interactions <sup>238-241</sup>
Olaparib	1	+	Yes	PARP1/2/3/4	+	11.9	55–60% in mice; 79% in dogs; <20% in rats	CYP3A4
Rucaparib	1	+	Yes	PARP1/2/3/4, TNKS1	+	25.9	36%	CYP enzymes
Niraparib	4	+	Weak	PARP1/2	++	48–51	75%	Dopamine, norepinephrine or serotonin transporters
Talazoparib	0.6	++	Weak	PARP1/2	–	90 ± 58 hours	41%	None
Veliparib	2	–	No	PARP1/2/3	+	4.1–8.2	NA	NA
Pamiparib	0.83	+	No	PARP1/2	++	NA	NA	NA
Fluzoparib	1.5	NA	NA	PARP1/2	NA	NA	35.8% in mice	NA

Figure 6: **PARP inhibitors pharmacological profile.** The reported table lists the pharmacological profile of the PARP inhibitors. The trapping activity of the PARP inhibitors has been used over the years as a reference value to determine the drug efficacy to induce a SL behaviour in combination with BRCA2 deficiencies. This figure has been previously published in Ref. [78]. CNS, central nervous system; CYP, cytochrome P450; IC<sub>50</sub>, half maximal inhibitory concentration; NA, not available; PARP, poly(ADP- ribose) polymerase; TNKS1, tankyrase 1; –, poor; +, modest; ++, good.

This recent hypothesis should be better investigated as it could provide valuable insights for developing more effective PARP inhibitors. What is clear is that PARPi treatment leads to SSB repair deficiencies with consequent accumulation of DSBs during the S-phase of the cell cycle. Up to date, the pharmacological profile of the clinically approved PARPi suggests that Talazoparib exhibit the best trapping activity (100-fold higher than Niraparib and higher than Olaparib and Rucaparib) and has no known off-target interaction [78][89] (Figure 5). In 2018, Talazoparib was approved by the FDA for germline BRCA-mutated (gBRCAm) HER2-negative locally advanced or metastatic breast cancer [90] and in 2023 for prostate cancer treatment [91]. Early-phase clinical trial have been initiated to prove Talazoparib efficacy in solid tumors including ovarian, prostate and pancreatic tumor [92][93][94]. Figure 7 summarizes the PARPi approvals by FDA starting from 2014.

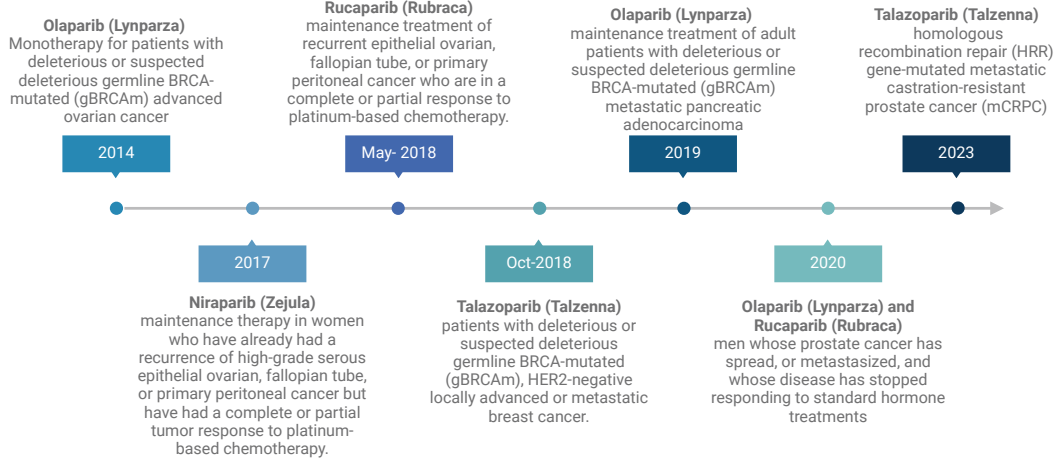


Figure 7: **Timeline of PARPi approved by FDA.** Timeline representation of the approved PARPi. The first approved drug was Olaparib in 2014 [77][95], followed by Niraparib in 2017 [96][97]. In 2018 Rucaparib [98][99] and Talazoparib [100][90] have been approved. Approval for more types of cancer followed in 2019 for Olaparib [101], in 2020 for Olaparib and Rucaparib [102] and in 2023 for Talazoparib [103].

### 0.2.2 Synthetic Lethality and FA pathway

Despite the clear advantage of using a treatment that aims to specifically target cancer cells, one of the main problem concerning the PARPi usage consists in PARPi resistance development. Cells might adapt to drug treatment in many ways: a) BRCA1/2 reverse mutation. In this case cancer cells might acquire new mutations that restores BRCA1/2 functions and, therefore, the HR pathway itself;

b) increase drug efflux which will provide the right metabolism of the drug inside the cells; c) epigenetic restoration which might affect BRCA1 expression levels rendering drug treatment ineffective [104][105][106][107][108]. The main alternatives to these acquired resistance include: 1) Combinational treatment with radiotherapy or immunotherapy; 2) Discovery of other biomarkers that might enhance or induce PARPi sensitivity; 3) Combination with other existing therapies [106]. As previously anticipated, the FA pathway is closely linked to HR through direct interactions with proteins like BRCA2 and RAD51. Therefore, studying the FA pathway and its connection to PARPi treatment could help identify new biomarkers for cancer therapy and potentially offer new strategies to overcome resistance to PARPi.

### 0.2.3 FA pathway and Pancreatic Cancer

Pancreatic cancer (PC) represents a good target for developing new therapeutical strategies. In fact it is one of the critical unmet challenges in oncology [109]. In the Phase III POLO trial, PC patients with BRCA1/2 mutations were treated with Olaparib [110][111]. This approach improved the Overall Survival (OS) of the patients, with a nearly 33% increase compared to the 17% OS observed in patients who did not receive the PARPi treatment. Additionally, PARPi-treated patients experienced a prolonged interval between chemotherapy sessions. However, the study's limitations include the relatively small population of PC patients with BRCA2 mutations, as well as the potential for PARPi resistance developing during treatment and restricting the efficacy of Olaparib to a limited subset of patients. Despite this type of advancements in cancer research and therapies, PC remains one of the most aggressive and lethal malignancies, with limited treatment options and poor survival outcomes [112][113][114]. PC accounts for approximately 3% of all cancer cases globally [115] yet it is the seventh leading cause of cancer-related deaths worldwide [109][116][117][118]. In the United States, for instance, pancreatic cancer makes up about 3% of all cancers [119] but is the fourth most common cause of cancer death. The 5-year survival rate is particularly poor, ranging from 5% to 12% depending on the population and healthcare system [120][121]. Even in developed countries with advanced medical technologies, only around 20% of patients survive one year after diagnosis [112]. The primary reason for this poor prognosis is that PC is usually diagnosed at an advanced stage. Over 80% of cases are detected after the disease has metastasized, making current treatment feasible only for a minority of patients [113]. PC can be categorized into exocrine and neuroendocrine subtypes, according to the pancreas compartment in which the tumor occurs. The exocrine compartment retains the digestion of carbohydrates, fats, and proteins function. The endocrine function of the pancreas is to regulate the glucose and metabolic homeostasis through the Islets of Langerhans [122][123]. Exocrine cancers are more common (95% of cases) than the endocrine forms (5%),

with pancreatic ductal adenocarcinoma (PDAC) being by far the most common exocrine cancer, accounting for over 90% of all cases [121] (Figure 8).

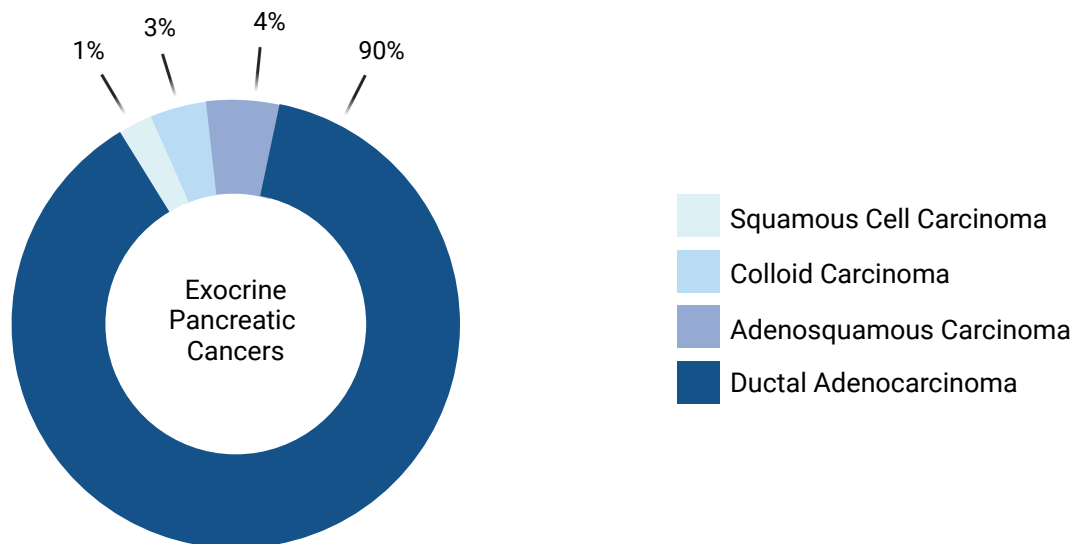


**Figure 8: Exocrine Pancreatic Cancers Pie Chart.** Exocrine Pancreatic Cancers account for 95% of all Pancreatic Cancer cases. Ductal Adenocarcinoma is by far the most common form of the exocrine cancer (90%) [124] and arises from the pancreatic duct which pumps digestive enzymes into the duodenum. Adenosquamous Carcinoma accounts for 0.5-4% of cases where malignant squamous cell grow together with ductal adenocarcinoma [125][126]. 1-3% of patients develop colloid carcinoma, also known as mucinous non-cystic carcinoma. This cancer is a histological variant of PDAC, where stromal mucin and floating malignant cells constitutes the 50% of the tumor volume [127][128]. The Squamous Carcinoma is an extremely rare form of exocrine carcinoma. It accounts for 1% of the cases and squamous epithelium is found in these patients [129][130].

Less common types of PC include acinar cell carcinoma (about 1-2% of cases), which originates from the enzyme-producing cells [131], and pancreatic neuroendocrine tumors (PNETs), which develop from the hormone-producing endocrine cells of the pancreas [132]. PNETs are relatively rare, constituting about 3-5% of PC. Although PNETs generally have a better prognosis than PDAC, the survival rate can vary depending on whether the tumor is functional (producing hormones) or non-functional (without producing hormones) [133]. The treatment of PC typically depends on the stage at diagnosis [134].

Surgery is potentially curative, but less than 20% of patients have a resectable disease at diagnosis. Chemotherapy, typically with drugs such as Gemcitabine and the FDA-approved FOLFIRINOX (a combination of Fluorouracil, Leucovorin,

Irinotecan, and Oxaliplatin) [135], is standard in both adjuvant and palliative settings [136]. Radiotherapy can also be applied, often in combination with chemotherapy, although its effectiveness in PC is limited [137]. The aforementioned genetic BRCA1/2 mutations are another alternative target, which may make patients eligible for PARPi like Olaparib. However, resistance to treatment remains a significant issue [138]. Different studies suggest that mutations in FA genes has been found in PC cells and patients. Mutations in FANCF and FANCM have been identified in patients with hereditary forms of the disease [139], while somatic mutations in FANCC and FANCG are associated with early-onset PC [140][141]. Additionally, both somatic mutations in FANCC and germline mutations in FANCG have been found in PC cells [142]. Genes such as FANCA, FANCC, FANCD2, FANCG, and FANCM are increasingly recognized as potential contributors to pancreatic cancer development [143][144][145][146]. These findings suggest that the FA pathway may affect pancreatic cancer, and targeting FA gene deficiencies could offer new avenues for treatment, especially in combination with PARP inhibitors, further enhancing SL strategies in PC therapy.

#### 0.2.4 FA genes correlation with PARPi

Different studies have aimed to investigate FA pathway to find among its genes new synthetic lethal partner for PARPi. FA defective cells have reduced viability after Olaparib treatment [147]. KO models for several FA genes, including FANCA, FANCC, FANCD2, FANCL and FANCI have shown heightened sensitivity to PARPi treatment [148][149][150][151][152]. Similarly, FANCM-deficient lymphoblasts also demonstrated increased sensitivity to PARPi [153]. Additionally, deficiency in FANCI and FANCD2 have been linked to enhanced PARPi sensitivity in ovarian cancer [150]. To predict genes associated with PARPi sensitivity, mainly CRISPR/Cas9 and RNAi screening methods have been used, with FA genes frequently identified in such screens [154][155][156][157][158]. Both methods rely on a library that enables Loss Of Function (LOF) studies for specific genes. However, RNAi screening is known for its limitations, such as off-target effects, cytotoxicity due to the delivery of shRNA or siRNA, and inconsistent knockdown efficacy across different genes and cell types [159][160][161]. In contrast, CRISPR/Cas9 high-throughput screens offer a more efficient approach to assessing gene essentiality. Nevertheless, the potential for in-frame mutations following Cas9-mediated DNA cuts can reduce screening accuracy, and off-target effects remain a concern with CRISPR/Cas9 as well [161][162][163]. In this thesis, more precise and reliable methods for screening FA genes will be evaluated as alternatives to existing techniques. One such method is the recently developed CRISPR-Select approach, which offers enhanced precision in gene editing [164].

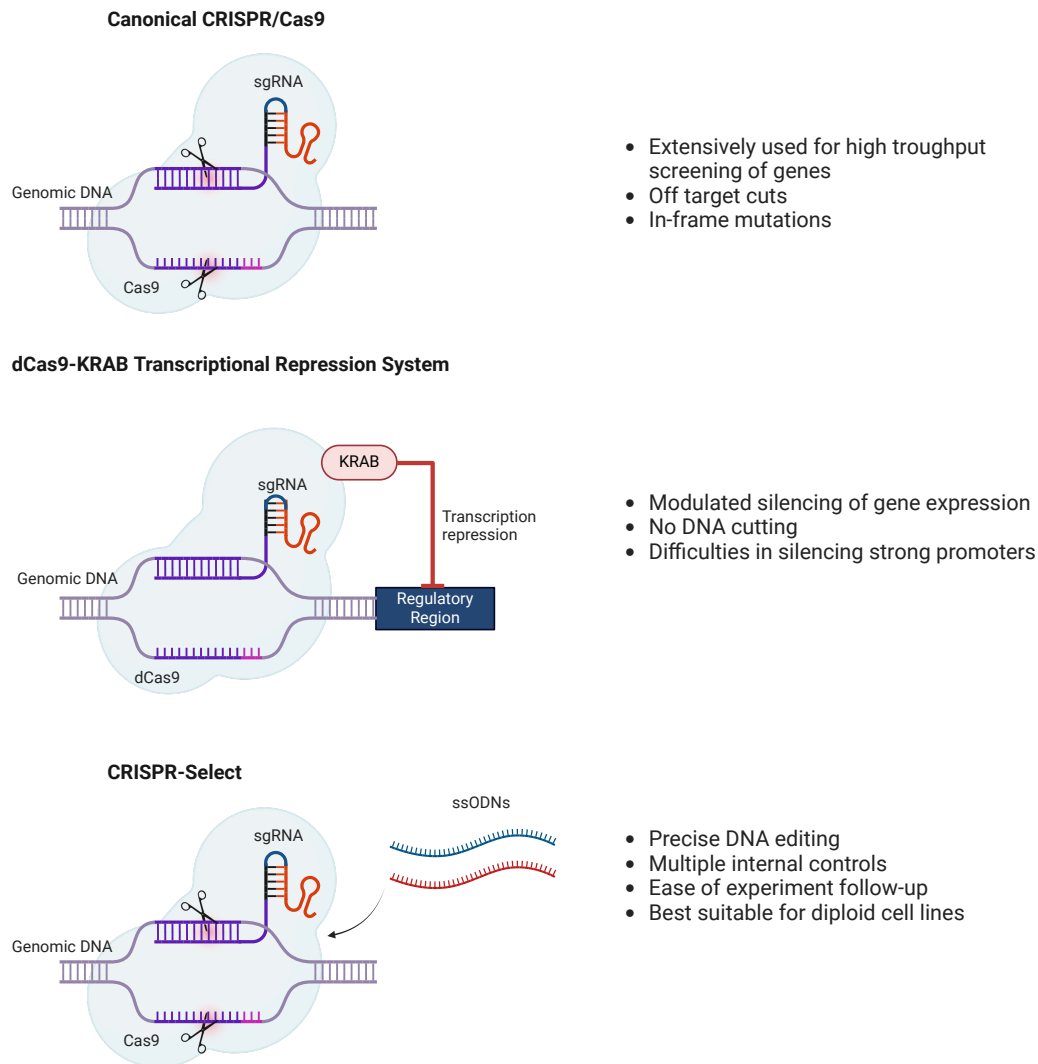


**Figure 9: Main features of CRISPR/Cas9, CRISPRi and CRISPR-Select.** CRISPR/Cas9 (up) is so far the main gene screening tool used [165][166]. The Cas9 enzyme is guided by the gRNA into the genomic region of interest to properly cut the DNA for its editing [167]. However, the off-target and in-frame mutations decrease the efficacy of the technique [168]. The CRISPRi tool (mid) is based on a catalytically inactive Cas9 fused with inhibitors for the transcription of the gene. This will result in a modulation of the gene expression without cutting the DNA. This approach can be difficult to use for inaccessible regions of the DNA (heterochromatin regions) or for strong promoters [169]. The CRISPR-Select tool (bottom) cuts the DNA in specific regions where single-stranded oligodeoxy nucleotides (ssODNs) will be integrated into the DNA for subsequent evaluation of their effect on cell survival. This tool is way more precise than the other two for its main internal controls but is mainly limited to diploid cell lines study

CRISPR-Select enables the assessment of the impact of mutations, such as those leading to protein truncation or functional alterations, on cell survival. As a second approach, CRISPR interference (CRISPRi) will be explored [158][170][171]. First introduced in 2013 [172], CRISPRi works by silencing the transcription of the target gene, bypassing the need for DNA cleavage by Cas9. This avoids complications linked to DNA cutting and it reduces the risk of off-target effects. By incorporating CRISPRi alongside other methods, there is potential to enhance the precision and efficiency of FA gene screening, overcoming some of the limitations of current techniques. Figure 9 illustrates the main differences between CRISPR-Select and CRISPRi, which will be better discussed in the following chapters.

### 0.2.5 DNA damaging drugs

To properly investigate FA genes, it is essential to use DNA-damaging drugs to induce DNA damage and, in turn, activate the cell's repair pathways. This approach ensures that the FA pathway is functioning within the cells, allowing for a comparison between scenarios where the pathway is either functional or non-functional in response to DNA damage. One of the drugs used for this purpose is Cisplatin, a platinum-based chemotherapeutic agent that has been extensively employed to treat various types of carcinomas and sarcomas [173]. Platinum-based drugs are among the most commonly used chemotherapy agents. In 1967, studies demonstrated that platinum compounds could inhibit *Escherichia coli* cell division and exert a cytotoxic effect on cancer cells [174]. Cisplatin was subsequently approved by the FDA for clinical use in 1978 for its efficacy, especially against testicular cancer [175]. Cisplatin works by binding to DNA, forming intra-strand DNA adducts between adjacent purine bases, which distorts the DNA structure and activates several DNA damage response pathways. These pathways include the activation of transduction cascades, such as p53 signalling, leading to cell cycle arrest, upregulation of pro-apoptotic genes, and downregulation of proto-oncogenes. It also triggers the nuclear excision repair (NER) system and activates the ATR pathway, which collectively hinders DNA synthesis and, subsequently, cell growth [176][177][178]. However, Cisplatin usage is associated with several side effects, such as nephrotoxicity, which can lead to kidney damage, and cardiotoxicity [179][180]. Furthermore, ototoxicity, or hearing loss, neurotoxicity, resulting in peripheral neuropathy, and gastrointestinal issues like nausea and vomiting, can occur after Cisplatin treatment [181]. Cisplatin causes also myelosuppression, which reduces bone marrow activity and the production of blood cells [182]. Another major challenge with Cisplatin is the development of drug resistance in cancer cells. One common mechanism of resistance is the increased DNA repair capacity of tumor cells, which enables them to survive despite Cisplatin-induced DNA damage. For example, overexpression of the ERCC1 protein enhances the efficiency of the NER pathway, thereby improving DNA repair [183]. Resistance can also arise from increased expression of efflux

pumps that remove Cisplatin from cells, lowering its intracellular concentration [184][185]. Additionally, cancer cells may alter their apoptotic pathways, becoming them less sensitive to DNA damage and reducing the likelihood of cell death [186]. These resistance mechanisms pose significant challenges to the long-term efficacy of Cisplatin therapy in many patients. Despite its drawbacks, Cisplatin is used in the treatment of PC, particularly in combination with Gemcitabine. This combination has shown moderate effectiveness in patients with advanced or metastatic PC [187][188][189]. In this thesis, Cisplatin will be used because it is relevant to PC treatment and, importantly, because it induces DNA damage, thereby activating DNA repair pathways such as FA and HR.

Another drug that will be used in the present study is Mytomycin C (MMC) an antibiotic originally isolated from *Streptomyces sandaensis* in 1988 [189]. MMC received FDA approval in 2020 for the treatment of upper tract urothelial cancer [190]. In cells, MMC creates interstrand crosslinks (ICLs) by forming covalent bonds between guanine bases on opposite strands of the DNA helix. These crosslinks inhibit the separation of DNA strands, which is necessary for replication and transcription. As a result, cells experience cell cycle arrest and eventually undergo apoptosis, especially in rapidly dividing cancer cells [3][191][192][193]. MMC typically forms these crosslinks in the minor groove of duplex DNA, particularly at 5'-CG-3' sites [20][194]. Unlike Cisplatin, MMC does not cause significant distortion of the DNA helix [195][196]. MMC is particularly effective in hypoxic conditions, which are common in many tumors, making it highly cytotoxic to solid tumors. Its application extends to treating various cancers, including gastric, pancreatic, and bladder cancers [197][198][199][200][201]. However, similar to Cisplatin, MMC can cause side effects and lead to the development of drug resistance. The most common side effect is myelosuppression, which decreases blood cell production and increases risk of infections, anemia, and bleeding [202][203]. Pulmonary toxicity is another concern, potentially resulting in conditions like interstitial pneumonitis or pulmonary fibrosis [204]. Drug resistance to MMC can arise through several mechanisms. One prominent pathway is the increased expression of detoxifying enzymes such as glutathione-S-transferase, which can deactivate MMC before it exerts its cytotoxic effects [205]. In this thesis, MMC will be used for its ability to form ICLs, which serve as the initial step in activating the FA pathway. Using MMC allows for the activation of this DNA repair pathway, enabling the study of how cells with functional or deficient FA pathways respond to the treatment.

## 0.3 Aim of the thesis

This thesis primarily aims to develop a methodological framework for investigating the FA pathway and its role in PARPi response. Although the FA pathway has been the focus of numerous studies, a comprehensive investigation covering all its proteins remains incomplete [206][207][208]. We hypothesize that the FA pathway plays a crucial role in DNA damage response and modulates sensitivity to PARPi in cancer treatment. This hypothesis is supported by multiple studies linking FA deficiencies to increased PARPi sensitivity [151][152][209]. However, these studies often lack a reliable and precise methodology to unequivocally determine the role of FA genes in this context. Two primary methods traditionally employed to study gene function are RNA interference (RNAi) and the CRISPR/Cas9 system. These methods have many off-target effects that might affect the result significance [210][211].

To address this issue, in this study we will utilize a recently developed technique, CRISPR-Select<sup>TIME</sup>, to specifically investigate the effects of mutations in FA genes (e.g. protein-truncating mutations) on cell survival over time [164]. The experimental model chosen for this approach is the MCF10A cell line which is a normal human breast epithelial cell line. This diploid cell line was selected to minimize confounding effects from other mutations, enabling a clear analysis of the specific mutation's impact on cell viability. This method will allow us to assess the precise role of the FA pathway in PARPi response within a normal cell model. The main limitation of the CRISPR-Select<sup>TIME</sup> tool lies in its optimal performance with diploid cell lines, such as MCF10A, which makes its application to PC cell lines more challenging. PC cell lines are typically aneuploid, complicating the tool's efficacy in this context. Therefore, in this thesis, CRISPR-Select<sup>TIME</sup> will primarily serve as a proof of concept to explore the correlation between FA pathway genes and Talazoparib sensitivity, rather than being directly applied to PC cell lines.

To develop a systematic study of FA gene deficiency in cancer cells, a second CRISP method will be applied, being cancer cells frequently aneuploid, and being CRISP-Select unsuitable for non-diploid cells. The CRISPR interference (CRISPRi) tool, a technique designed to silence gene expression at the transcriptional level [170], will therefore be employed. By silencing specific FA genes, we can observe the cellular consequences of FA pathway inactivation. CRISPRi experimental set up will be conducted in HeLa cells, a well-established cancer cell line with proficient DNA repair mechanisms, widely used in studies of DNA repair deficiencies [212][213][214][215][216]. This approach will enable us to evaluate the role of the FA pathway in the context of cancer, specifically how its disruption affects cell survival, in view of a potential future application of this approach to PC cell lines.

Both CRISPR-Select<sup>TIME</sup> and CRISPRi experimental strategies will be combined with drug treatments to assess the FA pathway's function under chemotherapeutic stress. Cisplatin will be used to observe how its DNA-damaging properties impact cells in our experimental models. Additionally, Mitomycin C (MMC) will be employed as it induces the formation of interstrand crosslinks (ICLs), a specific type of DNA damage that directly engages the FA pathway for repair. This allows us to study the FA pathway's activation and function in response to DNA damage that requires its intervention for resolution.

Furthermore, this thesis seeks not only to provide a method for studying the FA pathway but also to explore its connection to PDAC. Several studies have identified mutations in FA genes in PC patients. Our goal is to investigate the correlation between FA pathway dysfunction and PC progression, particularly its potential to influence PARPi sensitivity. To this end, we will utilize a PC cell line, PANC 03.27, with a known FA pathway deficiency, allowing us to assess its sensitivity to the PARPi Talazoparib without introducing additional genetic modifications. Consequently, the CRISPRi and CRISPR-Select<sup>TIME</sup> platforms offer promising alternatives for gene screening, though further optimization is needed for their application in PC models.

In summary, this thesis proposes innovative methodological approaches for studying the FA pathway in the context of PC, with the ultimate goal of improving our understanding of how FA pathway dysfunction influences Talazoparib response and developing targeted therapeutic strategies for FA-deficient cancers.

# Chapter 1

## Detection of Synthetic Letality between FANCA, FANCD2, FANCM and the PARPi Talazoparib in MCF10A cells by CRISPR-Select

### Introduction

Different methods have been used in research to investigate the role of FA pathway in cancer and drug response. A key strategy for elucidating the essentiality of a protein involves loss of function approaches by directly impairing protein activity using specific inhibitors or through genomic techniques, such as CRISPR-Cas9. The synthesis and use of inhibitors targeting the Fanconi Anemia (FA) pathway is notably challenging due to the interactions and ubiquitous role of FA proteins [11]. In fact, many FA proteins show multiple functions. FANCM has DNA-repair roles outside the FANCM pathway: it prevents the stalling of the replication fork through its ATPase activity and it can activate the ATR-mediated cell checkpoint [26]. The FA core-complex includes FANCA and FANCC whose roles have not been fully defined and are difficult to drug because of their multiple interactions with other proteins of the complex [41]. FANCD2 is the final effector of the pathway and its role in mRNA export and R-loop accumulation has been recently discovered [217]. These factors collectively highlight the complexities in designing selective and effective inhibitors for the FA proteins. As an alternative, the genomic approach of CRISPR/Cas9 has been used to discover genes involved in PARPi sensitivity in different cell lines, finding FANCA, FANCC, FANCD2 and FANCM among them

[157]. This result highlights the necessity to further investigate those genes. Despite the clear advantages of using CRISPR/Cas9 for extensive gene screening and identification of new drug targets in cancer research [218][219], its high on- and off-target score prevents its use as a tool for obtaining precise results [220][221]. In this chapter, a newly implemented method of CRISPR/Cas9 will be proposed as an alternative to overcome the current and intrinsic limits of this tool.

## 1.1 CRISPR-Select

### 1.1.1 Overview of the CRISPR-Select technique

In 2022, the labs of Claus Storgaard Sørensen and Morten Frödin co-developed the CRISPR-Select technique [164]. This method is based on an easy and precise tracking of a gene variant in a diploid cell to evaluate its cellular impact. This approach is a valid and advanced alternative to the current genome-editing tools and will be used to study the impact on cell proliferation/survival of FANCA, FANCD2 and FANCM genes. Moreover, CIS and Talazoparib treatment will be included to strengthen their role in DNA repair and PARPi sensitivity. Specific gene variants will be therefore designed to ensure the synthesis of a truncated protein that will promote a FA pathway-deficient condition. Among the three knock-in assays available (CRISPR-SelectTIME, CRISPR-SelectSPACE and CRISPR-SelectSTATE) this chapter will focus specifically on CRISPR-SelectTIME, providing a detailed exploration of its application and significance for this research.

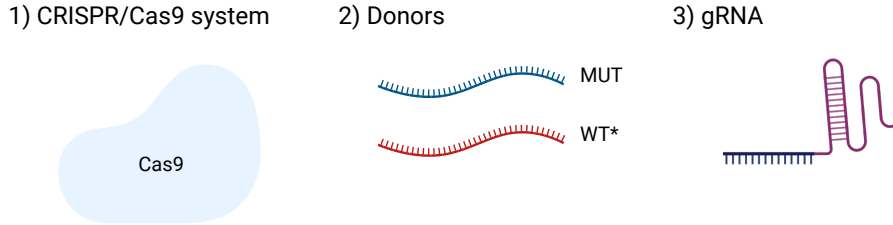
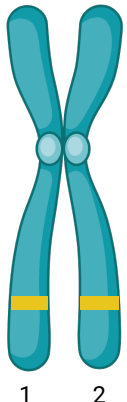


Figure 1.1: **CRISPR/Cas9 Cassette.** All the main components of the CRISPR-Select Cassette. 1) Cas9 enzyme. 2) Designed Donors containing the mutation to be studied (MUT) and the synonymous mutation used as control (WT\*). 3) Designed gRNA to properly guide the Cas9 enzyme to the genomic region of interest.

Briefly, the tool consists of a CRISPR/Cas9 cassette which includes (1) a CRISPR/ Cas9 system to cut the DNA at the site of interest, (2) a single-stranded oligodeoxy nucleotide (ssODN) repair template that carries the variant of interest and hereafter named MUT, (3) a second ssODN repair template with a synonymous mutation called WT\*, located at or near the same position as the variant of interest. These two ssODNs will hereafter be collectively referred to as "Donors". The guide

RNA (gRNA) is specifically chosen so that both the MUT and WT\* mutations lie within the seed region or protospacer-adjacent motif (PAM) of the CRISPR-Cas9 binding site, reducing the likelihood of post-knock-in recutting (Figure 1.1).



	Editing on Allele 1	Editing on Allele 2	Expected Effect
a)	MUT	Out of frame/InDel	Built-in Loss of Heterozygosity
b)	WT*	Out of frame/InDel	Built-in Loss of Heterozygosity
c)	WT*	WT*	Normal protein expression
d)	MUT	MUT	Mutant protein expression
e)	MUT	WT*	Partial MUT effect
f)	Out of frame/InDel	Out of frame/InDel	Protein loss
g)	WT	WT	No editing

Figure 1.2: **Most frequent CRISPR-Select<sup>TIME</sup> editing outcomes.** The CRISPR-Select<sup>TIME</sup> technique generates various editing outcomes following the delivery of the CRISPR/Cas9 cassette. Once the Cas9 enzyme, guided by the gRNA, introduces a targeted double-strand break at the specific gene locus, the cell's natural repair processes incorporate a new DNA sequence at the cut site. This sequence can be replaced by the MUT ssODN, the WT\* ssODN, or a sequence containing an out-of-frame or InDel mutation resulting from the Cas9-induced break. The preferred outcomes for accurately assessing the gene's specific impact are those that lead to a built-in Loss of Heterozygosity, as illustrated in scenarios a and b. These outcomes provide a clear context for studying the isolated effects of the gene, free from the influence of a second functional allele. Additionally, there is the possibility of no editing occurring in one or both alleles.

This cassette is delivered to the cell population of interest. This efficient system guarantees that the Cas9 is guided by the gRNA to the genomic region of interest, which will then be cut. The MUT and WT\* ssODNs (delivered in a 1:1 ratio) will serve as the template for the DNA repair and therefore will be integrated into the DNA. As a consequence, different editing outcomes will be obtained in different percentages and frequencies, depending on the template used by the cells for the repair (Figure 1.2). In the best-case scenario, one allele of the diploid cell will be affected by a disruptive genetic outcome (e.g. a frameshift mutation) (see section 1.1.2 for details) while the other will be replaced either by the MUT or the WT\* template. This will cause a built-in Loss of Heterozygosity (LOH) of the gene that can be easily analyzed through Next Generation Sequencing (NGS). By comparing two selected time points of the MUT:WT\* ratios over time, the tracked ssODN's

impact on cell proliferation/survival will be determined. In the following sections, each step of the technique will be explained in detail.

### 1.1.2 CRISPR-Select cassette design

The FANCA\_R880\* variant will be used as an example to explain and illustrate the method. Briefly, the website Benchling (<https://www.benchling.com/>) is used to import the reference sequence of the gene of interest from the Human Genome GRCh38 (Homo\_sapiens) as shown in Figure 1.3. Once imported, it is possible to see all the introns and exons of the gene. It is necessary now to select the region of interest where is located the variant to be studied. In our example, the R880 amino acid is located at the exon no. 28 of the FANCA gene (Figure 1.4).

Create DNA / RNA sequence

CREATE NEW UPLOAD FILES **IMPORT FROM DATABASE** SELECT CHROMOSOMAL REGION

Sequence  
FANCA

Genome  
GRCh38 Search Clear

Gene  
ENSG00000187741

Species  
GRCh38 (homo\_sapiens)

Ensembl version  
112

Location  
Chromosome 16 89,726,683—89,816,977 (-)  
☒ Import in sense orientation

Name  
FANCA-202 (ENST00000389301)

Transcript  
FANCA-202 (E...)

Import as  
Genomic sequence cDNA

Upstream bases  
0

Downstream bases  
0

Set nucleotide type\*  
DNA RNA

Set project folder\*  
FA\_Project

Set schema  
Select a schema...

Close Import

Figure 1.3: **Benchling website.** Example of how to use the Benchling Website. In this case, the requested gene sequence is the FANCA one from the GRCh38 (homo\_sapiens) genome. The "Genome sequence" and the "DNA" nucleotide type must be selected to obtain the complete sequence of the selected gene.

The resulting mutation originates a non-functional truncated protein. To obtain this, it is necessary to convert the sequence of the amino acid (CGA) into a stop codon (TGA). The Cytosine of the codon will be therefore taken as the starting

point for the gRNA design. From the Cytosine, it is necessary to select 45bp upstream and downstream of it and to copy it. This sequence will be pasted in the CRISPOR website (<http://crispor.gi.ucsc.edu/>) in the Step-1 box (Figure 1.5). In step 2, the genome of reference (GRCh38) is selected. Then, in step 3, NGG is selected as the PAM sequence and submitted. The submission output will be a list of gRNAs with respective PAM spread onto the submitted sequence (Figure 1.6).

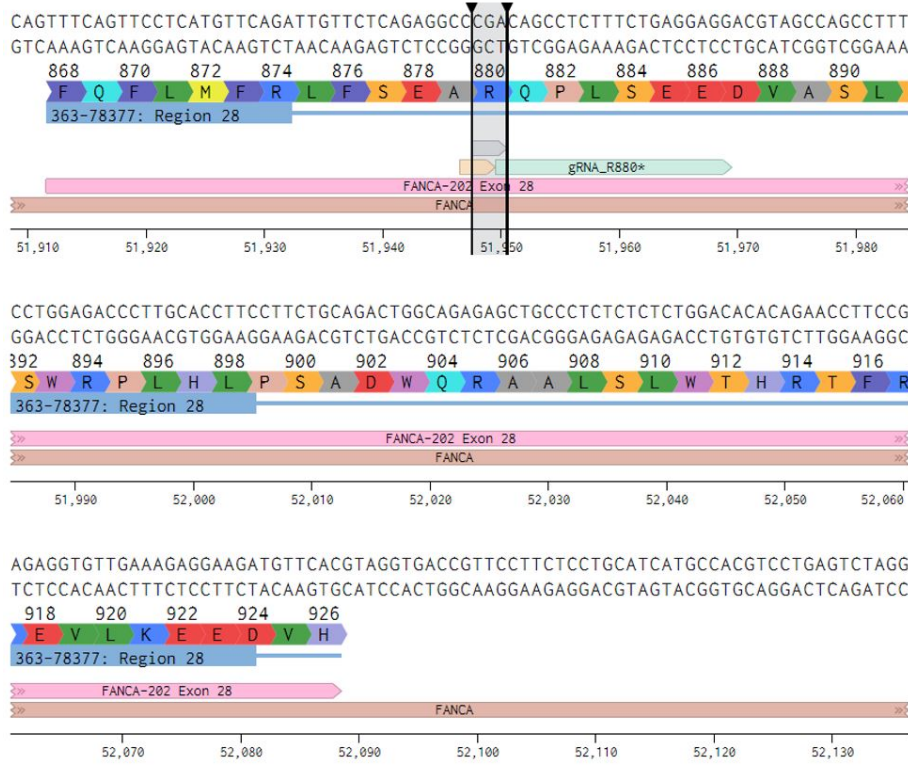
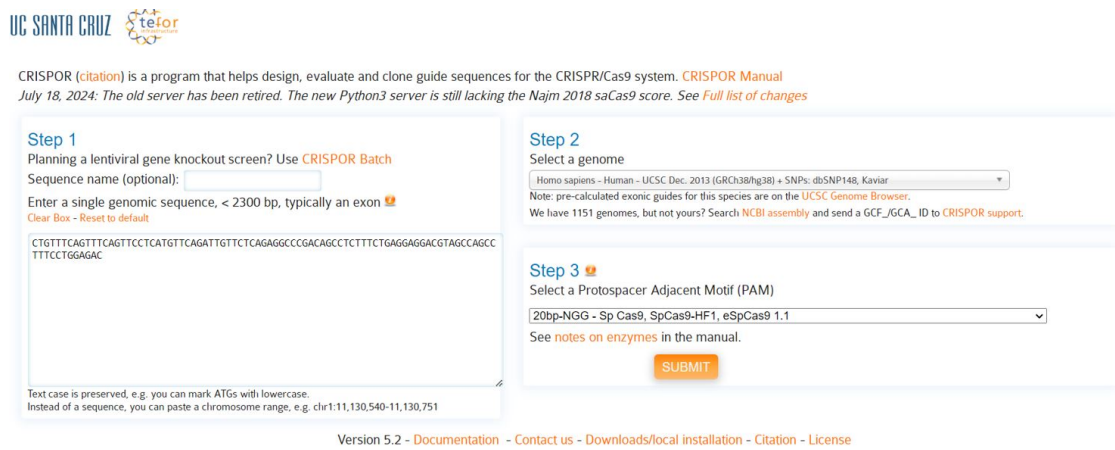



Figure 1.4: **Gene sequence in Benchling.** Once the request on Benchling has been submitted, the selected gene sequence will be provided as shown in this figure. Exons will be indicated with a bar (e.g. pink bar indicating FANCA Exon 28) where all the amino acids are mapped. Introns are shown as nucleotide sequences. The amino acid under investigation (e.g. R880) can be selected and saved in the website. It is also possible to map and save all the other necessary sequences (e.g. gRNA in green and relative PAM sequence in yellow)

As explained in section 1.1.5 of the Materials and Methods and in Figure 1.4, the selection of the gRNA is based on several critical parameters, including optimal specificity score, efficiency score, and minimal off-target effects. Another crucial metric is the Out-of-Frame (frameshift)/Insertion-Deletion (InDel) score. This score assesses the likelihood of inducing a frameshift or InDel modification

in at least one allele of the target gene. These modifications are essential for the CRISPR-Select assay in diploid cells for three reasons: 1) if one allele contains the WT\* sequence and the other allele undergoes a frameshift or InDel modification, the result is the production of a functional protein from the WT\* allele and a non-functional protein from the modified allele. This built-in LOH is necessary for assessing the impact of the WT\* protein over time. This allows to evaluate of the true neutrality of the WT\* sequence without interference from a fully functional WT allele, which cannot be distinguished by NGS. 2) A similar reason applies to the MUT sequence.




UC SANTA CRUZ 

CRISPOR (citation) is a program that helps design, evaluate and clone guide sequences for the CRISPR/Cas9 system. [CRISPOR Manual](#)  
 July 18, 2024: The old server has been retired. The new Python3 server is still lacking the Najm 2018 saCas9 score. See [Full list of changes](#)

**Step 1**

Planning a lentiviral gene knockout screen? Use [CRISPOR Batch](#)

Sequence name (optional):

Enter a single genomic sequence, < 2300 bp, typically an exon 

[Clear Box](#) - [Reset to default](#)

CTGTTTCAGTTTCAGTTCTCATGTTTCAGATTGTTCTCAGAGGCCGACAGCCTCTTCTGAGGAGGACGTAGCCAGCC  
 TTTCCTGGAGAC


Text case is preserved, e.g. you can mark ATGs with lowercase.  
 Instead of a sequence, you can paste a chromosome range, e.g. chr1:11,130,540-11,130,751

**Step 2**

Select a genome

Homo sapiens - Human - UCSC Dec. 2013 (GRCh38/hg38) + SNPs: dbSNP148, Kaviar

Note: pre-calculated exonic guides for this species are on the [UCSC Genome Browser](#).  
 We have 1151 genomes, but not yours? Search [NCBI assembly](#) and send a GCF\_ID to CRISPOR support.

**Step 3** 

Select a Protospacer Adjacent Motif (PAM)

20bp-NGG - Sp Cas9, SpCas9-HF1, eSpCas9 1.1

See [notes on enzymes](#) in the manual.

[SUBMIT](#)

Version 5.2 - [Documentation](#) - [Contact us](#) - [Downloads/local installation](#) - [Citation](#) - [License](#)

Figure 1.5: **CRISPOR website.** The CRISPOR website provides a list of mapped gRNA. To submit the request, 45bp upstream and downstream the mutation of interest must be copied and pasted in the "Step-1" box. Steps 2 and 3 consist of the selection of the reference genome (GRCh38\_Homo\_Sapiens) and the PAM sequence (NGG).

A frameshift or InDel modification in the second allele is necessary to precisely determine the long-term effects of the mutation. These effects will then be compared to those of the WT\* sequence using NGS analysis. 3) During data analysis, the ratio of frameshift/InDel to WT\* will be carefully monitored. This ratio provides clear evidence of the negative selection against cells harboring frameshift/InDel modifications within the same cell culture dish, thereby resulting in an internal control to verify the effectiveness of the CRISPR-Select technique.

## 1.1. CRISPR-SELECT

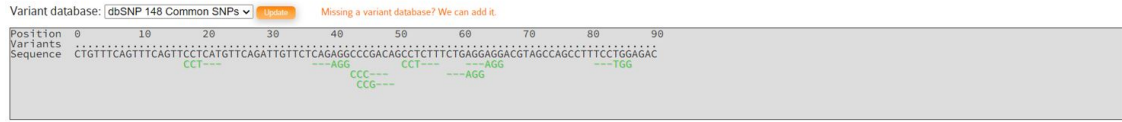
*Homo sapiens* (hg38), chr16:89764985-89765075, reverse genomic strand

Your input sequence is 91 bp long. It contains 8 possible guide sequences.

Shown below are their PAM sites and the expected cleavage position located -3bp 5' of the PAM site.

Click on a match for the PAM NGG below to show its 20 bp-long guide sequence. (Need help? Look at the [CRISPOR manual](#))

Colors green, yellow and red indicate high, medium and low specificity of the PAM's guide sequence in the genome.



### Predicted guide sequences for PAMs

Ranked by default from highest to lowest specificity score (Hsu et al., Nat Biotech 2013). Click on a column title to rank by a score.

If you use this website, please cite our [paper](#) in NAR 2018. Too much information? Look at the [CRISPOR manual](#).

Download as Excel tables: [Guides](#) / [Guides, all scores](#) / [Off-targets](#) / [Saturating mutagenesis assistant](#)

Position/ Strand	Guide Sequence + PAM + Restriction Enzymes + Variants <input type="checkbox"/> Only G- <input type="checkbox"/> Only GG- <input type="checkbox"/> Only A- <input type="checkbox"/>	Mit Specificity Score	CFD Spec. score	Predicted Efficiency <a href="#">Show all scores</a> Doench '16 Mor-Mateos Doench-RuleSet3	Outcome Out-of-Frame Lindel	Off-targets for 0-1-2-3-4 mismatches + next to PAM	Genome Browser links to matches sorted by CFD off-target score <input type="checkbox"/> exons only <input type="checkbox"/> chr16 only	
62 / fw	GGCCGACAGCCTCTTCTG AGG Enzymes: BseRI, BstDEI, Hpy188I Cloning / PCR primers	78	86	61	31	25	64 78 0-0-2-9-112 0-0-2-5-7 123 off-targets	4intergenic:RP11-430C1.1-RP11-457D20.2 4intergenic:RP11-178L8.6-C16orf95/RP11-178L8.4 4intron:SSBP2 <a href="#">show all...</a>

**Figure 1.6: gRNA selection in CRISPOR.** The CRISPOR website furnishes mapped gRNA sequence (with relative PAM sequence) around the submitted genome sequence. In the grey box, it is possible to see different suggested PAM sequences (green) below the submitted genome sequence. This green code indicates that all suggested PAM sequences have high specificity in the genome. Below the grey box, is possible to see the "Predicted guide sequences for PAMs" section. Here, all the gRNA sequences are listed with their relative scores. For simplicity, only one gRNA sequence is shown in this figure. The final selection of the gRNA will be guided by the comparisons of the predicted scores (e.g. MIT SSpecificity Score, Predicted Efficiency score, Off-target for 0-1-2-3-4 mismatches score) and by the proximity of the PAM sequence to the mutation under investigation.

Overall, the introduction of frameshift/InDel modifications acts as an internal positive control, ensuring the accuracy and reliability of the experimental results. For further detail on the NGS analysis for CRISPR-Select<sup>TIME</sup> see section 1.1.5 of this chapter. It is possible then to copy and paste the gRNA sequence to Benchling and annotate it (Figure 1.4). To design the MUT and WT\* sequences, it is sufficient to change the base of the codon of interest. In this case, CGA will become TGA for the MUT sequence. The WT\* sequence will be designed according to the codon usage table "Kazusa" (<https://www.kazusa.or.jp/codon/cgi-bin/showcodon.cgi?species=9606>) in order to choose a synonymous mutation that will not affect the translation process of the cells. In this case, CGA will become CGG (Arginine codon usage score of 10.4)(Figure 1.7). Finally, gRNA, MUT and WT\* sequences can be ordered and, therefore used for the next steps.

<i>Homo sapiens</i> [gbpri]: 93487 CDS's (40662582 codons)			
fields: [triplet] [frequency: per thousand] ([number])			
UUU 17.6(714298)	UCU 15.2(618711)	UAU 12.2(495699)	UGU 10.6(430311)
UUC 20.3(824692)	UCC 17.7(718892)	UAC 15.3(622407)	UGC 12.6(513028)
UUA 7.7(311881)	UCA 12.2(496448)	UAA 1.0( 40285)	UGA 1.6( 63237)
UUG 12.9(525688)	UCG 4.4(179419)	UAG 0.8( 32109)	UGG 13.2(535595)
CUU 13.2(536515)	CCU 17.5(713233)	CAU 10.9(441711)	CGU 4.5(184609)
CUC 19.6(796638)	CCC 19.8(804620)	CAC 15.1(613713)	CGC 10.4(423516)
CUA 7.2(290751)	CCA 16.9(688038)	CAA 12.3(501911)	CGA 6.2(250760)
CUG 39.6(1611801)	CCG 6.9(281570)	CAG 34.2(1391973)	CGG 11.4(464485)
AUU 16.0(650473)	ACU 13.1(533609)	AAU 17.0(689701)	AGU 12.1(493429)
AUC 20.8(846466)	ACC 18.9(768147)	AAC 19.1(776603)	AGC 19.5(791383)
AUA 7.5(304565)	ACA 15.1(614523)	AAA 24.4(993621)	AGA 12.2(494682)
AUG 22.0(896005)	ACG 6.1(246105)	AAG 31.9(1295568)	AGG 12.0(486463)
GUU 11.0(448607)	GCU 18.4(750096)	GAU 21.8(885429)	GGU 10.8(437126)
GUC 14.5(588138)	GCC 27.7(1127679)	GAC 25.1(1020595)	GGC 22.2(903565)
GUA 7.1(287712)	GCA 15.8(643471)	GAA 29.0(1177632)	GGA 16.5(669873)
GUG 28.1(1143534)	GCG 7.4(299495)	GAG 39.6(1609975)	GGG 16.5(669768)

Figure 1.7: **Codon usage table.** This codon usage table reports the frequency of the used codons in *Homo sapiens*. This table is necessary when designing synonymous mutations to guarantee the selection, and therefore expression, of proper codons.

### 1.1.3 CRISPR-Select cassette delivery

The designed cassette will then be delivered into the target cells, iCas9-MCF10A, which are immortalized normal human breast epithelial cells. This cell line was chosen for developing the CRISPR-Select tool because it offers an ideal system to uniquely assess the impact of a specific variant without interference from other cellular factors, such as additional mutations or dysfunctional pathways. Furthermore, as a diploid system, MCF10A cells provide an optimal genomic state for evaluating the built-in LOH within the gene of interest, offering a clean and controlled platform for gene function analysis. This cell line has already been engineered with and inducible form of Cas9. The first step for delivering the cassette will require the induction of the Cas9 expression through Doxycycline treatment of the cells 24h before the delivery (Figure 1.8). On Day 0, cells are being transfected by means of Lipofectamine RNAiMAX. The transfection solution consists of two carefully prepared mixtures. The first mix includes a 1:1 ratio of the Donors sequences. Maintaining this 1:1 ratio is critical to ensure that both sequences are integrated into the genome in approximately equal amounts, thereby establishing a reliable reference point for the experiment. The second mixture comprises the gRNA incubated and complexed with the trans-activating CRISPR RNA (tracrRNA).

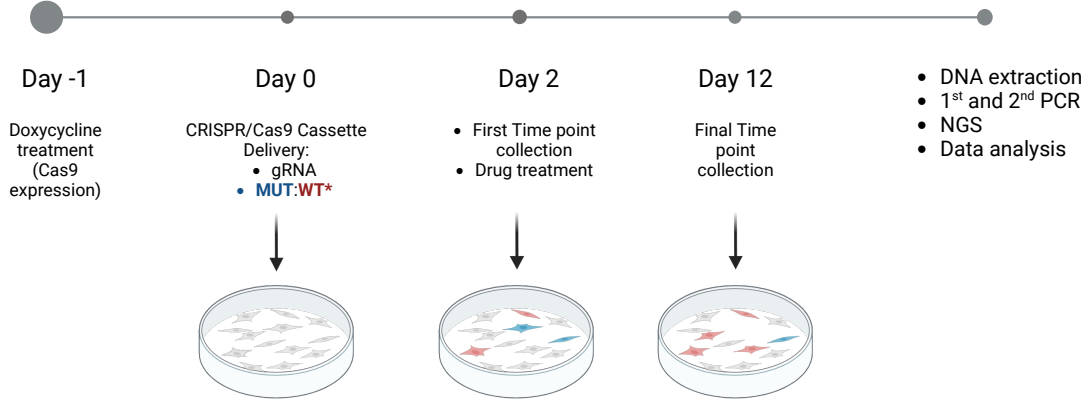


Figure 1.8: **CRISPR-Select<sup>TIME</sup> experiment.** Timeline illustration of the CRISPR-Select<sup>TIME</sup> experiment: On Day -1, iCas9-MCF10A cells are treated with doxycycline ( $1\mu\text{g}/\text{ml}$  to induce Cas9 expression. On Day 0, the CRISPR/Cas9 cassette is delivered into the cells using RNAiMax-Lipofectamine for transfection. The first key time point is Day 2, when half of the cells are trypsinized and collected. The remaining cells are reseeded and, when necessary, treated with drugs. On Day 12, all cells are collected for the final time point of the experiment. DNA is then extracted, and the region of interest is amplified through a two-step PCR process. The samples are subsequently prepared to create the final library for Next Generation Sequencing (NGS), followed by data analysis.

This complex formation is essential for accurately directing the Cas9 endonuclease to the specific genomic target, ensuring precise editing during the transfection process. The two mixes are then combined and delivered to the cells. As mentioned in section 1.1.1 and illustrated in Figure 1.2, different editing outcomes will be obtained and subsequently analyzed through NGS.

#### 1.1.4 Time-point collection and processing

To determine the variation of MUT:WT\* ratio over time, it is essential to collect samples at two specific time points following transfection. The first time point should be collected two days post-transfection, providing a baseline picture of the heterogeneous genomic status of the cells at Day 2, which serves as the reference point. The second time point should be collected 12 days post-transfection. The 10-day interval between these time points allows for a sufficient number of cell divisions, enabling the observation of how each mutation impacts cell proliferation and survival. To analyze the genomic changes, DNA will be extracted from the collected cells using the GenElute Mammalian Genomic DNA Miniprep Kit (Sigma). The gene of interest will then be amplified through the 1<sup>st</sup> PCR using primers that include specific adaptor sequences. These adaptors, unique to the forward and reverse primers, serve as a platform for the 2<sup>nd</sup> PCR step. In the 2<sup>nd</sup> PCR step,

unique barcodes are attached to the adaptor sequences of each sample’s primers, ensuring that each sample can be accurately identified and tracked throughout the subsequent analysis.

### 1.1.5 NGS data collection and analysis

Barcoded samples are sequenced through the MiSeq Illumina instrument according to the machine’s instructions. The results will be downloaded in FASTQ format. These data will be processed using the CRISPResso2 online tool using the default settings. The submitted data will produce a folder containing all the information for each sequence, and a web page summarizing all the information contained in the folder. The first histogram produced reports the alignment statistics of the run (Figure 1.9). In this case, an alignment percentage as close to 100% as possible is preferred.

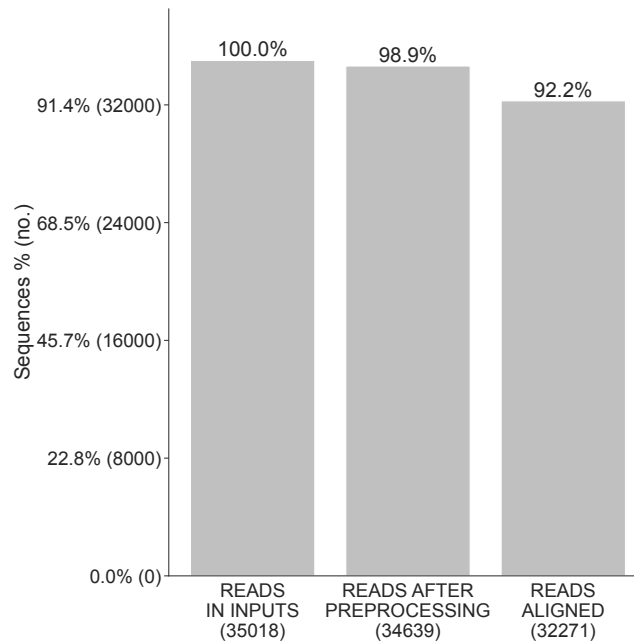


Figure 1.9: **Alignment statistics to the amplicons.** The number of reads in input FASTQ, after preprocessing, and after alignment to amplicons.

The second information from the analysis is an “Allele assignment” pie chart reporting the alignment and editing frequency of reads as determined by the percentage and number of sequence reads showing unmodified and modified alleles (Figure 1.10). A high percentage of modified reads is preferred as it reflects a good knock-in score. Another important pie chart is the one reflecting the Global frameshift analysis (Figure 1.11).

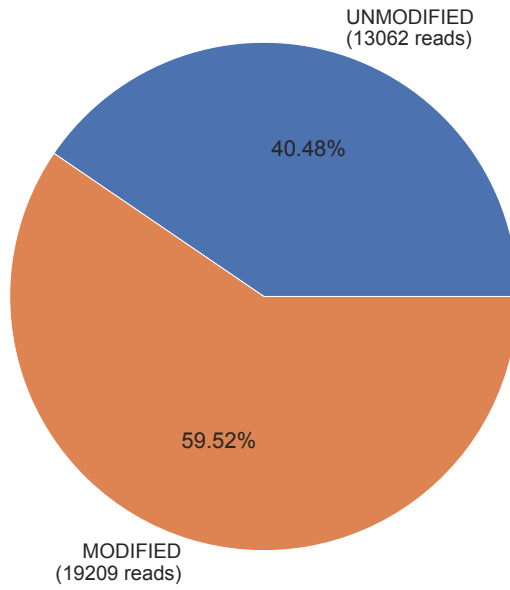


Figure 1.10: **Allele assignment.** Alignment and editing frequency of reads as determined by the percentage and number of sequence reads showing unmodified and modified alleles.

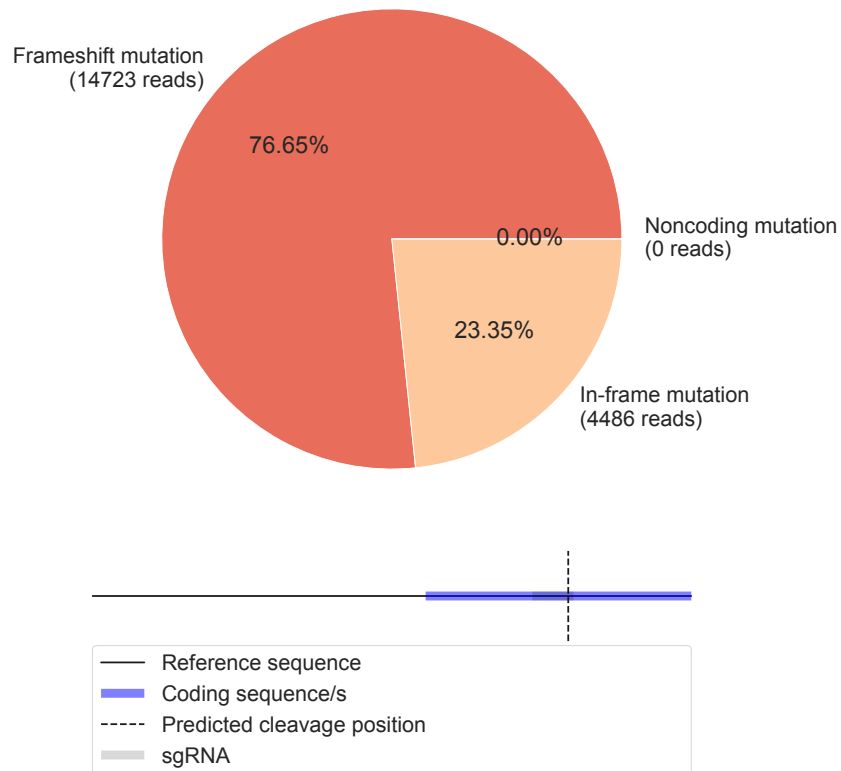


Figure 1.11: **Global frameshift analysis.** Frameshift analysis of coding sequence reads affected by modifications for all reads.

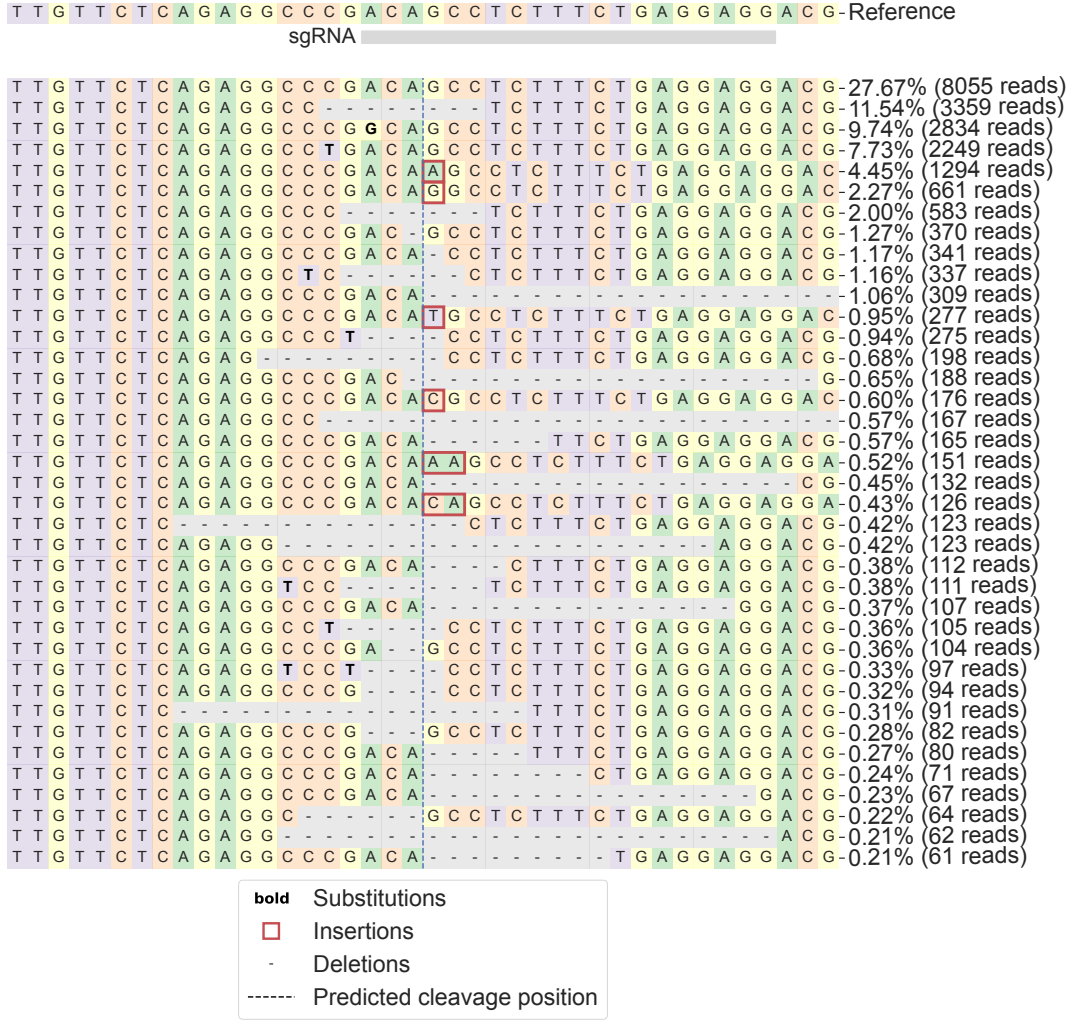


Figure 1.12: **Allele plot.** Visualization of the distribution of identified alleles around the cleavage site for the selected sgRNA. Nucleotides are indicated by unique colors (A = green; C = red; G = yellow; T = purple). Substitutions are shown in bold font. Red rectangles highlight inserted sequences. Horizontal dashed lines indicate deleted sequences. The vertical dashed line indicates the predicted cleavage site.

As discussed in section 1.1.2, the percentage of frameshift is expected to shift from high (day 2) to low (day 12) to ensure a good quality of the run and, therefore of the experiment. The final data of the analysis, is the Allele plot (Figure 1.12). An allele plot represents the sequences of detected alleles with a frequency greater than 0.20% using the gRNA as the reference sequence. The type of editing outcome of each allele is listed in the column preceding the sequences, with insertions and deletions indicated by (+) and (-), respectively. Within the sequences, mutations carried by the MUT and WT\* ssODN are highlighted in bold. Insertions are

marked by red boxes, while deletions are shown with dashed lines. The frequency percentage and the number of sequence reads for each allele are reported next to each sequence.

## 1.2 FANCA, FANCD2 and FANCM genes background

The FA pathway involves a series of complex steps involving approximately 27 different proteins, each playing a distinct role at various stages of the pathway [29]. To investigate the sensitivity of the FA pathway to the PARPi Talazoparib, this chapter focuses on the FANCA, FANCD2, and FANCM genes. These genes have been shown to enhance cell sensitivity to PARPi [157], and their involvement in different stages of the FA pathway allows for a comprehensive analysis of its key steps. The CRISPR-Select<sup>TIME</sup> method will be employed to assess the roles of these FA genes in cell proliferation, survival, and response to Talazoparib. This section will provide an overview of the three selected proteins, explaining the rationale behind their selection and the specific genomic variants to be studied.

### 1.2.1 FANCA

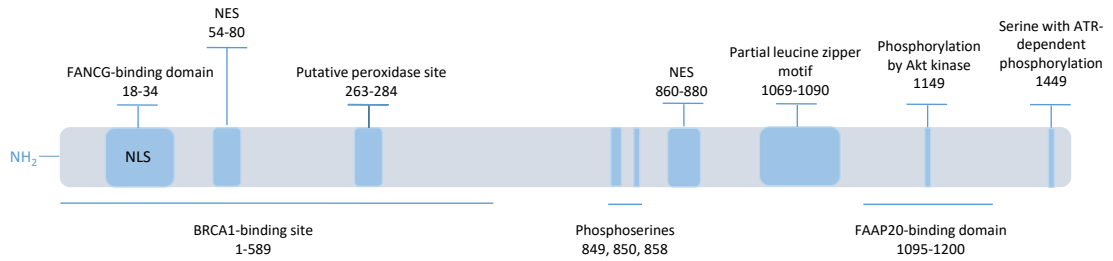


Figure 1.13: **FANCA gene, domains and sites.** A schematic representation of the FANCA protein highlights its known structural and functional domains. The amino-terminal region contains a nuclear localization signal (NLS) which overlaps with the FANCG binding site and the BRCA1 binding site. The carboxyl-terminal region features several critical sites, including a putative oxidase site, and a partial leucine zipper motif, followed by a FAAP binding site. This region includes a serine phosphorylation site at position 1149, targeted by Akt, and another serine phosphorylation site at position 1449, which is ATR-dependent. Nuclear export signals (NES) are distributed along the entire polypeptide chain.

The FANCA gene is involved in the core-complex formation of the pathway [31]. Deficiency of this gene has been correlated with genomic instability at stalled replication fork in human cells [29]. As reported in the introduction of this thesis,

FANCA forms also a sub-complex with FANCG to promote core complex localization and translocation within the nucleus<sup>1</sup>. FANCA silencing has been associated with cisplatin and PARPi sensitivity supporting the concept of SL involving FA proteins [11]. Altogether, these evidences supported the choice of this gene for the CRISPR-Select<sup>TIME</sup> analysis. When designing the specific mutation for this study, the domain structure of the FANCA gene was carefully considered (Figure 1.13). The chosen mutation needed to be positioned in a region that could potentially impair the protein's function without directly interfering with its interactions with other proteins. This approach ensures a controlled environment for studying the cellular effects of FANCA deficiency alone. For this reason, the ArgR880\* mutation was selected, classified as pathogenic according to the ClinVar database (<https://www.ncbi.nlm.nih.gov/clinvar/>).

### 1.2.2 FANCD2

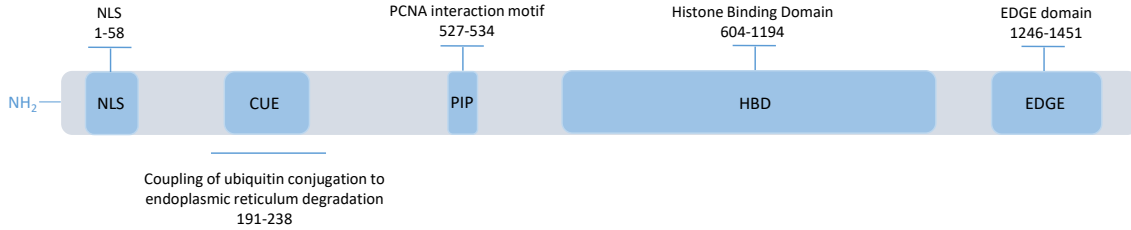


Figure 1.14: **FANCD2 gene domains.** FANCD2 has 5 domains that have been characterized: the C-terminal EDGE motif (necessary for complementation of the ICL sensitivity of FANCD2 patients cells); a histone binding domain important for chromatin binding and nuclear foci formation (H4K2me2); a highly conserved PIP motif (PCNA-interacting protein motif) for association of FANCD2 with PCNA and for FANCD2 monoubiquitination; an amino-terminal CUE (coupling of ubiquitin conjugation to endoplasmic reticulum degradation) domains (interaction with FANCI) and an N-terminal harbouring a NLS (Nuclear Localization Signal).

FANCD2 is the final effector of the FA pathway. Its monoubiquitination by the FA core-complex, together with the monoubiquitination of FANCI, forms the ID2 complex responsible for the endonucleases recruiting, which creates incisions in one DNA strand around the ICL site, unhooking the strands and generating a DSB that will then be repaired [11][42]. FANCD2 monoubiquitination is also involved in the maintenance of the genetically unstable common fragile sites (CFSs) and in replication fork stabilization [29]. Knockdown of FANCD2 in fibroblasts has been related to a PARPi sensitivity enhancement [148]. The gene structure of FANCD2 is reported in Figure 1.14. A K9\* mutation will be therefore introduced into the

FANCD2 gene. This early truncation mutation will result in a non-functional protein. The truncation is expected to disrupt both the transport and monoubiquitination of FANCD2, thereby obtaining a cell line with a defective FA pathway, which is crucial for studying the pathway's role in cell survival and PARPi resistance.

### 1.2.3 FANCM

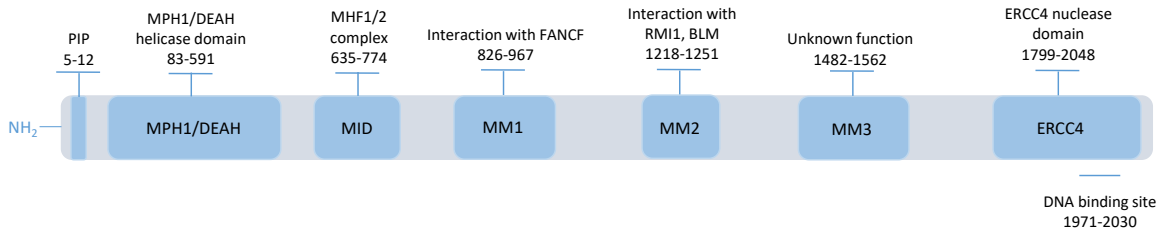


Figure 1.15: **FANCM gene domains.** FANCM consists of several distinct domains with specialized functions. The N-terminal PIP-box is responsible for interaction with proliferating cell nuclear antigen (PCNA). The DEAD/DEAH-motif provides ATPase activity essential for the protein's function. The MID-motif binds to the Major Use Histone Fold 1 and 2 (MHF1/2) heterotetramer. The MM1-motif facilitates interaction with FANCF within the FA core complex, while the MM2-motif connects with RecQ-Mediated Genome Instability protein 1 (RMI1), a part of the BTR complex alongside Bloom (BLM) and Topoisomerase IIIA (TOP3A). The ERCC4-motif is crucial for FANCM's heterodimerization with its obligatory partner, FAAP24 (Fanconi Anemia core complex-Associated Protein 24). The C-terminal HhH domain (amino acids 1971-2030) endows FANCM with DNA-binding capability. Additionally, FANCM includes the MM3 domain, whose function remains to be elucidated.

To summarize the FANCM roles, this protein shows ATPase and translocase activity. Specifically, the FANCM-FAAP24-MHF complex plays a critical role in recognizing various DNA structures, like an anchor that facilitates the recruitment and binding of the core-complex FA proteins to sites of ICLs [26][29]. The gene structure of FANCM is reported in Fig 1.15. The R658\* mutation located in the MHF motif of the gene has been selected. This region has been selected since mutations that affect either the combined DNA-binding surface or the protein-protein interactions within the MID-MHF complex result in compromised activation of the FA network and reduced genome stability [222].

## 1.3 Results

### 1.3.1 BRCA2 is a control gene for the CRISPR-Select<sup>TIME</sup> assay

To ensure the validity of the experiment, the well-characterized tumour suppressor gene BRCA2 was selected as a control. Two specific BRCA2 variants, D2723G and L2510P, were chosen based on their prior use by the developers of this technique [164]. The D2723G variant is a well-known loss-of-function (LOF) mutation that significantly impairs homologous recombination (HR)-mediated DNA repair, a critical process for cell proliferation. All the CRISPR-Select<sup>TIME</sup> data will be displayed in histograms which report the viability ratios of cells containing the MUT ssODN over the WT\* ssODN. As illustrated in Figure 1.16a, this variant leads to a marked decrease in cell survival by Day 12 of the assay, due to extensive cell death in those expressing the MUT ssODN. An essential metric for evaluating the efficacy of the gene-editing process is the knock-in (KI) efficiency, which represents the percentage of cells successfully edited to incorporate the variant of interest. Given the technique's high reproducibility and sensitivity, a threshold of 0.6% KI efficiency has been established. The D2723G variant exhibited a KI efficiency of 1.61%. In contrast, the L2510P variant induces a milder LOF effect on the BRCA2 gene (Figure 1.16a). This variant was selected for its moderate impact on cell survival by Day 12, which is crucial for evaluating the response of cells to drug treatment. Retaining a population of MUT-expressing cells throughout the experiment allows for an accurate assessment of the variant's drug response. Consequently, treatments with Cisplatin and Talazoparib were conducted. As reported in the introduction, Cisplatin was selected for its extensive use as an anticancer drug [223] while Talazoparib was chosen for its promising pharmacological profile with respect to the commonly used PARPi [78]. The results indicated that Cisplatin treatment led to a substantial reduction in cell survival, consistent with its known mechanism of action. Cisplatin forms interstrand and intrastrand DNA adducts that stall the DNA replication process and activate the DNA damage response [224]. This increases the mild BRCA2 deficiencies effect in the cells, impairing their ability to repair DNA and proliferate. On the other hand, Talazoparib treatment had a less pronounced but still significant effect on cell survival. This outcome aligns with the expected mechanism of Talazoparib as a PARPi, which traps PARP1 at single-stranded DNA lesions. Due to Talazoparib's high selectivity, it is less cytotoxic than Cisplatin, resulting in a more specific and less aggressive impact on cell survival. The observed effects are therefore more likely to reflect the variant's true response to the drug, regardless off-target toxicity. The KI efficiency for the L2510P variant is 6%.

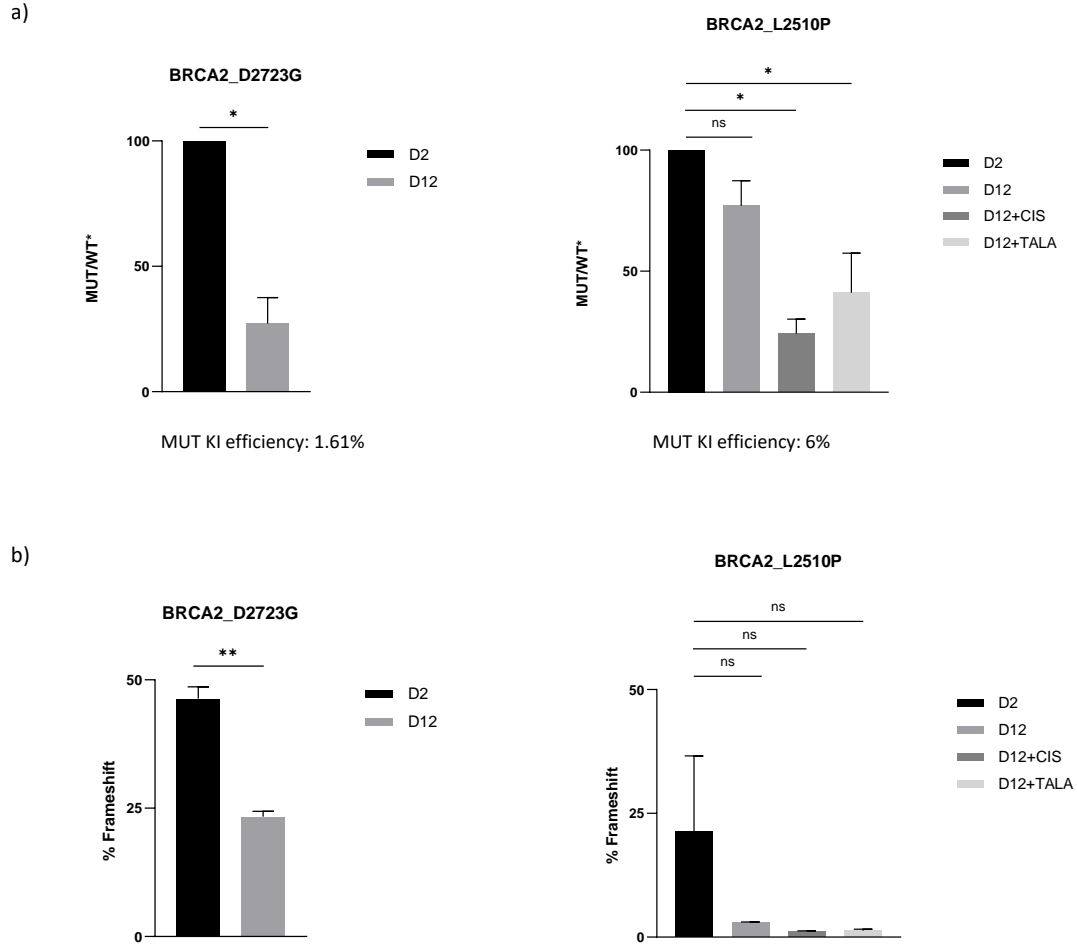


Figure 1.16: **BRCA2 control mutations.** CRISPR-Select<sup>TIME</sup> functional assay on BRCA2 variants D2723G and L2510P. The MUT:WT\* ratios were determined at the indicated day 2 and 12-time points with Cisplatin (CIS) (500nM) and Talazoparib (TALA) (2.5nM) treatment for BRCA2 L2510P variant only. The Day 12 time points are normalized to the respective Day 2 time points. Data are means  $\pm$  s.d. of  $n=3$  independent biological replicates and have been analyzed by two-tailed paired t-test \*( $P \leq 0.05$ ), \*\*( $P \leq 0.005$ ), ns= not significant ( $P \geq 0.05$ )

(a) MUT:WT\* ratios of BRCA2-D2723G (left) and L2510P (right) variants measured at D2 and D12 time points. Cisplatin and Talazoparib treatment are collected on Day 12. MUT Knock-in efficacies percentages are indicated below each histogram.

(b) Internal control of the experiment through measurement of the Frameshift percentage of BRCA2-D2723G (left) and L2510P (right) variants

The internal control for the experiment is represented by the Frameshift% (see Section 1.1.2) (Figure 1.16b). The Frameshift% data refers to the percentage of frameshift InDel mutations formed in one allele when the MUT or WT\* sequence

is present in the other allele. Ideally, a frameshift percentage of approximately 50% is anticipated, indicating that there is an equal likelihood of the MUT or WT\* sequence being present in the second allele. This balance is crucial for accurately assessing the internal control of the experiment. A decrease in the frameshift percentage over time, particularly from the D2 to D12 data points, is expected and would suggest that the non-functional protein resulting from the frameshift mutations is leading to cell death, especially if the targeted protein is essential for cell survival. Conversely, if the gene is not critical to cell viability, a reduction in frameshift percentage might be mild unless drug treatment is introduced, which could induce stress conditions. In this case, cells may activate compensatory survival pathways, highlighting the gene's role in response to drug-induced stress.

### **1.3.2 FANCA, FANCD2 and FANCM are synthetic lethal partners of the PARPi Talazoparib**

Given the validated efficacy of the CRISPR-Select<sup>TIME</sup> technique using BRCA2 control mutations, the Talazoparib response was assessed for the FA genes FANCA, FANCD2, and FANCM.

The CRISPR-Cassette was delivered to MCF10A-iCas9 cells for each pair of donor variants under investigation. The MUT:WT\* ratio at Day 2 was compared to the ratio at Day 12, with and without Cisplatin and Talazoparib treatments (Figure 1.17a). Notably, all tested mutations exhibited a mild decrease in MUT survival by Day 12, allowing for concurrent drug treatment analysis at this time point. As expected, Cisplatin treatment led to a more pronounced reduction in MUT survival over time compared to Talazoparib. Specifically, a 20% decrease in survival was observed after 12 days of Talazoparib treatment for the FANCA R880\* and FANCD2 K9\* mutations, while a 40% reduction was noted for the FANCM R658\* mutation. These results indicate that the mutations are not inherently toxic, as evidenced by the relatively modest decrease in MUT cell survival at Day 12. However, the findings also underscore that all tested mutations led to decreased cell fitness when exposed to Talazoparib. This data supports a synthetic lethal relationship between the tested mutations and Talazoparib, reinforcing previous studies that suggested this outcome. The reliability of these results is further proved by the frameshift percentages observed in the internal control analysis (Figure 1.17b).

### 1.3. RESULTS

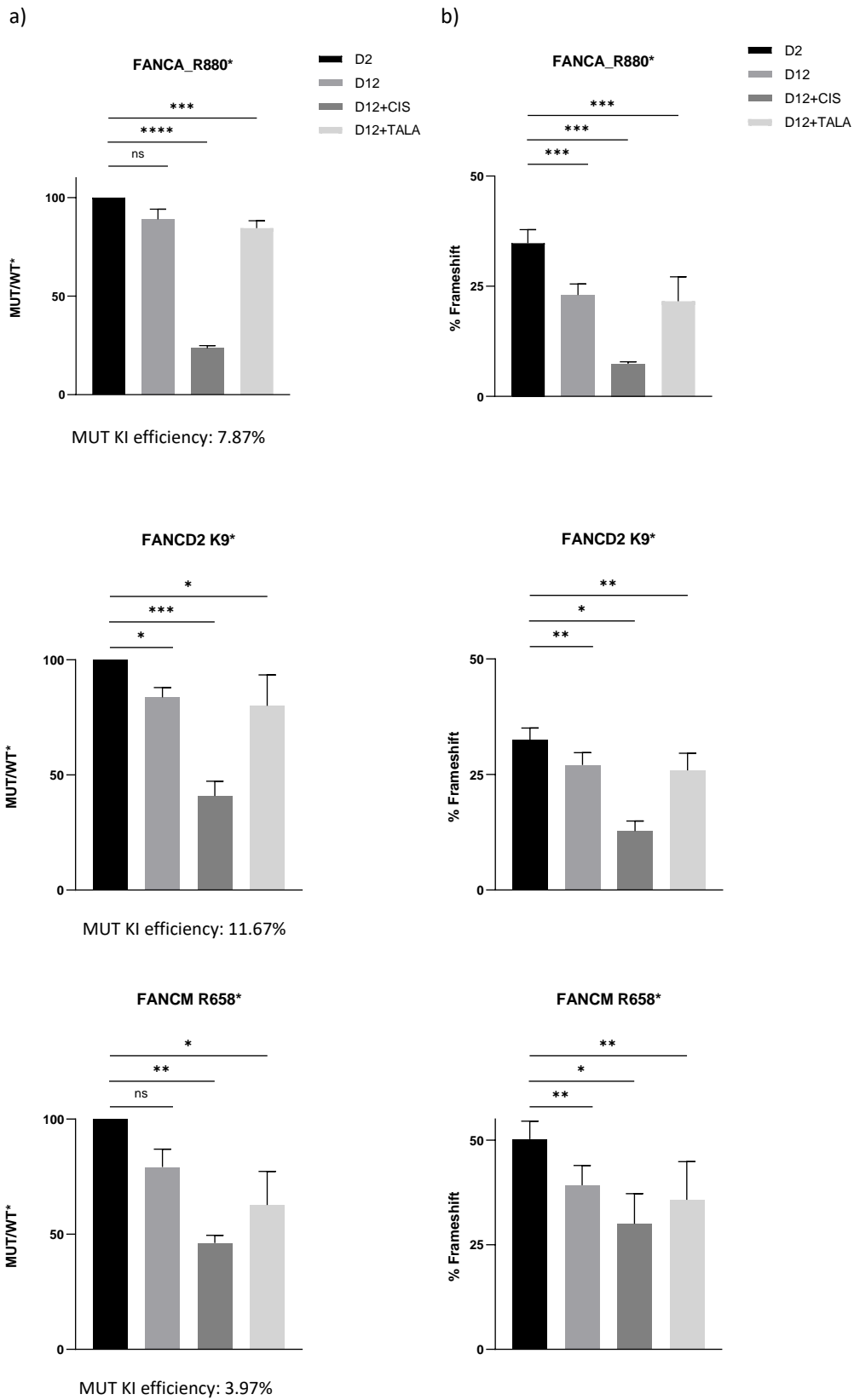


Figure 1.17 (*previous page*): **CRISPR-Select<sup>TIME</sup> and Fanconi Anemia genes.** CRISPR-Select<sup>TIME</sup> functional assay on FANCA R880\*, FANCD2 K9\* and FANCM R658\* variants. The MUT:WT\* ratios were determined at the indicated day 2 and 12 time points including Cisplatin (CIS) (500nM) and Talazoparib (TALA) (2.5nM) treatment. The Day 12 time points are normalized to the respective Day 2 time points. Data are means  $\pm$  s.d. of n=4 independent biological replicates and have been analyzed by two-tailed paired t-test \*( $P \leq 0.05$ ), \*\*( $P \leq 0.005$ ), \*\*\* ( $P \leq 0.0005$ ) \*\*\*\* ( $P \leq 0.00001$ ), ns= not significant ( $P \geq 0.05$ )

(a) MUT:WT\* ratios of FANCA-R880\* (top), FANCD2-K9\* L2510P (mid) and FANCM-R658\* (bottom) variants measured at D2 and D12 time points. Cisplatin and Talazoparib treatment are collected on Day 12. MUT Knock-in efficacies percentages are indicated below each histogram.

(b) Internal control of the experiment through measurement of the Frameshift percentage of FANCA-R880\* (top), FANCD2-K9\* L2510P (mid) and FANCM-R658\* (bottom) variants

## 1.4 Conclusions of Chapter 1

The CRISPR-Select<sup>TIME</sup> technique offers a highly sensitive and precise method for evaluating cell population survival over time. This is achieved through the delivery of a carefully designed CRISPR cassette to the target cells and the accurate detection of alleles via NGS. This powerful tool was used to assess the correlation between FANCA, FANCD2, and FANCM genes and their response to Cisplatin and Talazoparib. Cisplatin, a standard treatment for many DNA-repair-deficient tumors, was selected to evaluate survival responses to this treatment in the context of the tested mutations, taking into account the drug's inherent toxicity and side effects. Furthermore, Talazoparib, a PARPi with a promising pharmacological profile, characterized by effective PARP1 trapping and minimal off-target interactions, was used to explore the potential synthetic lethal partnerships with FANCA, FANCD2, and FANCM. The high editing efficiency of the selected mutations, combined with the robust quality of the frameshift percentage as an internal control, ensures that the results obtained are both reliable and reproducible. Previous valid studies have suggested a synthetic lethal relationship between these FA genes and Talazoparib, although they relied on less precise methods such as siRNA and RNAi [11] [148] [225]. The current approach, utilizing CRISPR-Select<sup>TIME</sup>, provides a more accurate validation, strengthening the idea that these FA genes could be viable synthetic lethal partners for PARPi treatments. This finding holds significant potential for stratifying patients for PARPi-based therapies and may have implications for adjusting treatment dosages. While these results are promising, further validation in models that better simulate in vivo conditions, such as organoids, is necessary. Nonetheless, these findings offer an optimistic perspective on the potential for new treatment strategies for patients with deficiencies in the FA pathway.

## Chapter 2

# Evaluation of the SL correlation between FANCC and Talazoparib in Pancreatic Cancer cell lines

### 2.1 Introduction

In the previous chapter, it was demonstrated that the FA genes FANCA, FANCD2, and FANCM contribute to sensitivity to the PARPi Talazoparib. This conclusion was reached using the advanced and precise CRISPR-Select<sup>TIME</sup> method in iCas9 MCF10A cells. These cells, being an immortalized normal diploid cell line, were selected to validate the concept. The normality of the cell line is advantageous as it minimizes potential side effects due to impaired cellular functions and genome alterations. Furthermore, the CRISPR-Select technique performs optimally in diploid cell lines due to its mechanism of action: introducing DNA cuts to create diverse editing outcomes across the two alleles, ideally resulting in an Out-of-Frame/InDel mutation in one allele and the mutation of interest in the other allele, thereby generating a built-in loss of heterozygosity. Achieving this specific scenario becomes challenging in cell lines with more than two alleles, where the increased number of potential editing outcomes reduces the overall efficiency of the technique. Consequently, while CRISPR-Select remains a robust and precise method, its optimal performance is better observed in normal diploid cell lines. These considerations present a challenge for validating results in a PC model, which is the aim of this part of the study. PC cell lines are often aneuploid and, therefore, unsuitable for the CRISPR-Select<sup>TIME</sup> assay. To address this issue, the commercially available PANC 03.27 cell line, a PDAC cell line already defective in the FANCC gene, was identified and used. This cell line provided a suitable platform for testing Talazoparib sensitivity in a model with an inherently deficient FA pathway.

### 2.1.1 FANCC protein Background

To investigate the correlation between FA pathway deficiency and Talazoparib sensitivity in a PC model, a suitable cell line was required. The commercially available PDAC cell line PANC 03.27 was identified as the most appropriate for this study. This cell line harbors a truncated form of the FANCC protein, expressing only six out of the 14 exons of the gene, making it an ideal model for examining the impact of FANCC deficiency on Talazoparib sensitivity in a PC context (Figure 2.1).

The FANCC protein is an integral component of the core complex of the FA pathway [31]. Specifically, FANCC forms a sub-complex with FANCE and FANCF, which serves as a critical bridge between FANCD2 and FANCM, facilitating the recognition and resolution of interstrand crosslinks (ICLs) in DNA [148]. Deficiency in FANCC has been shown to increase sensitivity to PARPi treatments and crosslinking agents such as mitomycin C (MMC) [149]. LOH in FANCC or FANCG is also associated with early-onset PC [29][31].

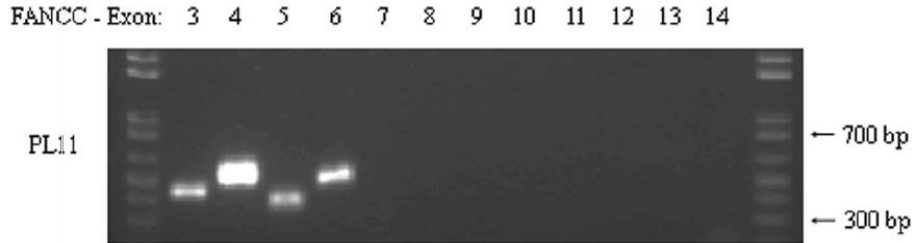


Figure 2.1: **FANCC exons in PANC 03.27 cells.** Evaluation of the exons expression of FANCC through PCR in PANC 03.27 cells (here indicated as PL11). This picture was taken from [142]

Examination of the UCSC Genome Browser (<https://genome.ucsc.edu/>) confirmed that no isoforms of the FANCC protein exist that are functional and include only the first six exons that only include the first six exons are functional (Figure 2.2). This observation further supports the selection of PANC 03.27 as a FANCC-deficient model, indicative of a defective FA pathway.

## 2.1. INTRODUCTION

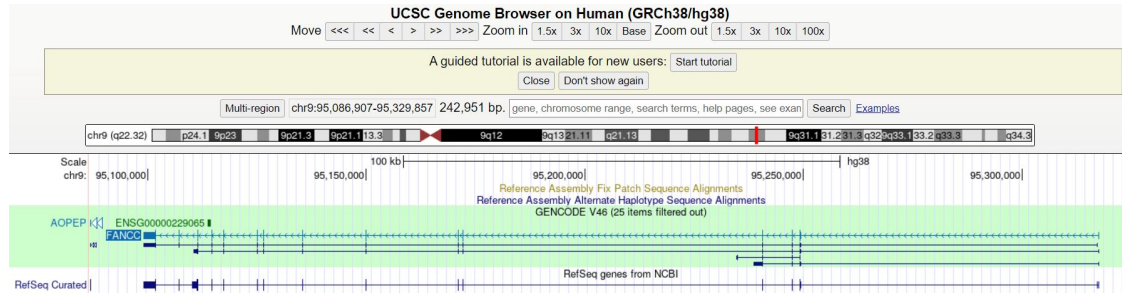


Figure 2.2: **UCSC data for FANCC isoforms expression.** Visual representation of the FANCC gene and its isoforms. The complete gene is depicted as a blue line, with arrows indicating the introns and lines representing the exons. The violet lines highlight the various gene isoforms (3).

## 2.2 Results

### 2.2.1 FANCC deficiency sensitizes cells to the PARPi Talazoparib in a PDAC cell model

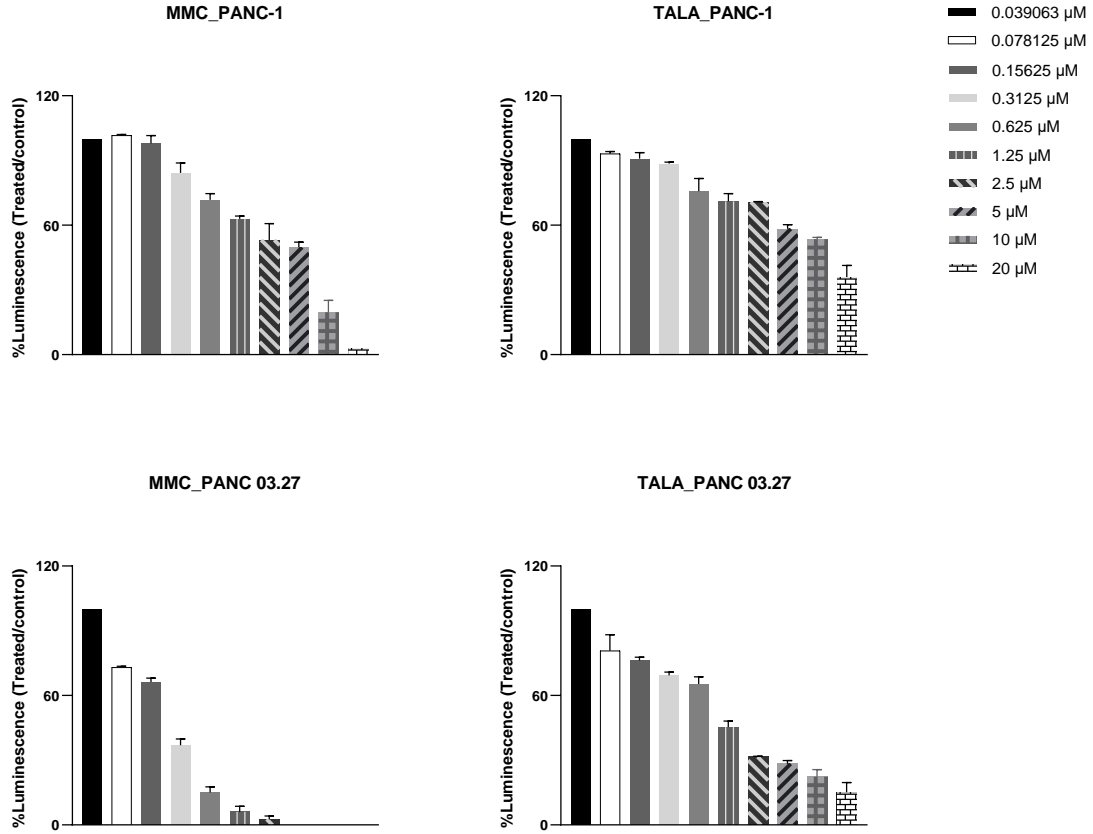


Figure 2.3: **Dose response curve for MMC and Talazoparib in PANC-1 and PANC 03.27 cells.** PANC-1 (top) and PANC 03.27 (bottom) cells treatment for 72h with Mytomicin C (MMC) and Talazoparib (TALA).

To establish an appropriate reference model for this study, the PC cell line PANC-1 was selected. This cell line has a functional FA pathway, making it suitable for comparing the role of FANCC in PARPi response between PANC 03.27 and PANC-1 cells. A cell viability assay was conducted to test this hypothesis (see Materials and Methods for details). The aim of this assay was to compare the survival rates of PANC 03.27 cells with those of PANC-1 cells under different treatment conditions. The first condition involved treatment with Mitomycin C (MMC), a crosslinking agent that induces interstrand crosslink (ICL) formation, thereby activating the FA repair pathway [192][17].

In a FANCC-deficient cell line, such treatment is expected to result in a significant reduction in cell viability compared to a cell line with an intact FA pathway. This outcome would serve to validate the experimental design and confirm the selection of the PANC-1 cell line as a control. In addition to MMC, Talazoparib treatment was also included in this evaluation. The primary goal of this treatment was to assess whether a Talazoparib-treated cell line, deficient in FANCC and consequently in the FA pathway, exhibits increased sensitivity to Talazoparib compared to PANC-1 cells with a functional FA pathway. A first dose-response curve was obtained to select the proper drug concentration for the cell treatment (Figure 2.3).

The cell viability assay was therefore performed, comparing non-treated cells survival with the treated ones with either MMC or Talazoparib. The results are displayed in Figure 2.4.

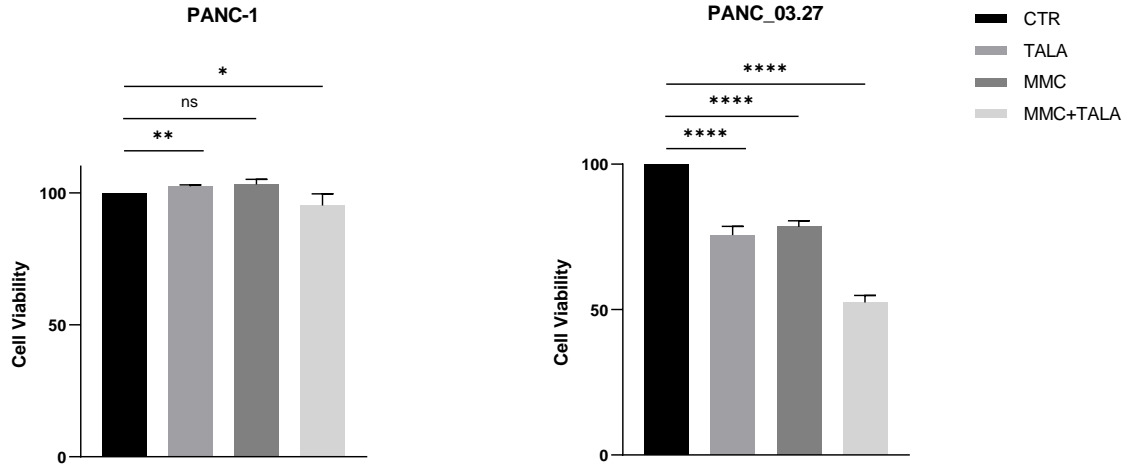


Figure 2.4: **Cell Viability Assay for FANCC.** PANC-1 (left) and PANC 03.27 (right) cells were both treated with  $0.8\mu\text{M}$  Mytomicin C (MMC) for 1 hour where indicated. This treatment was necessary to induce an ICL formation and, therefore, the activation of the FA pathway. Talazoparib (TALA) treatment was performed using  $0.8\mu\text{M}$  TALA for 72h. At the end of the assay, cell viability was measured using the Cell-TiterGlo kit. Data are means  $\pm$ s.d. of  $n=3$  independent biological replicates and have been analyzed by two-tailed paired t-test  $^*(P\leq 0.05)$ ,  $^{**}(P\leq 0.005)$ ,  $^{****}(P\leq 0.00001)$ , ns= not significant ( $P\geq 0.05$ )

As expected, no significant reduction in cell viability was observed in PANC-1 cells under any treatment condition. In contrast, a marked decrease in viability was detected in PANC 03.27 cells across all treatment conditions. These findings are particularly reliable, given the low drug concentrations used to separate the drug-specific effects from aspecific toxicity. Notably, a 25% reduction in viability was observed with Talazoparib treatment, a 22% reduction with Mitomycin C (MMC),

and a 50% reduction with the combined treatment of both drugs. The 25% viability reduction with Talazoparib treatment indicates that FANCC-deficient cells are indeed sensitive to PARP inhibition. The 22% reduction with MMC treatment suggests that interstrand crosslink (ICL)-induced DNA damage is more challenging to repair in FANCC-deficient cells. Finally, the significant 50% reduction in viability with combined Talazoparib and MMC treatment highlight the combined effects of ICL DNA damage and inhibited single-strand break (SSB) repair, enhanced by FANCC deficiency. These cumulative factors lead to a pronounced deficiency in DNA repair mechanisms, resulting in an increased cell death percentage. These crucial findings are consistent with those from the previous chapter, which demonstrated the sensitivity of FANCA, FANCD2, and FANCM deficiencies to Talazoparib. Together, these results strengthen the evidence for a correlation between FA pathway deficiencies and Talazoparib sensitivity, extending this relationship to FANCC gene in PC too.

### **2.2.2 FANCC-Mediated Talazoparib Sensitivity is associated with DNA Damage cell accumulation**

The obtained results suggest that the combined impairment of SSB repair by Talazoparib treatment and the FA pathway-mediated DNA repair leads to increased cell death. This finding prompted further investigation to define whether this outcome is due to the accumulation of DNA damage in cells that are unable to properly repair their DNA. To test this hypothesis, a Western blot analysis was conducted to assess the levels of  $\gamma$ H2AX phosphorylation in cells. The phosphorylation of H2AX at Ser-139 is an early marker of cellular response DSBs and is widely used as an indicator of DSB initiation, accumulation, and resolution [226]. The Western blot was performed on cells treated with MMC and Talazoparib, using the same incubation times and drug concentrations as described in the previous section (Section 2.3.1). Both PANC-1 and PANC 03.27 cells were analyzed under these conditions. The results shown in Figure 2.5 highlight a clear difference in  $\gamma$ H2AX expression between PANC-1 and PANC 03.27 cells under the various treatment conditions. In PANC-1 cells, no significant increase in  $\gamma$ H2AX levels was observed, regardless of the treatment applied. However, a different outcome was seen in PANC 03.27 cells, where treatment with MMC and Talazoparib led to an increase in  $\gamma$ H2AX levels, indicating a compromised DNA repair process and subsequent accumulation of DSBs. The combined treatment, as expected, exhibited a stronger effect, likely due to the simultaneous inhibition of both the SSB repair and FA pathways in these cells. Collectively, these findings support the hypothesis that Talazoparib treatment is more effective in FANCC-deficient PC cells, primarily due to the accumulation of DNA damage and the resultant impairment in DNA repair mechanisms.

## 2.2. RESULTS

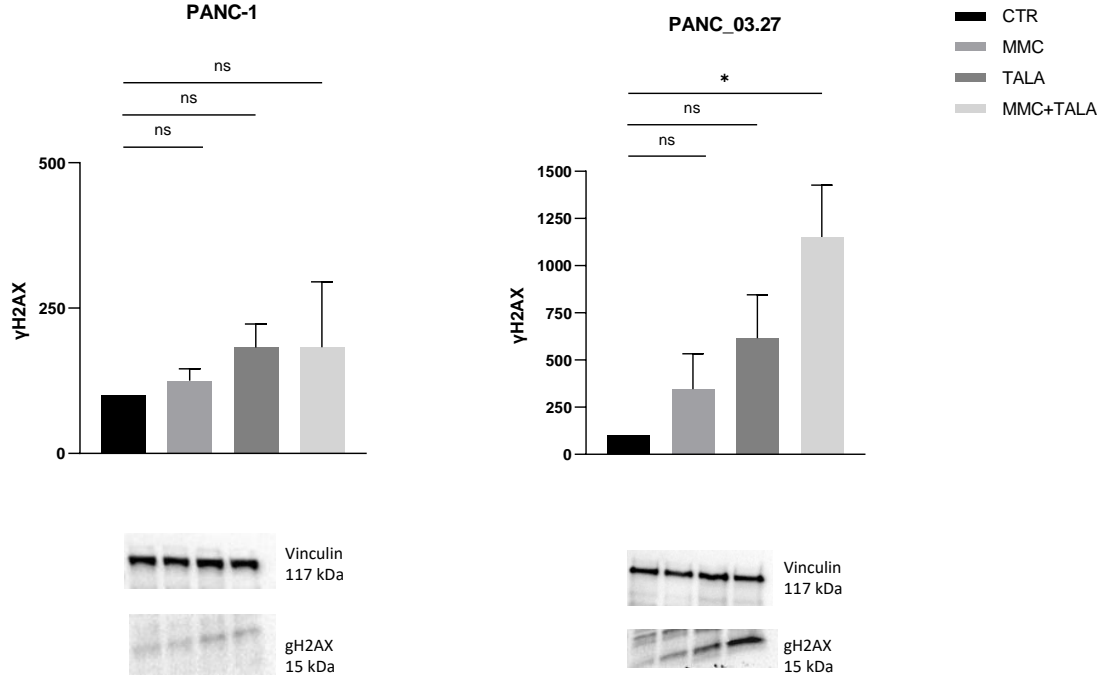


Figure 2.5: **Western Blot for  $\gamma$ H2AX expression levels.** PANC-1 (left) and PANC 03.27 (right) cells were both treated with  $0.8\mu\text{M}$  Mytomicin C (MMC) for 1 hour where indicated. This treatment was necessary to induce an ICL formation and, therefore, the activation of the FA pathway. Talazoparib (TALA) treatment was performed using  $0.8\mu\text{M}$  TALA for 72h. At the end of the treatment,  $\gamma$ H2AX levels were measured by means of Western Blot test. Data are means  $\pm$ s.d. of  $n=3$  independent biological replicates and have been analyzed by two-tailed paired t-test  $*(P \leq 0.05)$ , ns= not significant ( $P \geq 0.05$ )

## 2.3 Conclusions of Chapter 2

These findings underscore the complexity and significance of the FA pathway in cancer biology, particularly in the context of PC. The demonstrated sensitivity of PC cells to FA pathway deficiencies and Talazoparib treatment highlights the potential therapeutic implications of targeting this pathway. Currently, PARPi drugs like Olaparib are employed in the maintenance treatment of metastatic PC patients harboring BRCA1/2 mutations. Talazoparib has shown similar promise in this context [78][227][93]. However, a significant challenge remains, as patients often develop resistance to PARPi treatment through various mechanisms, such as the restoration of HR, stabilization of replication forks, and the emergence of peripheral neurotoxicity. Given these challenges, there is an urgent need to refine and improve therapeutic strategies for these patients. The results presented in this chapter suggest that subtyping PC patients based on FA pathway deficiencies could offer a new avenue for targeted treatment. Specifically, patients with defects in the FA pathway might benefit from PARPi therapy, expanding the potential patient population for this treatment approach. However, it is important to recognize that these findings are preliminary and focused solely on FANCC, one gene within the broader FA pathway. To develop a more comprehensive and clinically applicable hypothesis, it will be necessary to investigate the role of all FA genes in PARPi sensitivity and to establish more robust and representative cell models. The PANC 03.27 cell line, while useful for proving the concept in this study, is limited by its existing defect in FANCC, making it unsuitable for exploring other genes of the pathway. As a result, the following chapter will explore alternative methods and models to further elucidate the importance of the FA pathway in and its potential as a therapeutic target.

# Chapter 3

## Development of a cancer cell model to investigate the relationship between FA gene deficiency and Talazoparib effects

### 3.1 Introduction

In the previous chapters, the FANCA, FANCC, FANCD2, and FANCM genes were found to enhance sensitivity to Talazoparib, a critical discovery in understanding the relationship between the FA pathway and cancer treatment. This result was achieved using the advanced CRISPR-Select<sup>TIME</sup> technique for FANCA, FANCD2, and FANCM, and through studies on FANCC in PANC 03.27 cell lines. These results provide a strong foundation for an exploration of the connection between the FA pathway and Talazoparib sensitivity, with the goal of developing methods to study additional FA proteins.

Given the limitations of the CRISPR-Select<sup>TIME</sup> technique, which were discussed in Chapter 1, an alternative method is needed for further investigation. The focus of this chapter is, therefore, on establishing a precise, effective, and reproducible method to study the FA pathway's correlation with Talazoparib sensitivity with a strong focus on PC. The CRISPR-interference (CRISPRi) tool was selected as the most appropriate technique for this research and HeLa cells have been chosen as the model system. HeLa cells are widely used in the study of DNA repair pathways and, despite being a cancer cell line, they have an efficient DNA repair system [212][228][229][230]. The BxPC3 and Capan-1 PC cell lines have been selected to compare the FA pathway perturbation effect in a BRCA2-proficient (BxPC3) and BRCA2-deficient (Capan-1) cell model, therefore representing the two different subsets of PC patients of which this work is focused on. This approach will support the

continued exploration of the FA pathway and its potential as a therapeutic target in cancer treatment. Given the promising results obtained in PANC 03.27 cells (see Chapter 2) followed by studies on the FANCD2 gene, the FANCC gene will be first investigated to compare the findings obtained through the CRISPR-Select<sup>TIME</sup> technique. This comparison aims to evaluate whether the CRISPRi method effectively confirms the results previously obtained. By doing so, the chapter will assess the reliability and consistency of CRISPRi as a platform for FA genes study in PC cells.

## 3.2 CRISPR-interference

### 3.2.1 Overview of the CRISPR-interference

CRISPR-interference (CRISPRi) is a powerful and precise gene silencing tool derived from the CRISPR/Cas9 system [171]. Unlike the canonical CRISPR/Cas9 technique, which relies on creating double-strand breaks (DSBs) into a specific DNA site, CRISPRi employs a catalytically inactive form of Cas9 (dCas9). This modified enzyme retains its ability to bind DNA at a target site guided by a single guide RNA (sgRNA) but lacks the nuclease activity required for DNA cleavage. The dCas9 is fused to transcriptional repressors, such as KRAB (Krüppel-associated box), leading to the suppression of a gene expression by blocking the transcriptional machinery, at the promoter or within the coding region thereby inhibiting gene transcription without altering the DNA sequence [170] (Figure 3.1). This tool avoids the off-target effects that can arise from the DNA-cutting step in the canonical CRISPR/Cas9 system.

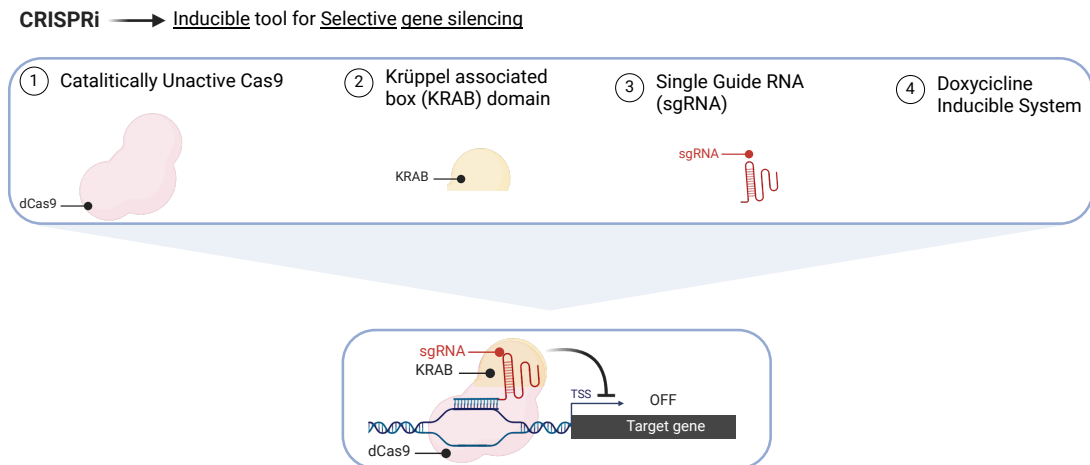


Figure 3.1: **CRISPRi components.** The CRISPRi tool is made of a catalytically inactive Cas9 (1) which is fused with a transcription repressive domain as the KRAB domain (2). The system is guided into the specific gene locus through the gRNA (3). The expression of the Cas9 is induced by treatment with Doxycycline (4). Altogether, this system lead to the transcription repression of the gene of interest.

One of the key advantages of CRISPRi is its ability to modulate gene expression reversibly and with high specificity. This makes it particularly valuable in the study of FA genes, where a complete knockout may lead to severe cellular phenotypes or even cell death. By fine-tuning the level of gene expression, CRISPRi enables the study of partial gene function and dosage effects, which are often critical in understanding the complex biology of FA proteins. Moreover, CRISPRi is a versatile

and scalable approach, well-suited for high-throughput screening of multiple genes within the FA pathway. This capability is particularly useful for identifying potential therapeutic targets and for exploring the broader network of gene interactions that influence sensitivity to PARPi. In this context, CRISPRi provides a powerful tool for elucidating the functional roles of FA genes in cancer biology and for advancing the development of targeted therapies.

### 3.2.2 sgRNA design

To effectively design sgRNAs for targeting FANCD2 and FANCC in CRISPRi experiments, two key resources were utilized. The first resource was an already published table of designed sgRNAs for the CRISPRi tool [231]. This table provides a list of 10 sgRNAs for each gene, categorized into "Top 5" and "Bottom 5" selections to distinguish the highest-performing sgRNAs from those with moderate efficacy. The critical metrics considered from this table were the Predicted Score and the Empirical Score. The Predicted Score is generated by an algorithm that predicts the efficacy of sgRNAs for targeting nuclease-dead Cas9 in CRISPRi. The Empirical Score, on the other hand, derives from experimental data, reflecting the actual performance of the sgRNAs. Higher scores in both categories indicate better sgRNA performance. The second resource used was the CRISPick tool, available at the Broad Institute's portal (<https://portals.broadinstitute.org/gppx/crispick/public>). CRISPick ranks and selects candidate CRISPRi sgRNA sequences based on their predicted on-target activity while minimizing off-target effects. To use this tool, the Reference Genome (Human GRCh38), the mechanism (CRISPRi), and the enzyme (typically SpyoCas9, which recognizes the NGG PAM sequence) were selected (Figure 3.2).

Figure 3.2: **CRISPick website, general settings.** On CRISPR-ick website is possible to select the reference genome (e.g. Human GRCh38) and the Mechanism under analysis, whether CRISPRko, CRISPRi or CRISPRa. Finally, it is possible to select the enzyme to work with (e.g. SpyoCas9).

**Target(s)**

☒ Quick gene lookup
 ☐ Bulk/Advanced targets
 ☐ Upload file

FANCD2 × ✓✕ Copy IDs

*Accepted target formats*

ID	Sequence	Coordinates
<b>Gene Symbol</b> ⓘ CDC5L, Brca1	<b>Raw</b> ⓘ TTGTAGCATCGCAGGTAGCAACAGTTACTAGG	<b>Point</b> ⓘ NC_000001.11:+127140001
<b>Gene ID</b> ⓘ 988	<b>FASTA</b> ⓘ >seq0	<b>Range</b> ⓘ NC_000001.11:-15000-16000
<b>Transcript ID</b> ⓘ NM_014911, NM_014911.1	TTGTAGCATCGCAGGTAGCAACAGTTACTAGG	<b>Ranges</b> ⓘ NC_000001.11:-12000-13000;15000-16000

☐ Library Mode <sup>NEW</sup> ⓘ

**CRISPick Quota** ⓘ

10 This tool will recommend the top N candidates according to:

- Raw ranking
- Cut position
- Mutual spacing

Figure 3.3: **CRISPick website, sgRNA selection.** The CRISPRick website allows to select the gene of interest (e.g. FANCD2) and to select the number of sgRNA to be designed (e.g. 10) in the CRISPRick quota box.

The target gene (e.g., FANCD2) and the desired output (e.g., 10 sgRNAs) were specified, followed by the data submission (Figure 3.3). The output includes two text files, being the Picking Summary file the most important one, as it contains scores and values for each sgRNA.

The key metrics considered for the final sgRNA selection were 1) CFD Score: This score represents the Cutting Frequency Determination, which calculates the potential off-target effects; 2) DHS Score: it refers to DNA hypersensitivity, indicating regions with high accessibility. A score closer to 1 is preferable; 3) On-Target Score: it measures the sgRNA's effectiveness relative to others targeting the same gene. A higher score, close to 1, indicates better performance.

The sgRNAs suggested by CRISPick were then compared with those from the published table. Preference was given to sgRNAs from the published table, especially if they had empirical scores. sgRNAs from CRISPick were selected when they targeted different regions of the gene to avoid redundancy and to explore a broader range of gene regions. Matching sgRNAs between the two sources were also prioritized. Ultimately, the sgRNAs with the best overall scores from both sources were selected. At least five sgRNAs, distributed across the gene sequence, were chosen for each gene to ensure adequate gene coverage. To map the sgRNA sequences onto the gene, the Benchling platform (<https://www.benchling.com/>) was used.

### 3.3 Results

#### 3.3.1 KRAB cell line generation

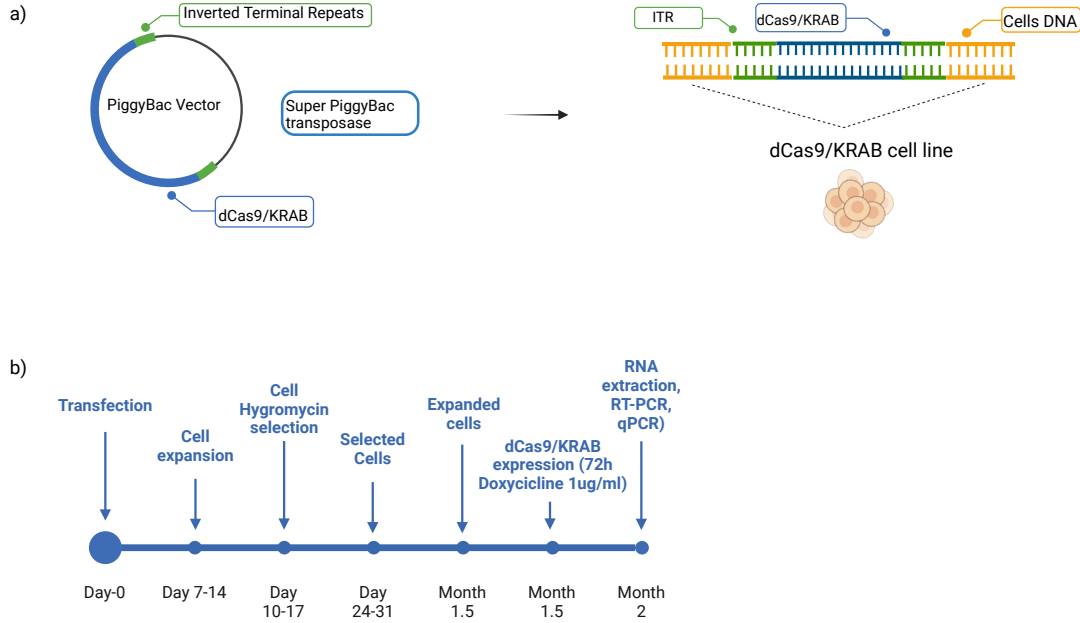


Figure 3.4: dCas9/KRAB cell line generation.

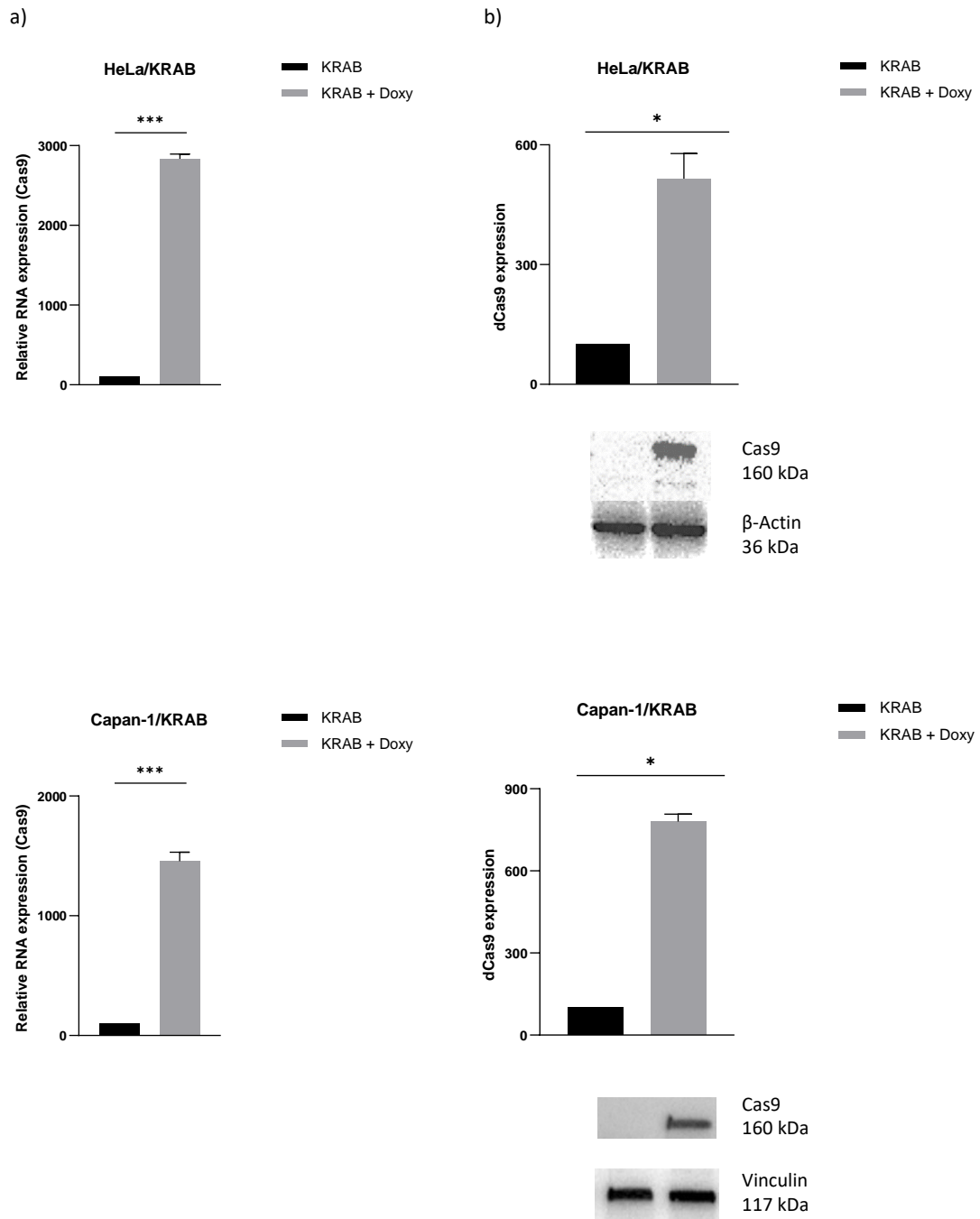
(a) Schematic representation of the PiggyBac Transposon system. It is possible to observe how the sequence of interest (dCas9/KRAB) and the ITR sequences are integrated into the genome

(b) Time Line for a complete dCas9/KRAB integration into cell DNA and validation through qPCR

HeLa cells and Capan-1 cells were transposed using a doxycycline-inducible dCas9/KRAB sequence by means of a PiggyBac (PB) transposon system. The PB transposon system utilizes a modified transposase enzyme to integrate a gene into a cell's genome. This system is composed of a PiggyBac Vector and the Super PiggyBac Transposase. The transposase recognizes specific Inverted Terminal Repeats (ITRs) within the transposon and efficiently inserts the ITRs along with the intervening DNA into the genome at TTAA sites. The Super PiggyBac Transposase is introduced into the cell through the Super PiggyBac Transposase Expression Vector, which is co-transfected with one or more PiggyBac Vectors (Figure 3.4a). In this experiment, a single PiggyBac vector was used to integrate the dCas9/KRAB sequence into the cells genome. The vector was designed with a Hygromycin resistance gene and a Doxycycline-inducible dCas9/KRAB sequence. Cells were transfected with the complete transposon system and allowed to proliferate for 1-2 weeks.

After this period, transposed cells were selected using 100  $\mu\text{g}/\text{ml}$  of Hygromycin-B, and the surviving cells were expanded. The expression of dCas9/KRAB was then induced by treating the cells with 1  $\mu\text{g}/\text{ml}$  of Doxycycline, and the gene expression level was quantified using qPCR. Figure 3.4.b illustrates the timeline and key steps involved in this transfection process. As anticipated, Doxycycline treated cells were then collected, and the dCas9/ KRAB levels were evaluated by qPCR (Figure 3.5a) and by WB (Figure 3.5b). These experiments proved that the cells have been correctly transposed and that they were suitable for the next steps.

### 3.3. RESULTS



**dCas9/KRRAB expression.** HeLa/KRAB cells and Capan-1/KRAB have been treated with 1 $\mu$ g/ml Doxycycline for 72h. After this incubation time, the dCas9/KRAB expression was measured at mRNA and protein level. Data are means  $\pm$ s.d. of n=3 independent biological replicates and have been analyzed by two-tailed unpaired t-test \*( $P \leq 0.05$ ), \*\*\*( $P \leq 0.0005$ ).

(a) qPCR for dCas9/KRAB mRNA. The relative expression of the gene is measured against the RPLPO gene expression

(b) Western Blot analysis for dCas9/KRAB protein expression. Proteins were extracted using RIPA buffer and 20  $\mu$ g of proteins were loaded

### 3.3.2 Stable sgRNA-expressing cells

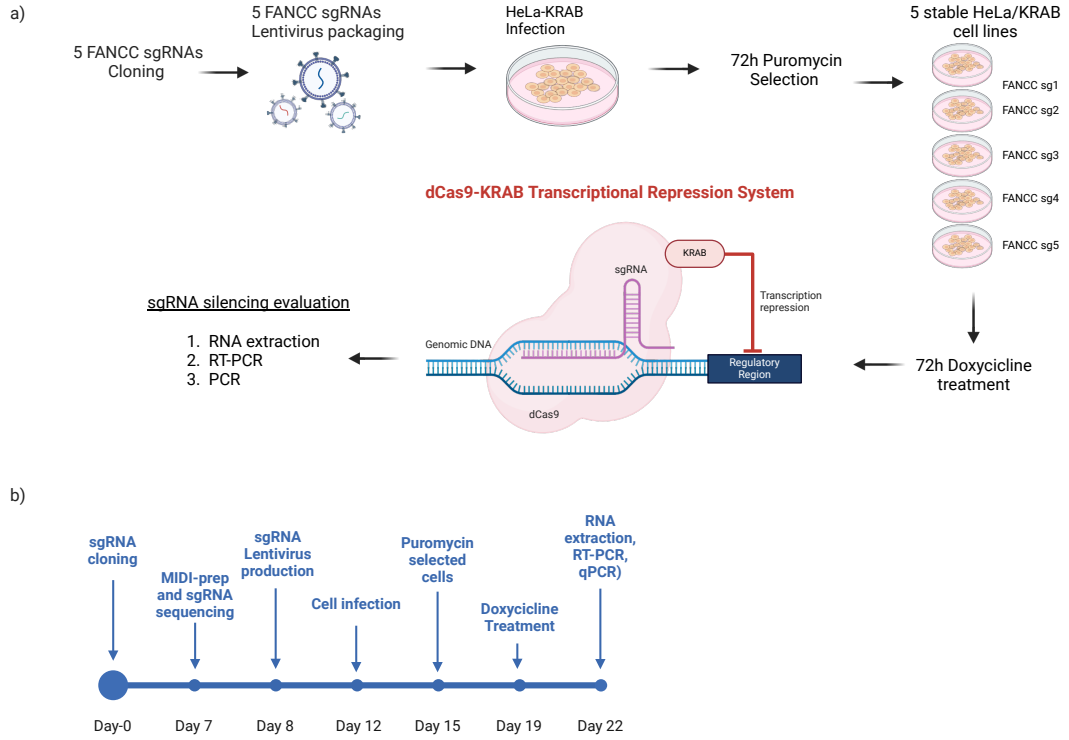


Figure 3.6: **Stable sgRNA-expressing cells generation.** All the main steps for a stable-expressing sgRNA cell line generation are reported here.

(a) The FANCC sgRNA are cloned and packed in lentiviral particles. Cells are then infected and selected by means of Puromycin (2 $\mu$ g/ml) for 72h. Stable sgRNA-expressing cell lines are obtained. Upon Doxycycline treatment, the Cas9/KRAB is expressed and gene silencing is obtained. The efficacy of the gene silencing is then evaluated through qPCR.

(b) Time Line for complete cloning and transfection of sgRNA into dCas9/KRAB cells

After generating the cell line expressing dCas9/KRAB upon Doxycycline induction, the next step was to clone the selected sgRNAs into these cells to create a stable sgRNA-expressing cell line. This allowed for the functional testing of

the selected sgRNAs within the cell line. To achieve this, each sgRNA was first cloned into a LentiGuide Puro plasmid (refer to Materials and Methods, section 4.5.3). The cloned sgRNA was then co-transfected into HEK293T cells along with viral packaging components to produce viral particles containing the sgRNA sequence. These viral particles were subsequently used to infect the KRAB cells in a fourth-generation lentiviral system, followed by selection using Puromycin. This process resulted in a stable cell line expressing the sgRNA of interest. At this point, Doxycycline was used to induce the expression of the dCas9/KRAB protein. The dCas9/KRAB complex was then guided to the specific genomic site by the specific sgRNA expressed in the cells, enabling targeted gene silencing. To verify the effectiveness of the gene silencing, mRNA was extracted from the cells, and qPCR analysis was performed. In Figure 3.6 is possible to appreciate the critical steps involved in generating a stable sgRNA-expressing cell line.

It is important to notice that KRAB cells stably expressing a non-targeting (NT) sgRNA were also produced as a control. This NT sgRNA does not match any sequence in the human genome (e.g., LacZ) and serves as a crucial control to ensure that any observed gene silencing effects are specific to the sgRNA targeting the gene of interest. For the purposes of the present thesis, five sgRNAs targeting FANCD2 were tested. An initial qPCR was conducted to assess FANCD2 mRNA levels in cells expressing sgRNA1 and in cells expressing the NT sgRNA. As shown in Figure 3.7a, sgRNA1 and sgRNA2 achieved the most effective gene silencing, with reductions of 97% and 94% in FANCD2 expression, respectively.

The lower silencing efficiency observed with the other sgRNAs may be attributed to various factors: 1) the target site may be located far from the transcription start site of the gene; 2) the target site may be located in a heterochromatin region, which is less accessible to the dCas9/KRAB complex; 3) the sgRNA targets a region that is influenced by a strong endogenous promoter or enhancer; 4) there is imperfect complementarity between the sgRNA sequence and the target DNA; 5) the sgRNA may have off-target effects; 6) The sgRNA itself may form secondary structures that reduce its efficiency in guiding the dCas9/KRAB complex to the target site. Based on the results, sgRNA1 was selected for further analysis. A WB was performed to assess FANCD2 protein levels in cells expressing sgRNA1 compared to those expressing the NT sgRNA (Figure 3.7b). The WB analysis revealed a 99% reduction in FANCD2 protein levels with sgRNA1, demonstrating a strong silencing effect, which was considered optimal for subsequent experiments.

As outlined in the introduction to this chapter, this part of the present study was undertaken to assess the silencing of the FANCC gene and compare these results with those previously obtained in PANC 03.27 cells. To this aim, five sgRNAs targeting the FANCC gene were cloned, and corresponding HeLa/KRAB and Capan-1 cell lines expressing these sgRNAs were generated following the same procedures used for the FANCD2 gene.

### 3.3. RESULTS

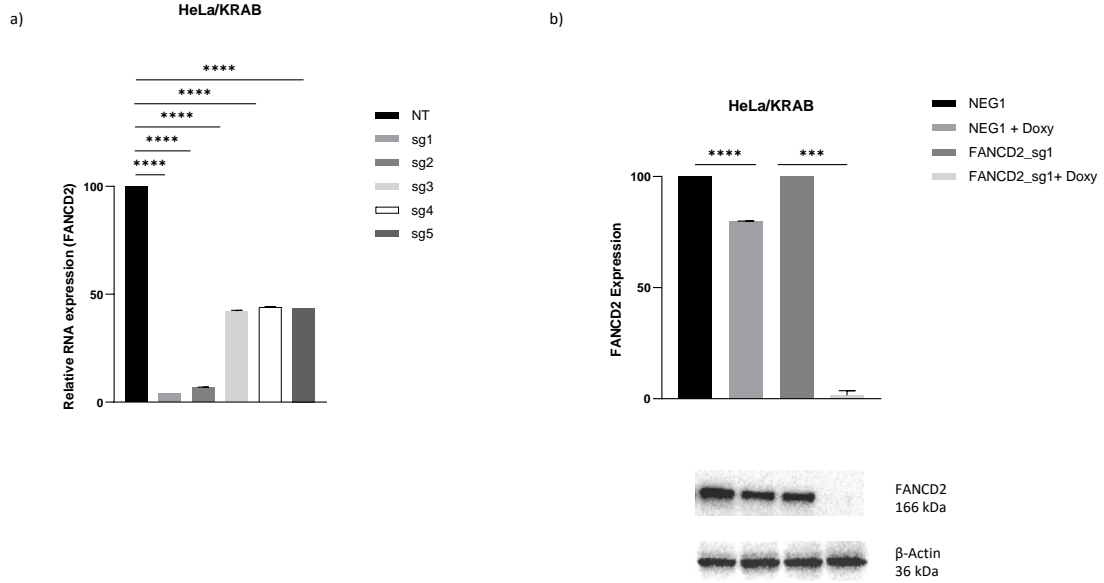


Figure 3.7: **FANCD2 expression in HeLa/KRAB cells.** HeLa/KRAB cells have been treated with 1 $\mu$ g/ml Doxycycline for 72h. After this incubation time, the mRNA and protein expression level of FANCD2 were measured. Data are means  $\pm$ s.d. of n=3 independent biological replicates and have been analyzed by two-tailed unpaired t-test, \*\*\*( $P \leq 0.0005$ ), \*\*\*\*( $P \leq 0.00001$ )

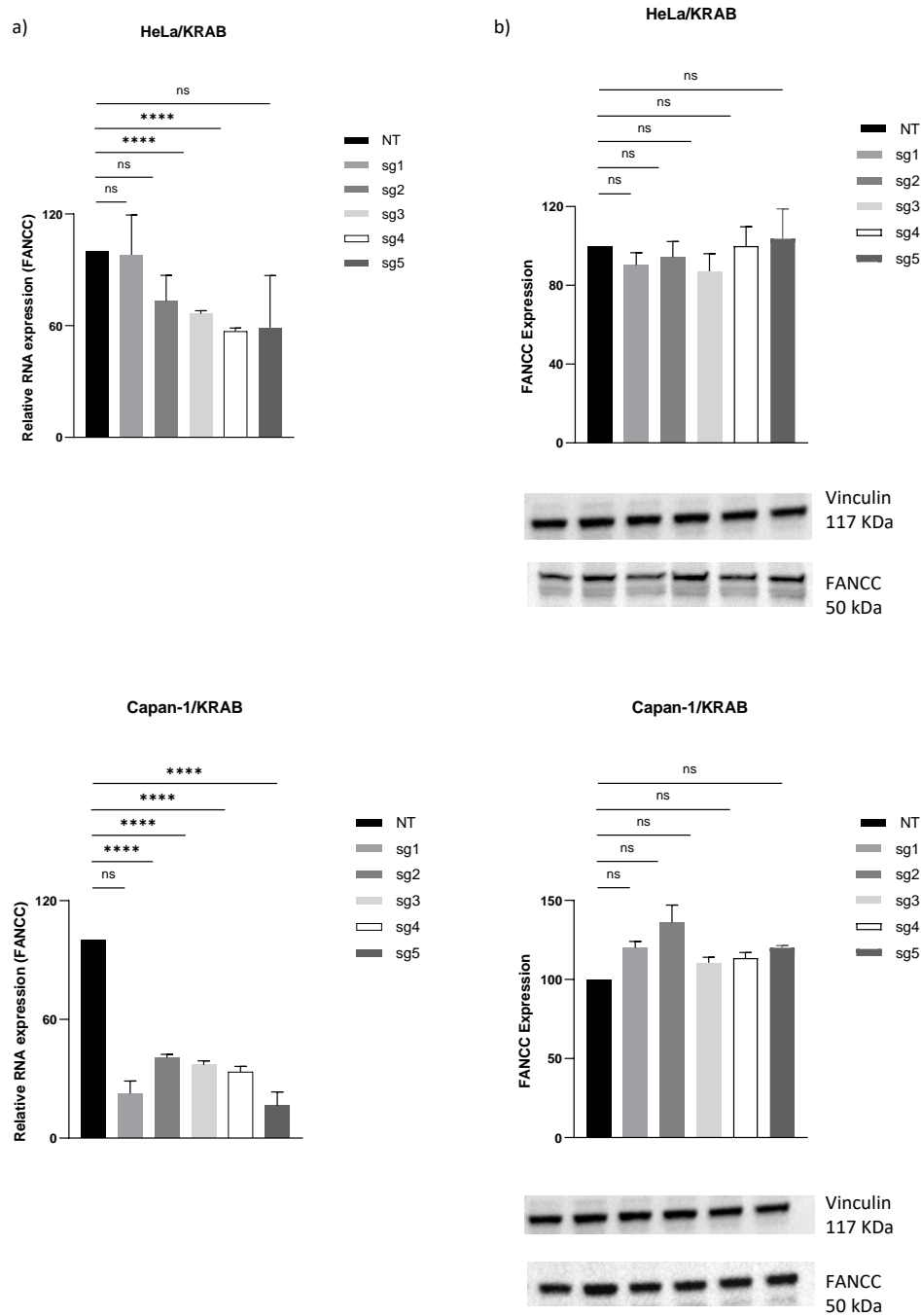
(a) qPCR of FANCD2 mRNA. The relative expression of the gene is measured against the RPLPO gene expression

(b) Western Blot analysis of FANCD2 protein expression. Proteins were extracted using RIPA buffer and 20  $\mu$ g of proteins were loaded

Unfortunately, when evaluating the gene silencing efficiency, none of the five sgRNAs achieved satisfactory levels of silencing in the HeLa/KRAB control cell line: 40% mRNA level decrease was the best result obtained using the sgRNA 4 (Figure 3.8a). As previously discussed in this section, several factors could have contributed to this outcome, such as issues of chromatin accessibility. FANCC was instead efficiently silenced in Capan-1 cells, reaching a 17% gene silencing when using the sgRNA 5. Despite the discrepancy between the model cell line and Capan-1 results, we proceeded to assess the protein expression levels to determine whether even a modest reduction in mRNA could lead to a decrease in FANCC protein levels.

Consistent with the mRNA results, there was no significant reduction in FANCC protein expression in HeLa/KRAB cells (Figure 3.8b). Unexpectedly, no protein silencing was achieved in Capan-1/KRAB cells too.

### 3.3. RESULTS



**FANCC expression in HeLa/KRAB cells.** HeLa/KRAB cells have been treated with 1 $\mu$ g/ml Doxycycline for 72h. After this incubation time, the mRNA and protein expression level of FANCC were measured. Data are means  $\pm$ s.d. of n=3 independent biological replicates and have been analyzed by two-tailed unpaired t-test, ns= not significant ( $P \geq 0.05$ ), \*\*\*( $P \leq 0.0005$ ), \*\*\*\*( $P \leq 0.00001$ ).  
*Following page*

(a) qPCR of FANCC mRNA. The relative expression of the gene is measured against the RPLPO gene expression

(b) Western Blot analysis of FANCC protein expression. Proteins were extracted using RIPA buffer and 20  $\mu$ g of proteins were loaded

This outcome could be attributed to the elevated expression levels of the FANCC gene in Capan-1 cells, making effective silencing more challenging. This hypothesis aligns with the known BRCA2 deficiency in Capan-1 cells, which may result in compensatory upregulation of alternative DNA repair pathways. These compensatory mechanisms could promote cell survival despite the loss of BRCA2 function, allowing the cells to bypass the defect and maintain genomic integrity.

Due to time constraints, these hypotheses could not be fully tested. Verifying the effectiveness of a sgRNA involves a long process, taking more than six months to properly assess the silencing effect and evaluate its efficacy. Given these results, the FANCC gene was not further used in the present thesis and the BxPC3 cells were not transposed with the dCas9/KRAB system. The BxPC3 cell line was intended to provide a PC model with a functional BRCA2 gene, allowing for the evaluation of FANCC silencing within a cancer-specific context. Therefore, further investigations are needed to elucidate the reasons behind the unsuccessful FANCC silencing and to optimize the conditions for effective gene repression in future studies.

The next sections will be focused on the FANCD2 silencing in HeLa/KRAB cells since this gene was nicely silenced in this model.

#### **3.3.3 FANCD2 silencing is not enhancing Talazoparib sensitivity in HeLa/ KRAB cells**

Given the results and the decision to focus exclusively on the FANCD2 gene, the next step involved evaluating the potential correlation between FANCD2 silencing and Talazoparib sensitivity. To achieve this, a cell viability assay was conducted using HeLa/KRAB-NT (non-targeting) and HeLa/KRAB-FANCD2-sg1 cells, both with and without Doxycycline treatment. Doxycycline was essential for inducing dCas9/KRAB expression, thereby enabling FANCD2 silencing in the HeLa/KRAB-FANCD2-sg1 cells. This setup allowed for a direct comparison between the silenced cells and the NT control. Both the NT control and HeLa/KRAB-FANCD2-sg1 cell lines were treated with either MMC, to induce DNA ICLs, or Talazoparib, to assess whether FANCD2 silencing might enhance Talazoparib sensitivity. Drug concentration was selected after a dose-response curve experiment (Figure 3.9).

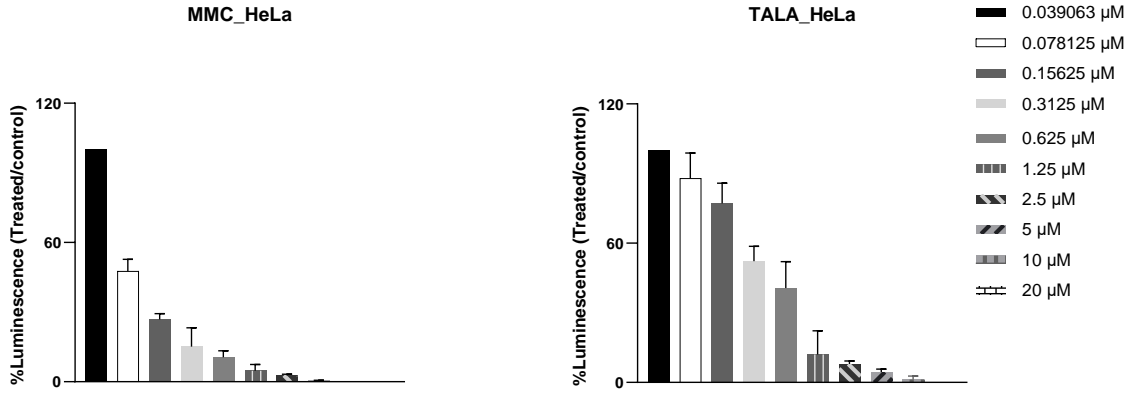


Figure 3.9: **Dose-response curve of MMC and Talazoparib in HeLa cells.** HeLa cells 72h treatment with Mytomicin C (MMC) and Talazoparib (TALA).

The combination of these treatments aimed to evaluate whether FANCD2 gene silencing resulted a reduction in cell survival (Figure 3.10).

Given the role of FANCD2 in the FA pathway, it was expected that silencing FANCD2 through CRISPRi would lead to increased sensitivity to Talazoparib in HeLa/KRAB cells, as similar results have been observed using the precise CRISPR-Select<sup>TIME</sup> technique. However, contrary to expectations, no significant differences in cell viability were observed between the FANCD2-silenced cells and the NT control cells. The cell viability trends across different treatments and cell lines were remarkably similar, which was unexpected. To verify that FANCD2 silencing had indeed occurred in the HeLa/KRAB-FANCD2-sg1 cells treated with Doxycycline, a WB analysis was performed. The successful silencing of FANCD2 was confirmed, ruling out the possibility of incomplete silencing as an explanation for the lack of response. One potential explanation for these unexpected results could be that the degree of gene repression achieved by CRISPRi was insufficient to fully disrupt the FA pathway. This incomplete disruption may have allowed some level of DNA repair to continue, thereby mitigating the expected sensitivity to PARPi. Additionally, it is possible that the cell viability assay used in this context was not the most suitable method for detecting subtle differences in cell survival, particularly when longer exposure times might be necessary to observe the true effects of FANCD2 silencing. To address this problem, the next section will focus on the  $\gamma$ H2AX damage signal in FANCD2-silenced cells.

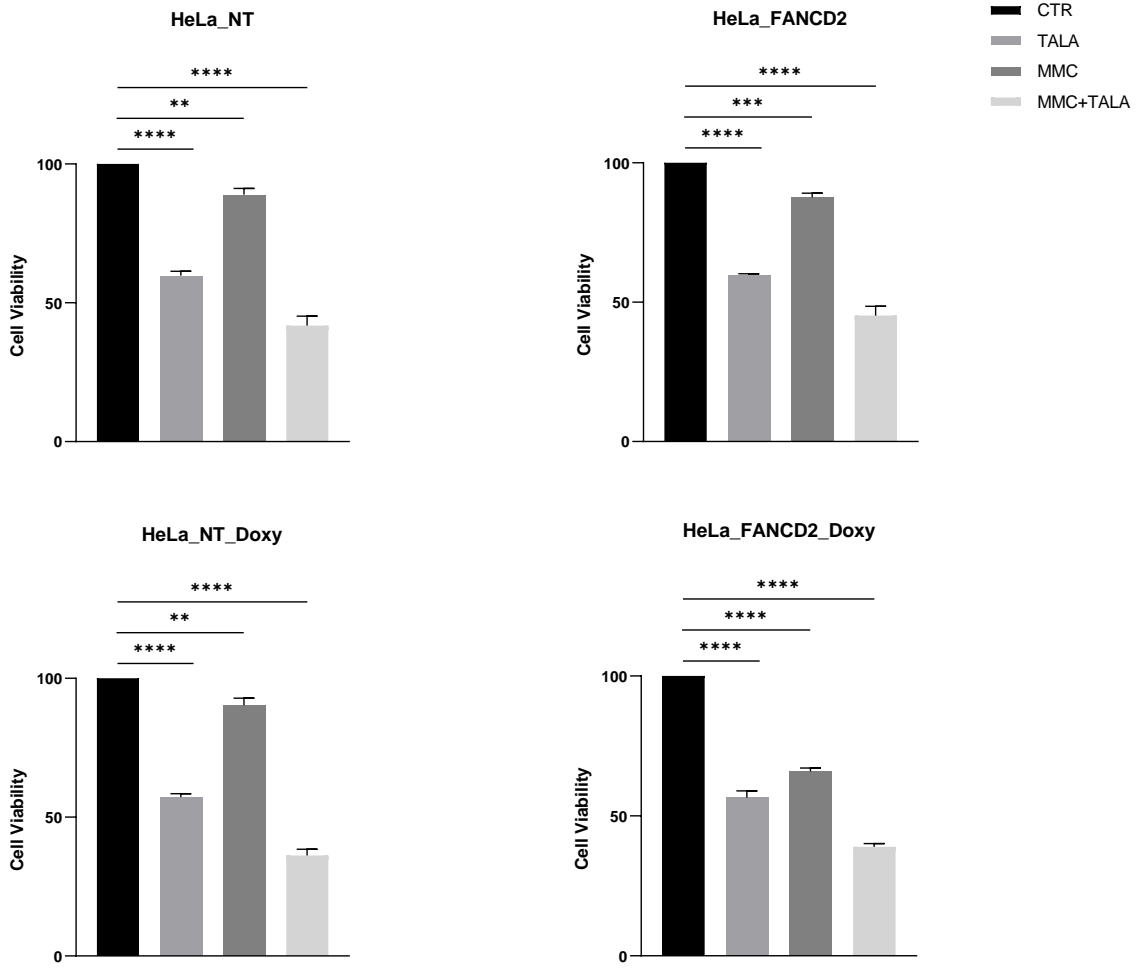


Figure 3.10: **Cell viability assay for FANCD2 silencing.** HeLa/KRAB-NT cells (left) and HeLa/KRAB-FANCD2 sg1 cells (right) were treated with 1  $\mu$ g/mL of Doxycycline for 72h (bottom). Where indicated, cells were treated with 125 nM MMC for 1 hour. This treatment was necessary to induce an ICL formation and, therefore, the activation of the FA pathway. Talazoparib (TALA) treatment was performed using 500 nM TALA for 72h. At the end of the assay, cell viability was measured using the Cell-TiterGlo kit. Data are means  $\pm$  s.d. of n=3 independent biological replicates and have been analyzed by two-tailed paired t-test \* (P $\leq$ 0.05), \*\* (P $\leq$ 0.005), \*\*\* (P $\leq$ 0.0005), \*\*\*\* (P $\leq$ 0.00001), ns= not significant (P $\geq$ 0.05).

### 3.3.4 3.3.3 FANCD2 gene silencing did not increase $\gamma$ H2AX levels in HeLa/KRAB cells

To further understand whether the FANCD2 gene silencing was actually affecting the DNA damage repair, an evaluation of  $\gamma$ H2AX levels on silenced and treated cells was carried out. This analysis was also aimed at elucidating why silencing the

### 3.3. RESULTS

FANCD2 gene does not lead to increased sensitivity to Talazoparib. Therefore, a WB analysis was performed on HeLa/KRAB-NT and HeLa/KRAB-FANCD2 sg1 cells. As done before, both cells were treated or not with Doxycycline. All cells were treated with MMC and Talazoparib either individually or in combination (Figure 3.11).

The results indicated a potential increase in  $\gamma$ H2AX levels in silenced cells; however, this increase was not significant when comparing silenced cells to controls. This finding suggests that although FANCD2 gene silencing does occur, it may not be sufficient to induce a DNA repair deficiency or increase Talazoparib sensitivity. These results also imply that the CRISPRi method, despite its advantages, may not be the optimal approach for this particular study.

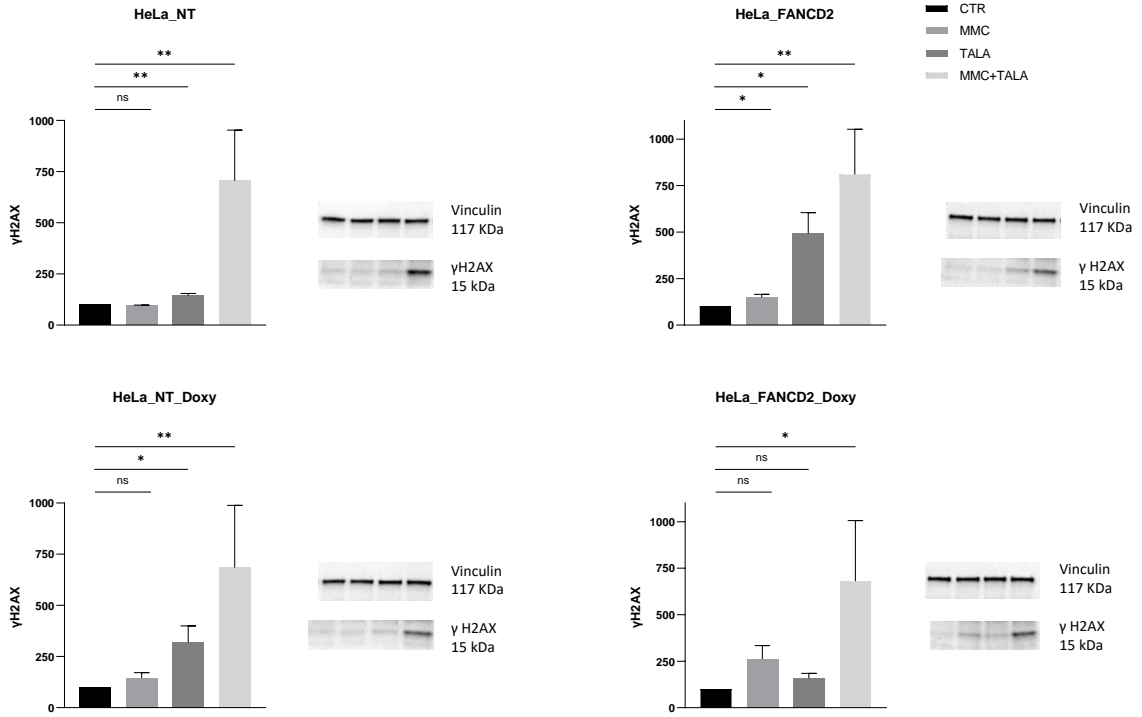


**Figure 3.11: Western Blot for  $\gamma$ H2AX expression levels on HeLa/KRAB cells.** HeLa/KRAB-NT cells and HeLa/KRAB-FANCD2 sg1 cells were treated with 1 $\mu$ g/mL Doxycycline for 72h (Bottom). Where indicated, cells were treated with 125 nM MMC for 1 hour. This treatment was necessary to induce an ICL formation and, therefore, the activation of the FA pathway. Talazoparib (TALA) treatment was performed using 500 nM TALA for 72h. At the end of the assay,  $\gamma$ H2AX expression levels were measured through WB. Data are means  $\pm$ s.d. of n=3 independent biological replicates and have been analyzed by two-tailed paired t-test (\*( $P \leq 0.05$ ), ns= not significant ( $P \geq 0.05$ )).

## 3.4 Conclusions of Chapter 3

In this chapter, the focus was on establishing a CRISPRi platform using HeLa cells to investigate the correlation between FA genes silencing, specifically FANCD2 and FANCC, and sensitivity to Talazoparib. HeLa cells were chosen for their proficiency in DNA repair, making them a suitable model system. The CRISPRi method was selected due to its ability to silence genes without inducing double-strand breaks, thus avoiding the off-target effects often associated with the canonical CRISPR/Cas9 system. Furthermore, the CRISPR-Select<sup>TIME</sup> tool could not be used, being unworkable in a triploid cell line. The initial experiments successfully generated HeLa cell lines expressing dCas9/KRAB upon Doxycycline induction. These cell lines were then transfected with sgRNAs targeting the FANCD2 gene. The effectiveness of FANCD2 silencing was confirmed through qPCR and WB analysis, which demonstrated a significant reduction in both mRNA and protein levels. This confirmed the successful establishment of the CRISPRi platform for FANCD2 in HeLa cells. Despite this success, when assessing the impact of FANCD2 silencing on Talazoparib sensitivity through a cell viability assay, no significant differences were observed between FANCD2-silenced cells and NT control cells. Furthermore, no significant increase in  $\gamma$ H2AX levels were obtained in FANCD2 silenced cells with or without PARPi treatment. This was unexpected, particularly given the role of FANCD2 in DNA repair and previous findings using CRISPR-Select<sup>TIME</sup>. The chapter also explored the silencing of the FANCC gene in HeLa and Capan-1 cells. Unfortunately, the CRISPRi method proved less effective for FANCC, with only modest reductions in mRNA and protein levels achieved. These results suggest the need for further optimization of the CRISPRi approach for FANCC, possibly by selecting alternative sgRNAs or modifying experimental conditions. The outcomes of this chapter underline the complexity of using CRISPRi for gene silencing and the necessity of validating results across different techniques. The unexpected lack of enhanced PARPi sensitivity in FANCD2-silenced HeLa cells suggests that further investigation is needed, possibly by employing alternative assays such as flow cytometry for cell cycle analysis or exploring synergy with other DNA damage-inducing agents. Overall, these findings establish a foundation for future research using the CRISPRi platform in HeLa cells and they also identify areas concerning FA pathway and PARPi sensitivity that require further exploration and optimization.

# Discussions, conclusions and Future perspective

The primary objective of this thesis was to identify and evaluate an appropriate methodology to verify the relationship between the FA pathway gene alterations and sensitivity to PARPi. Previous studies have explored the connection between the FA pathway and PARPi sensitivity using various approaches. For instance, DNA fiber assays in FANCD1-deficient cells demonstrated a correlation between FANCD1 and PARP1 activity. Specifically, depletion of FANCD1 leads to reduced PARP1 activity in S-phase by sequestration it in chromatin and resulting in resistance to PARPi. This indicates that PARPi resistance in FANCD1-deficient cells is due to the disruption of PARP1's replication function rather than its trapping. Given FANCD1's role in regulating PARP1 activity during replication, targeting FANCD1 could enhance PARPi effectiveness, offering potential therapeutic benefits. [151]. In siRNA-mediated FANCD1 gene silencing the DNA fiber assays revealed that FANCD1 promotes PARPi resistance [225]. The same study highlights the dual role of FANCD1 in counteracting the effects of PARPi. First, FANCD1 prevents the formation of ssDNA on the lagging strand, thereby inhibiting PARP1 trapping. Second, it promotes the repair of collapsed forks on the leading strand, which are generated by PARPi-induced ssDNA gaps [225]. FANCD2 loss has been shown to induce PARPi sensitivity through cell proliferation assays [209]. The relationship between REV1 (FANCD2) and PARPi resistance was established using loss-of-function shRNA assays [232]. Another study linked BRCA1/2 knockout to FANCD2 overexpression, leading to PARPi resistance as shown by cell survival assays [66]. This correlation is due to the ability of FANCD2 to recruit Pol $\theta$  to the DNA damage sites and, therefore, to stabilize the replication fork. Furthermore, non-functional FANCA was associated with PARPi sensitivity both in vitro and in vivo by disrupting the FA core-complex, as determined by dose-response curve analyses [233]. FANCC deficiency was similarly shown to cause PARPi sensitivity in FANCC-deficient fibroblasts using clonogenic survival assays [148]. This outcome might be linked to the involvement of FANCC in maintaining the G2 checkpoint for a proper DNA repair [234]. These studies, among others, highlight the significance of individual FA proteins in DNA repair deficiencies and their connection to

PARPi sensitivity. These findings are particularly relevant for cancer research, as they underscore the potential of targeting the FA pathway in cancer therapy. The concept of synthetic lethality, especially involving PARPi and BRCA1/2 defects, is already well-established among patients with breast, ovarian, and PCs [78]. However, despite the progress made, a gap in the development of an extensive, precise, and high-throughput screening method to comprehensively assess the relationship between FA proteins and PARPi sensitivity remains. Most of the existing studies have relied on siRNA and shRNA, which, while easy to use, are prone to off-target effects and may not be suitable for precise screening.

Some clinical studies have also pointed out the relevance of the FA pathway to cancer treatment and patient stratification. A germline mutation in FANCA has been found to sensitize ovarian cancer patients to PARPi treatment [150]. Inhibition of FANCI has a therapeutic relevance for Breast Cancer patients as it enhances the PARPi sensitivity in combination with BRCA1/2 deficiency [235]. Another study revealed how often (12.4%) Breast Cancer patients suitable for PARPi treatment carry germline variants in Fanconi Anemia genes, with a particular recurrence of FANCG alteration in Triple Negative Breast Cancer (TNBC) [236].

Given this context, our first goal was to employ an advanced and precise method to further validate the findings from previous studies, with a particular focus on FANCA, FANCD2, and FANCM. These genes were selected to cover different stages of the FA pathway: FANCM serves as the anchor protein for recruiting the complex to DNA interstrand crosslinks (ICLs); FANCA is part of the core complex, which is essential for guiding the E3 ubiquitin ligase to FANCD2; FANCD2 it is the final effector protein, working with FANCI to promote ICL resolution. To study these proteins, we used the CRISPR-Select<sup>TIME</sup> technique, which allows for the analysis of specific gene mutations and their effects on cell viability over time, complemented by Next-Generation Sequencing (NGS). This technique offers a high level of precision, as it includes internal and external controls, ensuring the reproducibility of results. We focused on one specific mutation for each gene: FANCA-R880\*, FANCD2-K9\*, and FANCM-R658\*. These mutations were designed to produce defective proteins with a mild impact on cell viability, allowing for further analysis of drug sensitivity in the edited cells. It is noteworthy that early truncation mutations were not feasible for FANCA and FANCM, as these did not result in observable changes in viability, likely due to exon-skipping events post-CRISPR/Cas9 editing [237]. Exon-skipping is a known cellular mechanism for essential genes, where cells avoid extreme genomic disruptions by skipping specific exons, thereby restoring the reading frame and producing a shorter, but potentially functional, protein. Indeed, FANCA (<https://depmap.org/portal/gene/FANCA?tab=overview>) and FANCM (<https://depmap.org/portal/gene/FANCM?tab=overview>) are classified as strongly essential for cell survival, as indicated in

the DepMap portal (<https://depmap.org/portal/>). This finding justified the design of mutations in other regions of these genes to induce the formation of truncated proteins that might retain some functionality. Although FANCD2 (<https://depmap.org/portal/gene/FANCD2?tab=overview>) is also categorized as essential, the K9\* mutation caused only a mild impact on cell viability, possibly due to a less effective exon-skipping mechanism. However, this is only one possible explanation, and further research is needed to fully understand the precise mechanisms. The CRISPR-Select<sup>TIME</sup> technique successfully demonstrated that mutations in FANCA, FANCD2, and FANCM contribute to Talazoparib sensitivity, thereby supporting previous findings. However, one limitation of this tool is that it performs optimally in diploid cells, and it has been applied in a normal-immortalized cell line to avoid background mutations/cellular altered processes. Overall, this part of the thesis supports the role of the FA pathway in PARPi sensitivity and highlights the potential of using advanced genome-editing techniques for precise and comprehensive studies in this field.

The findings presented in the Chapter 1 underscore the significance of studying the FA pathway. As the next step, we aimed to explore this pathway in PC cells. There is growing evidence linking FA pathway deficiencies to PC. For instance, one study reported that patients with germline PC often harbor mutations in the FANCM and FANCC genes [143]. Another study found that mutations in FANCC and FANCG may contribute to the early onset of PC [238]. Additionally, mutations in FANCA, FANCC, FANCG, and FANCM have been implicated in the development of PC [239][139].

Given these findings, in Chapter 2 the relation between a defective FA pathway and Talazoparib sensitivity has been investigated. We initially chose a cell line already defective in the FA pathway to ensure a clear understanding of the effects. For this purpose, we used PANC 03.27 cell lines, a PC cell line known to be deficient in FANCC. The results of this chapter highlighted that FANCC deficiency does indeed lead to Talazoparib sensitivity in PC cells. This finding is crucial as it connects FA pathway deficiencies with PARPi sensitivity in the context of PC, potentially offering new strategy for stratifying PC patients and tailoring their treatment with PARPi. Aware that these results were only preliminary, we investigated this correlation in Chapter 3.

Chapter 3 goal was to develop a tool to study all FA genes and their relationship with Talazoparib in a PC cell, starting from FANCC and FANCD2. The method chosen for this study was CRISPR interference (CRISPRi), a technique that stops gene transcription without altering the genome. CRISPRi was selected due to its precision and low risk of off-target effects, making it an ideal tool for this part of the research. Initially, we aimed to use a pancreatic cancer cell line to remain consistent with the main hypothesis. We, therefore, selected the two PC cells BxPC3 and

Capan-1 as models to test how the FANCC silencing mediated by CRISPRi affects a FA proficient cell line (BxPC3) and a BRCA2-deficient cell line (Capan-1).

These two cell lines more accurately represent the primary objectives of this work. The BxPC3 cell line reflects pancreatic cancer patients who are unlikely to receive PARPi treatment. By investigating FA gene silencing in this line, it is possible to assess whether a SL relationship exists between Talazoparib and FANCC, potentially enabling more precise gene screening for these patients. This could help identify those with a deficient FA pathway who may benefit from PARPi therapy. In contrast, the Capan-1 cell line represents patients who are already undergoing PARPi treatment. Studying FANCC gene silencing in this context can provide further insights into how cells with an additional FA pathway deficiency respond to PARPi, potentially providing more effective therapeutic strategies.

The HeLa cell line was instead selected as a DNA-repair proficient model system since the CRISPRi method has been fully tested in this cell line. CRISPRi was successfully implemented in HeLa and Capan-1 cells following a detailed and well-optimized protocol. While FANCD2 silencing was achieved in HeLa/KRAB cells, FANCC silencing was insufficient in both cell lines, as confirmed by Western blot analysis. The lack of effective silencing for FANCC could be attributed to various factors, such as poor chromatin accessibility, suboptimal sgRNA design, or the presence of a strong gene promoter.

This result necessitated to stop the experiments on BxPC3 cells, as it became clear that optimizing FANCC silencing in the HeLa/KRAB and Capan-1 cell lines was required before proceeding.

Given the silencing of FANCD2, we proceeded with further investigations on this gene in HeLa/KRAB cells. Surprisingly, FANCD2 silencing did not result in decreased cell viability or increased sensitivity to Talazoparib, which was unexpected, especially when comparing the results with the one obtained by CRISPR-Select<sup>TIME</sup>. This suggests that the HeLa cell line might not be the most suitable model for our study, as these results diverge from those observed in the previous chapters.

The outcome in HeLa cells could be due to the unique characteristics of this cell line. HeLa cells are derived from cervical cancer and are known for their robust growth and adaptability, which may affect how they respond to gene silencing, particularly with respect to the FA pathway. HeLa cells have complex genomic alterations and a highly efficient DNA repair system, which may compensate for the loss of FANCD2, thereby preventing the expected increase in Talazoparib sensitivity or decrease in cell viability. This compensation might be less effective or absent in other cancer cell types, such as PC cells, which could explain the differences observed and reported in Chapters 1 and 2.

This thesis has systematically explored the relationship between a few gene belonging to the FA pathway and sensitivity to Talazoparib, using different advanced

methodologies to enhance the precision and reliability of the findings. By utilizing CRISPR-Select<sup>TIME</sup>, the study demonstrated that mutations in key FA genes, specifically FANCA, FANCD2, and FANCM, contribute to increased Talazoparib sensitivity, confirming the relevance of the FA pathway in DNA repair deficiencies. The subsequent chapters extended this investigation to PC, revealing that FANCC deficiencies can also lead to enhanced sensitivity to PARPi, thereby proposing a potential strategy for patient stratification. Despite encountering challenges with the CRISPR interference (CRISPRi) approach in HeLa and Capan-1 cells, the research highlighted the complexity and cell-type specificity of FA pathway interactions, emphasizing the need for careful selection of model systems in future studies.

Future research should focus on identifying more suitable cancer cell models that better mimic the conditions observed in clinical settings, particularly for PC. Additionally, refining CRISPRi techniques to overcome current limitations, such as incomplete gene silencing, will be essential for enhancing the accuracy of gene function studies. Expanding the investigation to other FA genes and exploring their interactions with different DNA repair pathways could provide deeper insights into the mechanisms underlying PARPi sensitivity and resistance.

# Chapter 4

## Material and Methods

### 4.1 Cell Culture

#### 4.1.1 iCas9-MCF10A

iCas9-MCF10A clonal cell line with Cas9 expressed from stably integrated TRE3G Edit-R Inducible lentiviral Cas9 construct (Horizon, CAS11229) was a gift from Claus Storgaard Sørensen (Biotech Research & Innovation Centre, University of Copenhagen). iCas9-MCF10A was cultured in Dulbecco's Modified Eagle Medium /F12, HEPES (Thermo Fisher Scientific, 31330038) supplemented with 5% Horse Serum (Thermo Fisher Scientific, 26050088), 10  $\mu\text{g}/\text{ml}$  insulin (Sigma, I1882), 20 ng/ml EGF (Peprotech, AF-100-15), 0.5  $\mu\text{g}/\text{ml}$  hydrocortisone (Sigma, H0888) and 100 ng/ml cholera toxin (Sigma, C8052).

#### 4.1.2 PANC-1

PANC-1 (ATCC CRL-1469 <sup>TM</sup>) is a cell line isolated from the pancreatic duct of a metastatic epithelioid carcinoma. This was cultured in Dulbecco's Modified Eagle Medium (DMEM) supplemented with 10% Fetal Bovine Serum, 100 U/mL penicillin and 100 mg/mL streptomycin.

#### 4.1.3 PANC-03.27

PANC-03.27 (ATCC CRL-2549 <sup>TM</sup>) is an epithelial pancreatic adenocarcinoma cell line that was cultured in Dulbecco's Modified Eagle Medium (DMEM) supplemented with 15% Fetal Bovine Serum, 100 U/mL penicillin and 100 mg/mL streptomycin.

#### 4.1.4 HEK-293T

HEK-293T (ATCC CRL-3216 <sup>TM</sup>) is a highly transfectable epithelial-like cell. This cell line was cultured in Dulbecco's Modified Eagle's Medium (DMEM) supplemented with 10% Fetal Bovine Serum, 100 U/mL penicillin and 100 mg/mL streptomycin.

#### 4.1.5 HeLa-KRAB

HeLa-KRAB cells (Human cervical carcinoma) carrying the PB-TRE-dCas9-KRAB construct (see PiggyBac transposition below) were a gift from Carmela Rubolino (Francesco Nicassio's Genomic Science lab, IIT-CGS@SEMM). The cell line was cultured in Dulbecco's Modified Eagle Medium (DMEM) supplemented with 10% Tetracycline-FREE- Fetal Bovine Serum, 100 U/mL penicillin, 100 mg/mL streptomycin and 100  $\mu$ g/mL Hygromycin B.

#### 4.1.6 Capan-1

Capan-1 (ATCC HTB-79 <sup>TM</sup>) is an epithelial pancreatic adenocarcinoma cell line that was cultured in Iscove's Modified Dulbecco's Medium (IMDM) supplemented with 20% Fetal Bovine Serum, 2mM Glutamine, 100 U/mL penicillin and 100 mg/mL streptomycin. Capan-1-KRAB were cultured in the same medium as the parental cell line but using Tetracycline-FREE- Fetal Bovine Serum and 100  $\mu$ g/mL Hygromycin B.

### 4.2 CRISPR-Select Assay

#### 4.2.1 gRNA, donors and primers design

To create a unique gRNA targeting a sequence of interest, a single-stranded oligodeoxynucleotide (ssODN), the Benchling (<https://www.benchling.com/>) and CRISPOR (<http://crispor.gi.ucsc.edu/>) tools were utilized. The design process begins on Benchling by entering the gene of interest and selecting the human genome (GRCh38 / hg38) as the reference. The full gene sequence is displayed, and a 90-base region centered on the mutation of interest is selected. This sequence is then copied and pasted into CRISPOR as Step 1. Step 2 involves selecting the reference genome (GRCh38 /hg38), and Step 3 requires choosing the Protospacer Adjacent Motif (PAM) sequence (NGG). CRISPOR generates a list of 20-base long gRNAs with an NGG PAM sequence. For optimal selection, gRNAs with high MIT specificity scores (the higher the specificity score, the lower are off-target effects in the genome. The specificity score ranges from 0-100 and measures the uniqueness of a guide in the genome), high predicted efficiency scores (the higher the

efficiency score, the more likely is cleavage at the selected position), and low Off-Targets for 0-1-2-3-4 mismatches score (for each number of mismatches, the number of off-targets is indicated. Example: 1-3-20-50-60 means 1 off-target with 0 mismatches, 3 off-targets with 1 mismatch, 20 off-targets with 2 mismatches, etc.) have been considered. Additionally, a good Out-of-Frame/Indel score is crucial for successful CRISPR/Select outcomes. The final consideration is the proximity of the PAM sequence to the mutation. A closer PAM to the mutation site is preferred to a sequence with lower off targets score. Once the gRNA is selected, its sequence is copied back to Benchling to localize it within the gene sequence. To design donor sequences, 45 base pairs upstream and downstream of the target are selected. A MUT/WT\* design in the GG of the NGG or in the gRNA seed region is preferred to increase precision and avoid re-cutting. To design the MUT sequence, is sufficient to change the reference base to the mutated one (insertion/deletion/base exchange). To design the WT\* sequence, the Kazusa codon usage table (<https://www.kazusa.or.jp/codon/cgi-bin/showcodon.cgi?species=9606>) has been used, in order to select a high frequency change of the base that is not affecting the protein translation process. The primers for the specific MUT/WT\* sequences have been designed through Benchling selecting a region which includes at least the MUT/WT\*sequence and using the Wizard tool. The parameters used were the following: GC% (Min:50, Opt:51, Max:50), Tm (Min:55, Opt:62, Max:65), Size (Min:18, Opt:22, Max: 26), Amplicon size (Min:180, Opt:250, Max:300). The primers couple with the optimal scores have been selected for subsequent steps. The list of the used gRNAs (Table X.1), Donors (Table X.2) and primers (Table X.3) is below reported:

Gene	Target site	gRNA
BRCA2	D2723	TTATTGAACTTACAGATGGG
BRCA2	L2510	GGCAGTCTGTATCTTGCAA
FANCA	R880	ACAGCCTCTTTCTGAGGAGG
FANCD2	K9	AAGAAGACTGTCAAATCTG
FANCM	R658	TTTCGCTGCAAGTTCCGAGA

Table 4.1: **gRNA sequences.** Designed gRNAs for the genes and target sites reported in the table.

## 4.2. CRISPR-SELECT ASSAY

ssODN	ssODN sequence
BRCA2.D2723G_Reference	CTAGTAGTCAGATACCCAAAAAGTGGCCATTATTGAACCTACAGATGGGTGGTATGCTGTAA GGCCCAGTTAGATCCTCCCTCTTAGCT
BRCA2.D2723G.WT*	CTAGTAGTCAGATACCCAAAAAGTGGCCATTATTGAACCTACAGATGGGTGGTATGCTGTAA GGCCCAGTTAGATCCTCCCTCTTAGCT
BRCA2.D2723G_MUT	CTAGTAGTCAGATACCCAAAAAGTGGCCATTATTGAACCTACAGATGGGTGGTATGCTGTAA GGCCCAGTTAGATCCTCCCTCTTAGCT
BRCA2.L2510P_Reference	ATTAAGAAGAAACAAAGGCCAACGCGCTTTCCACAGCCAGGCAGTCTGTATCTTGCAAAAACATCCACTCTGCCTCGAATCTCTCTGAAAGCA
BRCA2.L2510P.WT*	ATTAAGAAGAAACAAAGGCCAACGCGCTTTCCACAGCCAGGCAGTCTGTATCTTGCAAAAACATCCACTCTGCCTCGAATCTCTCTGAAAGCA
BRCA2.L2510P_MUT	ATTAAGAAGAAACAAAGGCCAACGCGCTTTCCACAGCCAGGCAGTCTGTATCTTGCAAAAACATCCACTCTGCCTCGAATCTCTCTGAAAGCA
FANCA.R880*.Reference	TGTTCTCAGAGGCCCGCAGCCCTCTTTCTGAGGAGGACGTAGCCAGCCTTTCTGGAGACCC
FANCA.R880*.WT*	TGTTCTCAGAGGCCCGCAGCCCTCTTTCTGAGGAGGACGTAGCCAGCCTTTCTGGAGACCC
FANCA.R880*.MUT	TGTTCTCAGAGGCCCGCAGCCCTCTTTCTGAGGAGGACGTAGCCAGCCTTTCTGGAGACCC
FANCD2.K9*.Reference	GTGCACAAGACATTGGTCAAAATGGTTTCCAAAAGAAGACTGTCAAGATCTGAGGATAAAGAGAGCCTGACAGAAGATGCCTCCAGTAAGT
FANCD2.K9*.WT*	GTGCACAAGACATTGGTCAAAATGGTTTCCAAAAGAAGACTGTCAAGATCTGAGGATAAAGAGAGCCTGACAGAAGATGCCTCCAGTAAGT
FANCD2.K9*.MUT	GTGCACAAGACATTGGTCAAAATGGTTTCCAAAAGAAGACTGTCAAGATCTGAGGATAAAGAGAGCCTGACAGAAGATGCCTCCAGTAAGT
FANCM.R658*.Reference	GAAAAGAAACGTGATGAGACCCGAGTATGATCTTCTCTTCATTTCGAGATAGTGTTCAGAAATTGCAGAAATGCTTTCACAGCATCAGC
FANCM.R658*.WT*	GAAAAGAAACGTGATGAGACCCGAGTATGATCTTCTCTTCATTTCGAGATAGTGTTCAGAAATTGCAGAAATGCTTTCACAGCATCAGC
FANCM.R658*.MUT	GAAAAGAAACGTGATGAGACCCGAGTATGATCTTCTCTTCATTTCGAGATAGTGTTCAGAAATTGCAGAAATGCTTTCACAGCATCAGC

Table 4.2: **Donors sequences.** Designed Donors for the genes and target sites reported in the table. Reference sequences are also reported

Gene_Target	Primer_Forward	Primer_Reverse
BRCA2.T2723	CTGACATAATTTTCATTGAGCGCA	CCACCAGTTCTGCTCCATGA
BRCA2.L2510	CAAGTCTTCAGAATGCCAGAGA	CACTCTGTCATAAAAGCCATCA
FANCA.R880	CATTTGCTCAGCCACTCACA	CCCTCTCTCTCTGGACACAC
FANCD2.K9	TCTGTTTCCCGATTTTGCTCT	CCTGTAGCAATGTGTGAGGC
FANCM.R658	TTCAAGTAACAGGCAGGTCC	ACGACCTGCTAAGTAAGAACAG

Table 4.3: **Primers sequences.** Designed Primers for the genes and target sites reported in the table.

To prepare the samples for next-generation sequencing (NGS), adaptor sequences were integrated into each primer. The specific adaptor sequences attached to the forward and reverse primers are reported in Table X.4.

Adaptor_FWD	Adaptor_REV
ACACTCTTTCCCTACACGACGCTCTTCCGATCT	TGACTGGAGTTCAGACGTGTGCTCTTCCGATCT

Table 4.4: **Adaptors sequences.** Designed Adaptors for the 1<sup>st</sup>PCR Primers

### 4.2.2 Cell transfection

On Day -1, 200,000 iCas9-MCF10A cells were seeded in a 6-well plate containing 2 mL medium supplemented with 1  $\mu$ g/mL Doxycycline to induce Cas9 expression. On day 0, cells with 50%-70% confluency were transfected. Briefly, 7.5  $\mu$ l Lipofectamine RNAiMAX (Thermo Fisher Scientific, 13778) were added in a RNase-free tube together with 125  $\mu$ l OptiMEM (Thermo Fisher Scientific, 31985062) and 10 pmol each of the variant (MUT) and WT\* ssODN in 2  $\mu$ l. In another RNase-free tube, 75 pmol each of crRNA and tracrRNA in 7.5  $\mu$ l were mixed followed by a 10-minute incubation at room temperature to allow complex formation. After incubation, 125  $\mu$ l OptiMEM was added and then mixed with the Lipofectamine solution to let all incubate for other 10 min at room temperature. The prepared transfection solution was then gently added dropwise to the iCas9\_MCF10A cells in fresh medium containing doxycycline. Cells were then left for 48h in the incubator

at 37°C with 5% CO<sub>2</sub>. On Day 2, cells were detached from the 6-well plate using Trypsin. Half of the cells were harvested to capture the Day 2 time point, while the remaining cells were re-seeded into a 6-cm dish. If required, cells were treated the following day with 2.5 nM the PARP inhibitor Talazoparib (Axon Medchem, 2502) or 500 nM Cisplatin until Day 12, at which point the cells were harvested. Harvested cells were then centrifuged at 300g for 3 minutes, and the pellet was used for DNA extraction.

### 4.2.3 DNA extraction

The GenElute Mammalian Genomic DNA Miniprep Kit (Sigma) was used for the extraction of DNA. Initially, each cell pellet was resuspended in 200  $\mu$ L Resuspension Solution, followed by the addition of 20  $\mu$ L RNase A, with the mixture incubated for 2 min at room temperature. Subsequently, 20  $\mu$ L Proteinase K solution was added to the sample, along with 200  $\mu$ L Lysis Solution C (B8803). The mixture was vortexed for 15 seconds and then incubated at 55°C for 10 minutes to ensure thorough lysis. During this incubation, 500  $\mu$ L Column Preparation Solution was added to each pre-assembled GenElute™ Miniprep Binding Column and centrifuged at  $12,000 \times g$  for 1 minute to prepare the column. Following the incubation, 200  $\mu$ L 95%/100% ethanol was added to the lysate, mixed thoroughly for 5-10 seconds, and then transferred to the prepared columns, followed by centrifugation at  $>6,500 \times g$  for 1 minute to bind the DNA. The binding columns were washed twice. 500  $\mu$ L Wash Solution were used for the first wash followed by  $>6,500 \times g$  for 1 minute. The second wash was performed by adding 500  $\mu$ L Wash Solution and centrifuging it at  $12,000 \times g$  for 5 minutes to ensure complete removal of contaminants. The elution step was performed as follows: 20  $\mu$ L nuclease-free water was added to the column, incubated at room temperature for 5 minutes, and then centrifuged for 1 minute at  $>6,500 \times g$ . The eluted DNA was subsequently quantified using a Nanodrop spectrophotometer and used for 1<sup>st</sup> and 2<sup>nd</sup> PCR.

### 4.2.4 1<sup>st</sup> and 2<sup>nd</sup> PCR

One hundred ng DNA, corresponding to approximately 17,000 diploid cells, was used to perform the first round of PCR. The following reagents were used: 25  $\mu$ L Phusion U Green Multiplex PCR Master Mix (Thermo Fisher Scientific, F564L), 1.5  $\mu$ L Primer Mix (5  $\mu$ M FWD/REV), 100 ng DNA, and ddH<sub>2</sub>O to reach a final volume of 25  $\mu$ L. The reaction conditions were set as follows: initial denaturation at 98°C for 1 min (1 cycle), followed by 35 cycles of 98°C for 10 sec, a gradual annealing from 60°C (decreasing by 0.1°C per cycle) for 30 sec, and elongation at 72°C for 15 sec, with a final extension at 72°C for 15 sec (1 cycle), and then hold at 4°C. The products from the first PCR were assessed using 1% agarose gel electrophoresis.

For the second PCR, unique barcodes were appended to each sample to facilitate library preparation and subsequent NGS sequencing. The reagents used for the 2nd PCR were the following: 6.5  $\mu\text{L}$  Phusion U Green Multiplex PCR Master Mix (Thermo Fisher Scientific, F564L), 1.5  $\mu\text{L}$  barcodes, 1.5  $\mu\text{L}$  PCR product from the first run, ddH<sub>2</sub>O up to 12.5  $\mu\text{L}$ . The reaction conditions were the following: initial denaturation at 98°C for 30 sec (1 cycle), followed by 8 cycles of 98°C for 10 sec, annealing at 65°C for 30 sec, and elongation at 72°C for 15 sec, with a final extension at 72°C for 5 min (1 cycle), then hold at 4°C. The results of the 2nd PCR were evaluated through 1% gel Agarose sample run using the 1st PCR samples as reference. Samples with matching primers or similar lengths were pooled and run on a 1% agarose gel. After gel run, DNA fragments were extracted using the QIAquick® Gel Extraction Kit (Qiagen, cat. nos. 28704, 28706). DNA bands were excised from the gel using the x-tracta gel extraction tool (Merck, Z722390) and collected in 1.5 mL tubes. Three volumes of Buffer QG were added to the gel slices, and the mixture was incubated at 50°C for 10 minutes to dissolve the gel. Then, 1 gel volume of isopropanol was added, and the mixture was loaded to QIAquick columns and centrifuged at 13,000 x g for 1 min. 500  $\mu\text{L}$  Buffer QG were added and the samples centrifuged at 13,000 x g for 1 min. For the washing step, 750  $\mu\text{L}$  Buffer PE were added to the columns and incubated for 5 min at room temperature and then centrifuged at 13,000 x g for 1 min. Finally, 20  $\mu\text{L}$  nuclease-free water was added to the center of each column, incubated for 5 min, and centrifuged to elute the purified DNA. The purified DNA was then ready for the next step in the NGS workflow.

### 4.2.5 NGS

The DNA samples extracted from the 2nd PCR were quantified using the Qubit dsDNA HS Assay Kit (Q32854). From each sample, 10 ng was pooled together to create a sequencing library. The pooled library was then diluted to a final concentration of 4 nM in 100  $\mu\text{L}$  nuclease-free water. To prepare the library for sequencing, 5  $\mu\text{L}$  the 4 nM library was mixed with 5  $\mu\text{L}$  of freshly prepared 0.2N NaOH for denaturation. This 10  $\mu\text{L}$  mixture was then combined with 990  $\mu\text{L}$  HT1 buffer from the MiSeq Reagent Kit v2 (Illumina, MS-102-2002), yielding a final library concentration of 20 pM. To achieve the optimal concentration for sequencing, the 20 pM library was further diluted to 12 pM in a 600  $\mu\text{L}$  solution. Additionally, 20% of this final solution was replaced with 20% of a 12.5 pM PhiX control library. The PhiX is a control library from the PhiX virus serves as a sequencing control to ensure accuracy during the run. Finally, the entire 600  $\mu\text{L}$  of the prepared library mixture was loaded into the NGS sequencing chamber, initiating the sequencing process. NGS data were processed through the CRISPResso2 online tool using default settings (<https://crispresso.pinellolab.partners.org/submission>).

## 4.3 Cell Viability Assay

The cell viability assay was performed in 96-well plates (Corning 96-well Solid White Flat Bottom). On Day 0, PANC 03.27 and PANC 01 cells were seeded at a density of 5,000 cells per well in 100  $\mu$ l DMEM, while HeLa-KRAB cells were seeded at a density of 2,000 cells per well in 100  $\mu$ l DMEM. The following day, the medium was replaced with 100  $\mu$ l fresh medium containing the relevant drug where needed. The drugs used in this study were Mitomycin C and Talazoparib. Mitomycin C was obtained from Abcam (Cat. Ab120797), and Talazoparib was purchased from TargetMol (Cat. T6253). PANC 03.27 cells were treated with 0.8  $\mu$ M Mitomycin C and 0.8  $\mu$ M Talazoparib for 72 h, while HeLa-KRAB cells were treated with 125 nM Mitomycin C and 500 nM Talazoparib for the same duration. Following the 72-hour treatment period, cell viability was assessed using the CellTiter-Glo Luminescent Cell Viability Assay (Promega). In brief, 100  $\mu$ l of the CellTiter-Glo Reagent provided by the kit was added to each well, followed by a 10-minute incubation in the dark. Post-incubation, the 96-well plate was analyzed using a GloMax<sup>®</sup> Spectrophotometer to measure the luminescent signal from each well. The luminescence is directly proportional to the ATP content, which correlates with the number of viable cells in each well.

## 4.4 Western Blot

For whole cell lysis, harvested cell culture pellets were rinsed twice with PBS. Cell pellet was lysed in RIPA buffer (10mM Tris-HCl pH 8, 0, 1% Triton, 150mM NaCl, 0.1% SDS, 0.1%NaDeoxycholate, 1mM EDTA, 1mM DTT, 50x cocktail protease inhibitor Roche (cat. ROCHE 11836170001)). Cell lysis was incubated on ice for 15 min. The lysates were centrifuged for 15 min at 13000 x g at 4°C. Supernatant (total protein lysate extraction) was quantified using Bradford Assay (Bio-Rad Protein Assay Dye Reagent Concentrate, cat. 5000006) which uses Coomassie G-250 dye in a colorimetric reagent for the detection and quantitation of total protein. Western blot analysis was performed using Criterion<sup>™</sup> TGX Stain-Free<sup>™</sup> Precast Gels, gradient 4-15% (Bio-Rad). Proteins were transferred to a nitrocellulose membrane using the Trans-Blot Turbo<sup>™</sup> Transfer System (Bio-Rad) in Transfer buffer. The membrane was then incubated with the primary antibody (diluted 1:1000-1:2000 in 5% BSA in 1X TBS with 1% Tween-20) followed by the secondary antibody (diluted 1:10000 in 5% BSA in 1X TBS with 1% Tween-20). After three washes in 1X TBS with 1% Tween-20 5 min each, the membrane was acquired using the ChemiDoc XRS+ Imaging System (Bio-Rad) via a chemiluminescence reaction with a 1:1 solution of Clarity<sup>™</sup> Western ECL Substrate (Peroxide solution) and Clarity<sup>™</sup> Western ECL Substrate (Luminol/Enhanced solution). The Cas9 antibody was obtained from Cell Signaling (Ref. 7A9-3A3) (1:1000);  $\gamma$ H2AX (ab11174), FANCD2

(ab108928) (1:1000), and FANCC (ab97575) (1:1000) antibodies were acquired from Abcam; Vinculin (V9131) (1:2000) and Actin (A4700) (1:1000) antibodies were purchased.

## 4.5 Stable dCas9-KRAB cell line production

### 4.5.1 PB-TRE-dCas9-KRAB plasmid generation

The PB-TRE-dCas9-KRAB plasmid was a gift from Bianca Giuliani (Francesco Nicassio's lab). The KRAB domain sequence was amplified by PCR from the pHAGE TRE-dCas9-KRAB (Addgene plasmid #50917) and cloned in frame into the PBTRE-dCas9-VPR backbone (Addgene plasmid #63800) within the AscI/Age I sites. Sanger Sequencing was used to verify the cloning efficacy.

### 4.5.2 PiggyBac Transposition

The day before transposition cells were seeded at 60-70% confluency in six well plates. Cells were transfected according to Lipo3000 protocol (Thermo Fisher Scientific) with 500 ng transposon DNA (PB-TREdCas9-KRAB) and 200 ng Super-PiggyBac transposase helper plasmid (Systems Bioscience). The DNA was first diluted in 125  $\mu$ L Opti-MEM (Thermo Fisher Scientific) along with 5  $\mu$ L P3000 transfection reagent. Separately, 7.5  $\mu$ L Lipofectamine 3000 were mixed in 125  $\mu$ L Opti-MEM and thoroughly vortexed. The DNA solution and Lipofectamine mix were combined in a 1:1 ratio and incubated at room temperature for 20 minutes. This mixture was then added dropwise to the cells in fresh media. After 72 h post-transfection, the cells were selected with 200  $\mu$ g/mL Hygromycin B for two weeks.

### 4.5.3 LentiGuide cloning

The LentiGuide Puro (Addgene #52963) cloning was made within the BsmBI (Esp3I) sites. Restriction digestion was performed using 5 $\mu$ g plasmid, 5 $\mu$ L Tango Buffer 10X (Thermo Fisher Scientific), 3 $\mu$ L Esp3I 10U/ $\mu$ L (Thermo Fisher Scientific), 20mM DTT and H<sub>2</sub>O up to 50  $\mu$ L. The reaction was incubated for 2h at 37°C. Digested plasmid was purified from a 1.5% agarose gel. The dephosphorylation step was made using the purified plasmid (up to 1 $\mu$ g), 2 $\mu$ L Phosphatase buffer 10X (Roche), 1U Alkaline Phosphatase 1U/ $\mu$ L (Roche) and H<sub>2</sub>O up to 20  $\mu$ L. The reaction was incubated at 35°C for 10 min, then 75°C for 2 min and finally at 4°C. sgRNAs oligos were purchased as Oligos with compatible ends for BsmBI cut sites by Sigma-Aldrich. Forward and Reverse oligos were annealed using the following reagents: 1 $\mu$ L T4 ligation buffer 10X (NEB), 0.5 $\mu$ L T4 Polynucleotide Kinase 10U/ $\mu$ L (PNK)(NEB), 1 $\mu$ L Oligo FWD 100 $\mu$ g, 1 $\mu$ L Oligo REV 100 $\mu$ g and H<sub>2</sub>O up

to 6.5  $\mu$ l. The reaction was divided into three steps: a Phosphorylation step at 37°C for 30 min, a Denaturation step at 95°C for 5 min, an Oligo annealing step from 95°C to 25°C 0.1°C/s, and a final hold at 4°C. Annealed Oligos were diluted in H<sub>2</sub>O for subsequent ligation. The reagents used for the ligation reaction between annealed Oligos and the dephosphorylated plasmid were: up to 1 $\mu$ g dephosphorylated plasmid, 1 $\mu$ l diluted annealed Oligos (1:200), 2 $\mu$ l DNA dilution buffer (Roche) 5X and H<sub>2</sub>O up to 10 $\mu$ l. After mixing well the reagents, 10 $\mu$ l T4 ligation buffer 10X (Roche) and 5U T4 ligase 5U/ $\mu$ l (Roche) were added. This solution (ligation mix) was incubated 5min RT. Two  $\mu$ l ligation mix were then used for subsequent transformation in Stbl3 cells. STBl3 cells are Chemically Competent E. coli cells designed for cloning direct repeats found in lentiviral expression vectors. Briefly, Stbl3 cells with 2 $\mu$ l ligation mix were incubated on ice for 30 minutes. Heat shock at 42°C for 1 minute and incubation on ice for 2 minutes followed. 90  $\mu$ l L Broth (LB) were added and the suspension was shaken at 225 rpm for 60 minutes at 37°C. Bacteria were seeded in LB AGAR + 50 $\mu$ g/mL Ampicillin plates and incubated the plates Over Night (ON) at 37°C. Once the colonies were grown, 1 colony per plate was incubated during the day at 37 °C in LB + Ampi medium, 1:500 Ampicillin. A mini prep kit (QIAprep Spin Miniprep Kit, QIAGEN) was used to extract DNA and the samples were sent to Sanger Sequencing to verify the insertion of the sgRNA of interest. Subsequently, a maxi prep was performed using NucleoBond Xtra Maxi kit to extract the sgRNA plasmids

#### 4.5.4 sgRNAs design

The sgRNAs included in the library are derived from two sources: 1) sgRNAs targeting the "essential genes set" were selected from previously published sgRNA libraries (Horlbeck et al., 2016); 2) sgRNAs were designed using the CRISPick tool by inputting the genomic coordinates of the predicted TSS, using default settings, and choosing sgRNAs from the top 10 recommended by the tool. The sgRNA sequences (Table X.5) and Primers (Table X.6) used are below reported:

sgRNA	Forward	Reverse
LacZ	CACCGTGCTGCAAGGCGATTAAGT	AAACACTTAATCGCCTTGCAGCAC
GAL4	CACCGATGTGGTCATTCGTCATGA	AAACTCATGACGAATGACCACATC
FANCC sg1	CACCGGTCCCGCGGTTCGCCCCGGCAG	AAACCTGCCGGGCGACCGCGGGACC
FANCC sg2	CACCGGGGTCTGGCCGACACGTCAG	AAACCTGACGTGTCGGCCAGACCCC
FANCC sg3	CACCGGGAGGGCGACCGGCTCAAAG	AAACCTTTGAGCCGGTCGCCCTCCC
FANCC sg4	CACCGGAGGCCGACGAACGCAGCGA	AAACTCGCTGCGTTCTGCGGCCTCC
FANCC sg5	CACCGGAGCCACCGCCCCGGGATCTG	AAACCAGATCCCGGGCGGTGGCTCC
FANCD2 sg1	CACCGGGAAGTCGAAAACCTACGGG	AAACCCCGTAGTTTTCGACTTTCCC
FANCD2 sg2	CACCGGCGGTGAGTAAGTGGAGCAA	AAACTTGCTCCACTTACTCACCGCC
FANCD2 sg3	CACCGGCTTAGAGATTAGGCCGCAG	AAACCTGCGGCCTAATCTCTAAGCC
FANCD2 sg4	CACCGGCGGCCCGGACTTAGAGATT	AAACAATCTCTAAGTCCGGGCCGCC
FANCD2 sg5	CACCGGTAAATGCGGAAACGAGAA	AAACTTCTCGTTTCCGCATTTTACC

Table 4.5: sgRNA sequences.

Primers	Forward	Reverse
FANCC	TCAAGGTCTTGGGTATGCACC	GCCATTTCGCCTTTGAGTGTTAAA
FANCD2	AAAACGGGAGAGAGTCAGAATCA	ACGCTCACAAGACAAAAGGCA

Table 4.6: Primers sequences.

#### 4.5.5 Lentiviral production and sgRNA delivery

HEK293T cells were seeded 24 h before transfection at 70-80% confluency in 6-well plates containing DMEM media with Glutamax, supplemented with 10% Tetracycline-FREE FBS and 100  $\mu\text{g}/\text{mL}$  Penicillin/Streptomycin. The sgRNAs were packaged using the psPAX2 (gag&pol) and VSV-G (envelope) plasmids, following the Lipofectamine 3000 transfection protocol. The transfection was performed preparing two mixes. The first one (Lipo mix) was prepared using 125  $\mu\text{L}$  Opti-MEM and 4  $\mu\text{L}$  Lipofectamine 3000. The second one (DNA mix) was prepared using 125  $\mu\text{L}$  Opti-MEM, 1.8  $\mu\text{g}$  Plasmid sgRNA, 1.35  $\mu\text{g}$  psPAX2, 0.45  $\mu\text{g}$  vsv-g, 5  $\mu\text{L}$  p3000. The two mixes were united 1:1 and incubated at room temperature (RT) for 20 min. The final mix was then added dropwise to cells with 1.5 mL of fresh media that was replaced after 12-16 h. Supernatant was collected 24 h after media replacement and centrifuged to remove cell debris, filtered through 0.22  $\mu\text{m}$  syringe filters. Filtered supernatant was used for subsequent cells infection. For cell transduction, 350.000 Capan-1 cells were seeded per well of 6W plates 12-16 h prior to transduction. 8  $\mu\text{g}/\text{mL}$  polybrene was added to the undiluted lentiviral supernatant to a final concentration of 1  $\mu\text{g}/\text{mL}$ . Transduction was usually carried out over-day and then media was changed. 2  $\mu\text{g}/\text{mL}$  Puromycin selection was started 72 h after the end of infection. Stable cell lines expressing dCas9-KRAB sgRNA were treated with 1  $\mu\text{g}/\text{mL}$  Doxycycline to induce gene silencing.

## 4.6 Evaluation of gene expression levels

### 4.6.1 Total RNA extraction

Total RNA extraction was carried out using the miRNeasy Micro Kit (Qiagen). The samples were prepared according to the guidelines in the miRNeasy Micro Handbook. The cells were collected by centrifugation, resuspended in 700  $\mu$ L QIAzol Lysis Reagent, and left to incubate at room temperature for 5 minutes. Subsequently, 140  $\mu$ L chloroform were added, and the mixture was vortexed for 15 seconds before a 2-3 minute incubation at room temperature. The samples were then centrifuged at 12,000 x g for 15 minutes at 4°C. The upper aqueous phase was carefully transferred to a fresh tube, followed by the addition of 1.5 volumes of 100% ethanol. The mixture was then loaded onto an RNeasy MinElute spin column and centrifuged at >8000 x g for 15 seconds. The flow-through was discarded, and the column was washed with 350  $\mu$ L RWT buffer. DNA was removed with DNase treatment on the columns, prepared by diluting 10  $\mu$ L DNase I (Qiagen) in 70  $\mu$ L RDD buffer and incubating at room temperature for 15 minutes. The columns were then washed with 350  $\mu$ L RWT buffer, followed by two washes with 500  $\mu$ L RPE buffer, each with centrifugation at >8000 x g for 15 seconds and 2 minutes, respectively. The columns were further centrifuged to remove any residual ethanol. RNA was eluted in RNase-free water and quantified using a NanoDrop UV-Vis Spectrophotometer (Thermo Scientific). The RNA samples were then stored at -80°C.

### 4.6.2 mRNA retrotranscription

Total RNA was retro-transcribed in cDNA according to SuperScript VILO cDNA synthesis kit. The reagent used for the retrotranscription were: 100-1  $\mu$ g RNA, 4  $\mu$ L 5X VILO Reaction Mix, 2  $\mu$ g 10X SuperScript Enzyme Mix and H<sub>2</sub>O up to 20  $\mu$ L. The reaction was performed in a thermal cycler. The conditions used for each steps were: 10 min at 25°C for the Annealing step; 60 min at 42°C for the Extension step; 5 min at 85°C for the Enzyme inactivation step; hold at 4°C for the Incubation step. cDNA was stored at -20°C for subsequent amplification.

### 4.6.3 RT-qPCR

Expression levels of target protein coding genes were detected by Real-Time quantitative PCR (RT-qPCR) with Fast SYBR Green reagents (Life Technologies). For each cDNA sample, a reaction was set-up as follows: 10  $\mu$ L 2X Fast SYBR Master Mix, 2  $\mu$ L Forward and reverse primers 3.3  $\mu$ M, 1-5 ng/ $\mu$ L Template cDNA, Nuclease-free H<sub>2</sub>O up to 20  $\mu$ L. Reactions were carried out in BIORAD CFX Real-Time PCR detection system under the following cycling conditions: Initial denaturation at 95°C for 15 min; Denaturation at 94°C for 15 seconds (39 cycles); Annealing

at 55°C for 30 seconds (39 cycles); Extension at 70°C for 30 seconds (39 cycles). Experiments were conducted in triplicate. Raw Ct data were processed using Microsoft Excel (Microsoft). To normalize the data,  $\Delta$  Ct values were calculated by comparing them to the Ct values of the housekeeping gene RPLPO. The results are presented in terms of relative RNA expression, using the  $2^{-\Delta Ct}$  formula. Primer pairs were designed with the help of the Primer3 software for computer-assisted primer design. The sequences of the used primers are below reported:

Gene	Forward	Reverse
RPLPO	CAGCAGTTTCTCCAGAGC	TTCATTGTGGGAGCAGAC
FANCC	TCAAGGTCTTGGGTATGCACC	GCCATTTCGCCTTTGAGTGTTAAA
FANCD2	AAAACGGGAGAGAGTCAGAATCA	ACGCTCACAAGACAAAAGGCA
dCas9	GATCGCAAAGTCTGAGCAGG	CTACCCTTGTCCCACACGAT

Table 4.7: **Primers sequence for RT-qPCR.**

# Bibliography

- [1] Giuseppina Giglia-Mari, Angelika Zotter, and Wim Vermeulen. Dna damage response. *Cold Spring Harbor perspectives in biology*, 3(1):a000745, 2011.
- [2] Razqallah Hakem. Dna-damage repair; the good, the bad, and the ugly. *The EMBO journal*, 27(4):589–605, 2008.
- [3] Nimrat Chatterjee and Graham C Walker. Mechanisms of dna damage, repair, and mutagenesis. *Environmental and molecular mutagenesis*, 58(5):235–263, 2017.
- [4] Ruixue Huang and Ping-Kun Zhou. Dna damage repair: historical perspectives, mechanistic pathways and clinical translation for targeted cancer therapy. *Signal transduction and targeted therapy*, 6(1):254, 2021.
- [5] Yan Xu, Hui Li, Fan Yang, Dingpeng Yang, and Bin-Bing S Zhou. Cell plasticity and genomic instability in cancer evolution. *Genome Instability & Disease*, 1:301–309, 2020.
- [6] Gustavo S França, Maayan Baron, Benjamin R King, Jozef P Bossowski, Alicia Bjornberg, Maayan Pour, Anjali Rao, Ayushi S Patel, Selim Misirlioglu, Dalia Barkley, et al. Cellular adaptation to cancer therapy along a resistance continuum. *Nature*, pages 1–8, 2024.
- [7] Yucui Zhao, Tingting Lu, Yanwei Song, Yanqin Wen, Zheng Deng, Jiahui Fan, Minghui Zhao, Ruyi Zhao, Yuntao Luo, Jianzhu Xie, et al. Cancer cells enter an adaptive persistence to survive radiotherapy and repopulate tumor. *Advanced Science*, 10(8):2204177, 2023.
- [8] Nigel J O’Neil, Melanie L Bailey, and Philip Hieter. Synthetic lethality and cancer. *Nature Reviews Genetics*, 18(10):613–623, 2017.
- [9] Jeremy Setton, Michael Zinda, Nadeem Riaz, Daniel Durocher, Michal Zimmermann, Maria Koehler, Jorge S Reis-Filho, and Simon N Powell. Synthetic lethality in cancer therapeutics: the next generation. *Cancer discovery*, 11(7):1626–1635, 2021.
- [10] Grzegorz Nalepa and D Wade Clapp. Fanconi anaemia and cancer: an intricate relationship. *Nature Reviews Cancer*, 18(3):168–185, 2018.
- [11] Sarah J Taylor, Mark J Arends, and Simon P Langdon. Inhibitors of the fanconi anaemia pathway as potential antitumour agents for ovarian cancer. *Exploration of targeted anti-tumor therapy*, 1(1):26, 2020.

- [12] Wenjun Liu, Anna Palovcak, Fang Li, Alyan Zafar, Fenghua Yuan, and Yanbin Zhang. Fanconi anemia pathway as a prospective target for cancer intervention. *Cell & bioscience*, 10:1–14, 2020.
- [13] Qian-Wen Liu, Zhi-Wen Yang, Qing-Hai Tang, Wen-Er Wang, Da-Sheng Chu, Jin-Feng Ji, Qi-Yu Fan, Hong Jiang, Qin-Xin Yang, Hui Zhang, et al. The power and the promise of synthetic lethality for clinical application in cancer treatment. *Biomedicine & Pharmacotherapy*, 172:116288, 2024.
- [14] Xinlin Xu, Yixi Xu, Ruiyuan Guo, Ran Xu, Congcong Fu, Mengtan Xing, Hiroyuki Sasanuma, Qing Li, Minoru Takata, Shunichi Takeda, et al. Fanconi anemia proteins participate in a break-induced-replication-like pathway to counter replication stress. *Nature Structural & Molecular Biology*, 28(6):487–500, 2021.
- [15] Alfredo Rodríguez and Alan D’Andrea. Fanconi anemia pathway. *Current Biology*, 27(18):R986–R988, 2017.
- [16] Raphael Ceccaldi, Prabha Sarangi, and Alan D D’Andrea. The fanconi anaemia pathway: new players and new functions. *Nature reviews Molecular cell biology*, 17(6):337–349, 2016.
- [17] Lily C Wang and Jean Gautier. The fanconi anemia pathway and icl repair: implications for cancer therapy. *Critical reviews in biochemistry and molecular biology*, 45(5):424–439, 2010.
- [18] MD Tischkowitz and SV Hodgson. Fanconi anaemia. *Journal of medical genetics*, 40(1):1–10, 2003.
- [19] Stephan Lobitz and Eunike Velleuer. Guido fanconi (1892–1979): a jack of all trades. *Nature Reviews Cancer*, 6(11):893–898, 2006.
- [20] Satoru Hashimoto, Hirofumi Anai, and Katsuhiko Hanada. Mechanisms of interstrand dna crosslink repair and human disorders. *Genes and Environment*, 38:1–8, 2016.
- [21] Andrew J Deans and Stephen C West. Dna interstrand crosslink repair and cancer. *Nature reviews cancer*, 11(7):467–480, 2011.
- [22] Hannah L Williams, Max E Gottesman, and Jean Gautier. The differences between icl repair during and outside of s phase. *Trends in Biochemical Sciences*, 38(8):386–393, 2013.
- [23] Yutong Xue, Yongjiang Li, Rong Guo, Chen Ling, and Weidong Wang. Fancm of the fanconi anemia core complex is required for both monoubiquitination and dna repair. *Human molecular genetics*, 17(11):1641–1652, 2008.
- [24] Yuyong Tao, Changjiang Jin, Xu Li, Shali Qi, Lingluo Chu, Liwen Niu, Xuebiao Yao, and Maikun Teng. The structure of the fancm–mhf complex reveals physical features for functional assembly. *Nature communications*, 3(1):782, 2012.
- [25] Min Huang, Jung Min Kim, Bunsyo Shiotani, Kailin Yang, Lee Zou, and Alan D D’Andrea. The fancm/faap24 complex is required for the dna interstrand crosslink-induced checkpoint response. *Molecular cell*, 39(2):259–268,

- 2010.
- [26] Xiaoyu Xue, Patrick Sung, and Xiaolan Zhao. Functions and regulation of the multitasking fancm family of dna motor proteins. *Genes & Development*, 29(17):1777–1788, 2015.
  - [27] Alberto Ciccia, Chen Ling, Rachel Coulthard, Zhijiang Yan, Yutong Xue, Amom Ruhikanta Meetei, El Houari Laghmani, Hans Joenje, Neil McDonald, Johan P de Winter, et al. Identification of faap24, a fanconi anemia core complex protein that interacts with fancm. *Molecular cell*, 25(3):331–343, 2007.
  - [28] George-Lucian Moldovan and Alan D D’Andrea. How the fanconi anemia pathway guards the genome. *Annual review of genetics*, 43(1):223–249, 2009.
  - [29] Joshi Niraj, Anniina Färkkilä, and Alan D D’Andrea. The fanconi anemia pathway in cancer. *Annual review of cancer biology*, 3(1):457–478, 2019.
  - [30] Yaling Huang, Justin WC Leung, Megan Lowery, Nobuko Matsushita, Yucan Wang, Xi Shen, Do Huong, Minoru Takata, Junjie Chen, and Lei Li. Modularized functions of the fanconi anemia core complex. *Cell reports*, 7(6):1849–1857, 2014.
  - [31] Chenchen Dan, Hongjing Pei, Buzhe Zhang, Xuan Zheng, Dongmei Ran, and Changzheng Du. Fanconi anemia pathway and its relationship with cancer. *Genome Instability & Disease*, 2(3):175–183, 2021.
  - [32] Shengliu Wang, Renjing Wang, Christopher Peralta, Ayat Yaseen, and Nikola P Pavletich. Structure of the fa core ubiquitin ligase closing the id clamp on dna. *Nature structural & molecular biology*, 28(3):300–309, 2021.
  - [33] Andrew J Deans and Stephen C West. Fancm connects the genome instability disorders bloom’s syndrome and fanconi anemia. *Molecular cell*, 36(6):943–953, 2009.
  - [34] Eunyoung Jeong, Seong-Gyu Lee, Hyun-Suk Kim, Jihyeon Yang, Jinwoo Shin, Youngran Kim, Jihan Kim, Orlando D Schärer, Youngjin Kim, Jung-Eun Yeo, et al. Structural basis of the fanconi anemia-associated mutations within the fanca and fancg complex. *Nucleic acids research*, 48(6):3328–3342, 2020.
  - [35] Dipesh Kumar Singh, Rigel Salinas Gamboa, Avinash Kumar Singh, Birgit Walkemeier, Jelle Van Leene, Geert De Jaeger, Imran Siddiqi, Raphael Guerois, Wayne Crismani, and Raphael Mercier. The fancf–fance–fancf complex is evolutionarily conserved and regulates meiotic recombination. *Nucleic Acids Research*, 51(6):2516–2528, 2023.
  - [36] Susan M Gordon, Noa Alon, and Manuel Buchwald. Fancf, fancf, and fancd2 form a ternary complex essential to the integrity of the fanconi anemia dna damage response pathway. *Journal of Biological Chemistry*, 280(43):36118–36125, 2005.
  - [37] France Léveillé, Miriam Ferrer, Annette L Medhurst, El Houari Laghmani, Martin A Rooimans, Patrick Bier, Jurgen Steltenpool, Tom A Titus, John H

- Postlethwait, Maureen E Hoatlin, et al. The nuclear accumulation of the fanconi anemia protein fance depends on fancc. *DNA repair*, 5(5):556–565, 2006.
- [38] Francesca E Morreale, Alessio Bortoluzzi, Viduth K Chaugule, Connor Arkinson, Helen Walden, and Alessio Ciulli. Allosteric targeting of the fanconi anemia ubiquitin-conjugating enzyme ube2t by fragment screening. *Journal of medicinal chemistry*, 60(9):4093–4098, 2017.
- [39] Yingying Zhang, Xiaowei Zhou, Lixia Zhao, Chao Li, Hengqi Zhu, Long Xu, Liran Shan, Xiang Liao, Zekun Guo, and Peitang Huang. Ube2w interacts with fanc1 and regulates the monoubiquitination of fanconi anemia protein fancd2. *Molecules and cells*, 31(2):113–122, 2011.
- [40] Yuichi J Machida, Yuka Machida, Yuefeng Chen, Allan M Gurtan, Gary M Kupfer, Alan D D’Andrea, and Anindya Dutta. Ube2t is the e2 in the fanconi anemia pathway and undergoes negative autoregulation. *Molecular cell*, 23(4):589–596, 2006.
- [41] Michael F Sharp, Rohan Bythell-Douglas, Andrew J Deans, and Wayne Crismani. The fanconi anemia ubiquitin e3 ligase complex as an anti-cancer target. *Molecular Cell*, 81(11):2278–2289, 2021.
- [42] Kimon Lemonidis, Connor Arkinson, Martin L Rennie, and Helen Walden. Mechanism, specificity, and function of fancd2-fanci ubiquitination and deubiquitination. *The FEBS Journal*, 289(16):4811–4829, 2022.
- [43] Martin L Rennie, Connor Arkinson, Viduth K Chaugule, Rachel Toth, and Helen Walden. Structural basis of fancd2 deubiquitination by usp1- uaf1. *Nature Structural & Molecular Biology*, 28(4):356–364, 2021.
- [44] Fengshan Liang, Adam S Miller, Simonne Longerich, Caroline Tang, David Maranon, Elizabeth A Williamson, Robert Hromas, Claudia Wiese, Gary M Kupfer, and Patrick Sung. Dna requirement in fancd2 deubiquitination by usp1-uaf1-rad51ap1 in the fanconi anemia dna damage response. *Nature communications*, 10(1):2849, 2019.
- [45] Vibe H Oestergaard, Frederic Langevin, Hendrik J Kuiken, Paul Pace, Wojciech Niedzwiedz, Laura J Simpson, Mioko Ohzeki, Minoru Takata, Julian E Sale, and Ketan J Patel. Deubiquitination of fancd2 is required for dna crosslink repair. *Molecular cell*, 28(5):798–809, 2007.
- [46] Jung Min Kim, Kalindi Parmar, Min Huang, David M Weinstock, Carrie Ann Ruit, Jeffrey L Kutok, and Alan D D’Andrea. Inactivation of murine usp1 results in genomic instability and a fanconi anemia phenotype. *Developmental cell*, 16(2):314–320, 2009.
- [47] Masamichi Ishiai. Regulation of the fanconi anemia dna repair pathway by phosphorylation and monoubiquitination. *Genes*, 12(11):1763, 2021.
- [48] David Lopez-Martinez, Marian Kupculak, Di Yang, Yasunaga Yoshikawa,

- Chih-Chao Liang, Ronghu Wu, Steven P Gygi, and Martin A Cohn. Phosphorylation of fancd2 inhibits the fancd2/fanci complex and suppresses the fanconi anemia pathway in the absence of dna damage. *Cell reports*, 27(10):2990–3005, 2019.
- [49] Pablo Alcón, Shabih Shakeel, Zhuo A Chen, Juri Rappsilber, Ketan J Patel, and Lori A Passmore. Fancd2–fanci is a clamp stabilized on dna by monoubiquitination of fancd2 during dna repair. *Nature structural & molecular biology*, 27(3):240–248, 2020.
- [50] Martin L Rennie, Kimon Lemonidis, Connor Arkinson, Viduth K Chaugule, Mairi Clarke, James Streetley, Laura Spagnolo, and Helen Walden. Differential functions of fanci and fancd2 ubiquitination stabilize id2 complex on dna. *EMBO reports*, 21(7):e50133, 2020.
- [51] Winnie Tan, Sylvie van Twest, Andrew Leis, Rohan Bythell-Douglas, Vincent J Murphy, Michael Sharp, Michael W Parker, Wayne Crismani, and Andrew J Deans. Monoubiquitination by the human fanconi anemia core complex clamps fanci: Fancd2 on dna in filamentous arrays. *elife*, 9:e54128, 2020.
- [52] Renjing Wang, Shengliu Wang, Ankita Dhar, Christopher Peralta, and Nikola P Pavletich. Dna clamp function of the monoubiquitinated fanconi anaemia id complex. *Nature*, 580(7802):278–282, 2020.
- [53] Irene Garcia-Higuera, Toshiyasu Taniguchi, Shridar Ganesan, M Stephen Meyn, Cynthia Timmers, James Hejna, Markus Grompe, and Alan D D’Andrea. Interaction of the fanconi anemia proteins and brca1 in a common pathway. *Molecular cell*, 7(2):249–262, 2001.
- [54] Kimiyo N Yamamoto, Shunsuke Kobayashi, Masataka Tsuda, Hitoshi Kurumizaka, Minoru Takata, Koichi Kono, Josef Jiricny, Shunichi Takeda, and Kouji Hirota. Involvement of slx4 in interstrand cross-link repair is regulated by the fanconi anemia pathway. *Proceedings of the National Academy of Sciences*, 108(16):6492–6496, 2011.
- [55] Yonghwan Kim, Gabriella S Spitz, Uma Veturi, Francis P Lach, Arleen D Auerbach, and Agata Smogorzewska. Regulation of multiple dna repair pathways by the fanconi anemia protein slx4. *Blood, The Journal of the American Society of Hematology*, 121(1):54–63, 2013.
- [56] Daisy Klein Douwel, Rick ACM Boonen, David T Long, Anna A Szypowska, Markus Räschle, Johannes C Walter, and Puck Knipscheer. Xpf-ercc1 acts in unhooking dna interstrand crosslinks in cooperation with fancd2 and fancp/slx4. *Molecular cell*, 54(3):460–471, 2014.
- [57] Juan P Trujillo, Leonardo B Mina, Roser Pujol, Massimo Bogliolo, Joris Andrieux, Muriel Holder, Beatrice Schuster, Detlev Schindler, and Jordi Surallés. On the role of fan1 in fanconi anemia. *Blood, The Journal of the American Society of Hematology*, 120(1):86–89, 2012.
- [58] Alexandra Vaisman, John P McDonald, and Roger Woodgate. Translesion

- dna synthesis. *EcoSal plus*, 5(1):10–1128, 2012.
- [59] Kanchan D Mirchandani, Ryan M McCaffrey, and Alan D D’Andrea. The fanconi anemia core complex is required for efficient point mutagenesis and rev1 foci assembly. *DNA repair*, 7(6):902–911, 2008.
  - [60] Xuan Li and Wolf-Dietrich Heyer. Homologous recombination in dna repair and dna damage tolerance. *Cell research*, 18(1):99–113, 2008.
  - [61] Youngho Kwon, Heike Rösner, Weixing Zhao, Platon Selemenakis, Zhuoling He, Ajinkya S Kawale, Jeffrey N Katz, Cody M Rogers, Francisco E Neal, Aida Badamchi Shabestari, et al. Dna binding and rad51 engagement by the brca2 c-terminus orchestrate dna repair and replication fork preservation. *Nature communications*, 14(1):432, 2023.
  - [62] Tohru Miura, Yoshimasa Yamana, Takehiko Usui, Hiroaki I Ogawa, Masa-Toshi Yamamoto, and Kohji Kusano. Homologous recombination via synthesis-dependent strand annealing in yeast requires the irc20 and srs2 dna helicases. *Genetics*, 191(1):65–78, 2012.
  - [63] Anna H Bizard and Ian D Hickson. The dissolution of double holliday junctions. *Cold Spring Harbor perspectives in biology*, 6(7):a016477, 2014.
  - [64] Wenpeng Liu, Piotr Polaczek, Ivan Roubal, Yuan Meng, Won-chae Choe, Marie-Christine Caron, Carl A Sedgeman, Yu Xi, Changwei Liu, Qiong Wu, et al. Fancd2 and rad51 recombinase directly inhibit dna2 nuclease at stalled replication forks and fancd2 acts as a novel rad51 mediator in strand exchange to promote genome stability. *Nucleic Acids Research*, 51(17):9144–9165, 2023.
  - [65] Koichi Sato, Mayo Shimomuki, Yoko Katsuki, Daisuke Takahashi, Wataru Kobayashi, Masamichi Ishiai, Hiroyuki Miyoshi, Minoru Takata, and Hitoshi Kurumizaka. Fanci-fancd2 stabilizes the rad51-dna complex by binding rad51 and protects the 5′-dna end. *Nucleic acids research*, 44(22):10758–10771, 2016.
  - [66] Zeina Kais, Beatrice Rondinelli, Amie Holmes, Colin O’Leary, David Kozono, Alan D D’Andrea, and Raphael Ceccaldi. Fancd2 maintains fork stability in brca1/2-deficient tumors and promotes alternative end-joining dna repair. *Cell reports*, 15(11):2488–2499, 2016.
  - [67] Johanna Michl, Jutta Zimmer, Francesca M Buffa, Ultan McDermott, and Madalena Tarsounas. Fancd2 limits replication stress and genome instability in cells lacking brca2. *Nature structural & molecular biology*, 23(8):755–757, 2016.
  - [68] Th Dobzhansky. Genetics of natural populations. xiii. recombination and variability in populations of drosophila pseudoobscura. *Genetics*, 31(3):269, 1946.
  - [69] John C Lucchesi. Synthetic lethality and semi-lethality among functionally related mutants of drosophila melanogaster. *Genetics*, 59(1):37, 1968.
  - [70] Kevin M Hennessy, Angela Lee, Ellson Chen, and David Botstein. A group of interacting yeast dna replication genes. *Genes & development*, 5(6):958–969,

- 1991.
- [71] ALAN Bender and John R Pringle. Use of a screen for synthetic lethal and multicopy suppressor mutants to identify two new genes involved in morphogenesis in *saccharomyces cerevisiae*. *Molecular and cellular biology*, 1991.
  - [72] Sebastian MB Nijman. Synthetic lethality: general principles, utility and detection using genetic screens in human cells. *FEBS letters*, 585(1):1–6, 2011.
  - [73] Donal P McLornan, Alan List, and Ghulam J Mufti. Applying synthetic lethality for the selective targeting of cancer. *New England Journal of Medicine*, 371(18):1725–1735, 2014.
  - [74] Biyu Zhang, Chen Tang, Yanli Yao, Xiaohan Chen, Chi Zhou, Zhiting Wei, Feiyang Xing, Lan Chen, Xiang Cai, Zhiyuan Zhang, et al. The tumor therapy landscape of synthetic lethality. *Nature communications*, 12(1):1275, 2021.
  - [75] Meiyi Ge, Jian Luo, Yi Wu, Guobo Shen, and Xi Kuang. The biological essence of synthetic lethality: Bringing new opportunities for cancer therapy. *MedComm–Oncology*, 3(1):e70, 2024.
  - [76] Shijie Li, Win Topatana, Sarun Juengpanich, Jiasheng Cao, Jiahao Hu, Bin Zhang, Diana Ma, Xiujun Cai, and Mingyu Chen. Development of synthetic lethality in cancer: molecular and cellular classification. *Signal Transduction and Targeted Therapy*, 5(1):241, 2020.
  - [77] Geoffrey Kim, Gwynn Ison, Amy E McKee, Hui Zhang, Shenghui Tang, Thomas Gwise, Rajeshwari Sridhara, Eunice Lee, Abraham Tzou, Reena Philip, et al. Fda approval summary: olaparib monotherapy in patients with deleterious germline brca-mutated advanced ovarian cancer treated with three or more lines of chemotherapy. *Clinical cancer research*, 21(19):4257–4261, 2015.
  - [78] Mariana Paes Dias, Sarah C Moser, Shridar Ganesan, and Jos Jonkers. Understanding and overcoming resistance to parp inhibitors in cancer therapy. *Nature reviews Clinical oncology*, 18(12):773–791, 2021.
  - [79] M Rose, JT Burgess, K O’Byrne, DJ Richard, and E Bolderson. Parp inhibitors: clinical relevance, mechanisms of action and tumor resistance. *front cell dev biol*. 2020; 8: 564601, 2020.
  - [80] Yolanda Jerez, Ivan Márquez-Rodas, Inmaculada Aparicio, Manuel Alva, Miguel Martín, and Sara López-Tarruella. Poly (adp-ribose) polymerase inhibition in patients with breast cancer and brca 1 and 2 mutations. *Drugs*, 80:131–146, 2020.
  - [81] Parasvi S Patel, Arash Algouneh, and Razq Hakem. Exploiting synthetic lethality to target brca1/2-deficient tumors: where we stand. *Oncogene*, 40(17):3001–3014, 2021.
  - [82] Christopher J Lord and Alan Ashworth. Parp inhibitors: Synthetic lethality in the clinic. *Science*, 355(6330):1152–1158, 2017.

- [83] Thomas Helleday. The underlying mechanism for the parp and brca synthetic lethality: clearing up the misunderstandings. *Molecular oncology*, 5(4):387–393, 2011.
- [84] Shuangying Li, Liangliang Wang, Yuanyuan Wang, Changyi Zhang, Zhenya Hong, and Zhiqiang Han. The synthetic lethality of targeting cell cycle checkpoints and parps in cancer treatment. *Journal of Hematology & Oncology*, 15(1):147, 2022.
- [85] P Lesueur, F Chevalier, JB Austry, W Waissi, H Burckel, G Noel, et al. Poly-(adp-ribose)-polymerase inhibitors as radiosensitizers: a systematic review of pre-clinical and clinical human studies. *oncotarget*. 2017; 8: 69105–24, 2019.
- [86] Bella Kaufman, Ronnie Shapira-Frommer, Rita K Schmutzler, M William Audeh, Michael Friedlander, Judith Balmaña, Gillian Mitchell, Georgeta Fried, Salomon M Stemmer, Ayala Hubert, et al. Olaparib monotherapy in patients with advanced cancer and a germline brca1/2 mutation. *Journal of clinical oncology*, 33(3):244–250, 2015.
- [87] Y Pommier and J Murai. Classification of parp inhibitors based on parp trapping and catalytic inhibition, and rationale for combinations. *Annals of Oncology*, 26:ii8, 2015.
- [88] Michalis Petropoulos, Angeliki Karamichali, Giacomo G Rossetti, Alena Freudenmann, Luca G Iacovino, Vasilis S Dionellis, Sotirios K Sotiriou, and Thanos D Halazonetis. Transcription–replication conflicts underlie sensitivity to parp inhibitors. *Nature*, 628(8007):433–441, 2024.
- [89] Laura Cortesi, Hope S Rugo, and Christian Jackisch. An overview of parp inhibitors for the treatment of breast cancer. *Targeted oncology*, 16(3):255–282, 2021.
- [90] FDA/ Food and Drug Administration. Fda approves talazoparib for gbrcam her2-negative locally advanced or metastatic breast cancer, 2018/ 2018.
- [91] FDA/ Food and Drug Administration. Fda approves talazoparib with enzalutamide for hrr gene-mutated metastatic castration-resistant prostate cancer, 2023/ 2023.
- [92] Taofeek K Owonikoko, Mary W Redman, Lauren A Byers, Fred R Hirsch, Philip C Mack, Lawrence H Schwartz, Jeffrey D Bradley, Thomas E Stinchcombe, Natasha B Leighl, Tareq Al Baghdadi, et al. Phase 2 study of talazoparib in patients with homologous recombination repair–deficient squamous cell lung cancer: Lung-map substudy s1400g. *Clinical lung cancer*, 22(3):187–194, 2021.
- [93] Andrei Kachmazov, Larisa Bolotina, Anna Kornietskaya, Olesya Kuznetsova, Maxim Ivanov, and Alexander Fedenko. Complete response to talazoparib in patient with pancreatic adenocarcinoma harboring somatic palb2 mutation: A case report and literature review. *Frontiers in Oncology*, 12:953908, 2022.
- [94] Arjun Mittra, Geraldine H O’Sullivan Coyne, Jennifer Zlott, Shivaani Kumar, Robert Meehan, Lawrence Rubinstein, Lamin Juwara, Deborah Wilsker,

- Jiuping Ji, Brandon Miller, et al. Pharmacodynamic effects of the parp inhibitor talazoparib (mdv3800, bmn 673) in patients with brca-mutated advanced solid tumors. *Cancer Chemotherapy and Pharmacology*, 93(3):177–189, 2024.
- [95] AZ/ AstraZeneca. Lynparza approved by the us food and drug administration for the treatment of advanced ovarian cancer in patients with germline brca-mutations, 2014/ 2014.
- [96] FDA/ Food and Drug Administration. Niraparib (zejula), 2017/ 2017.
- [97] NCI/ National Cancer Institute. Fda approves niraparib as maintenance therapy for recurrent ovarian cancer, 2017/ 2017.
- [98] FDA/ Food and Drug Administration. Fda approves rucaparib for maintenance treatment of recurrent ovarian, fallopian tube, or primary peritoneal cancer, 2018/ 2018.
- [99] NCI/ National Cancer Institute. Rucaparib approved as maintenance treatment for some recurrent ovarian cancers, 2018/ 2018.
- [100] Sheridan M Hoy. Talazoparib: first global approval. *Drugs*, 78(18):1939–1946, 2018.
- [101] FDA/ Food and Drug Administration. Fda approves olaparib for gbrcam metastatic pancreatic adenocarcinoma, 2019/ 2019.
- [102] NCI/ National Cancer Institute. With two fda approvals, prostate cancer treatment enters the parp era, 2020/ 2020.
- [103] FDA/ Food and Drug Administration. Fda approves talazoparib with enzalutamide for hrr gene-mutated metastatic castration-resistant prostate cancer, 2023/ 2023.
- [104] He Li, Zhao-Yi Liu, Nayiyuan Wu, Yong-Chang Chen, Quan Cheng, and Jing Wang. Parp inhibitor resistance: the underlying mechanisms and clinical implications. *Molecular cancer*, 19:1–16, 2020.
- [105] Yu-Yi Chu, Clinton Yam, Hirohito Yamaguchi, and Mien-Chie Hung. Biomarkers beyond brca: promising combinatorial treatment strategies in overcoming resistance to parp inhibitors. *Journal of biomedical science*, 29(1):86, 2022.
- [106] Xiaoyu Fu, Ping Li, Qi Zhou, Ruyuan He, Guannan Wang, Shiya Zhu, Amir Bagheri, Gary Kupfer, Huadong Pei, and Juanjuan Li. Mechanism of parp inhibitor resistance and potential overcoming strategies. *Genes & diseases*, 11(1):306–320, 2024.
- [107] Elena Giudice, Marica Gentile, Vanda Salutari, Caterina Ricci, Lucia Musacchio, Maria Vittoria Carbone, Viola Ghizzoni, Floriana Camarda, Francesca Tronconi, Camilla Nero, et al. Parp inhibitors resistance: mechanisms and perspectives. *Cancers*, 14(6):1420, 2022.
- [108] Kasper Fugger, Graeme Hewitt, Stephen C West, and Simon J Boulton. Tackling parp inhibitor resistance. *Trends in cancer*, 7(12):1102–1118, 2021.

- [109] Andrew McGuigan, Paul Kelly, Richard C Turkington, Claire Jones, Helen G Coleman, and R Stephen McCain. Pancreatic cancer: A review of clinical diagnosis, epidemiology, treatment and outcomes. *World journal of gastroenterology*, 24(43):4846, 2018.
- [110] Heng Zhu, Miaoyan Wei, Jin Xu, Jie Hua, Chen Liang, Qingcai Meng, Yiyin Zhang, Jiang Liu, Bo Zhang, Xianjun Yu, et al. Parp inhibitors in pancreatic cancer: molecular mechanisms and clinical applications. *Molecular cancer*, 19:1–15, 2020.
- [111] Hedy L Kindler, Pascal Hammel, Michele Reni, Eric Van Cutsem, Teresa Macarulla, Michael J Hall, Joon Oh Park, Daniel Hochhauser, Dirk Arnold, Do-Youn Oh, et al. Overall survival results from the polo trial: a phase iii study of active maintenance olaparib versus placebo for germline brca-mutated metastatic pancreatic cancer. *Journal of Clinical Oncology*, 40(34):3929–3939, 2022.
- [112] Jorg Kleeff, Murray Korc, Minoti Apte, Carlo La Vecchia, Colin D Johnson, Andrew V Biankin, Rachel E Neale, Margaret Tempero, David A Tuveson, Ralph H Hruban, et al. Pancreatic cancer. *Nature reviews Disease primers*, 2(1):1–22, 2016.
- [113] Prashanth Rawla, Tagore Sunkara, and Vinaya Gaduputi. Epidemiology of pancreatic cancer: global trends, etiology and risk factors. *World journal of oncology*, 10(1):10, 2019.
- [114] Qi Li, Zijian Feng, Ruyi Miao, Xun Liu, Chenxi Liu, and Zhen Liu. Prognosis and survival analysis of patients with pancreatic cancer: retrospective experience of a single institution. *World Journal of Surgical Oncology*, 20(1):11, 2022.
- [115] NCI/ National Cancer Institute. Cancer stat facts: Pancreatic cancer, 2024/2024.
- [116] Irena Ilic and Milena Ilic. International patterns in incidence and mortality trends of pancreatic cancer in the last three decades: A joinpoint regression analysis. *World Journal of Gastroenterology*, 28(32):4698, 2022.
- [117] Lola Rahib, Benjamin D Smith, Rhonda Aizenberg, Allison B Rosenzweig, Julie M Fleshman, and Lynn M Matrisian. Projecting cancer incidence and deaths to 2030: the unexpected burden of thyroid, liver, and pancreas cancers in the united states. *Cancer research*, 74(11):2913–2921, 2014.
- [118] Rebecca L Siegel, Kimberly D Miller, Nikita Sandeep Wagle, and Ahmedin Jemal. Cancer statistics, 2023. *CA: a cancer journal for clinicians*, 73(1), 2023.
- [119] ACS/ American Cancer Society. Key statistics for pancreatic cancer, 2024/2024.
- [120] Giuseppe Lippi and Camilla Mattiuzzi. The global burden of pancreatic cancer. *Archives of Medical Science*, 16(1), 2020.
- [121] Christopher J Halbrook, Costas A Lyssiotis, Marina Pasca di Magliano,

- and Anirban Maitra. Pancreatic cancer: Advances and challenges. *Cell*, 186(8):1729–1754, 2023.
- [122] Andrew D Rhim and Ben Z Stanger. Molecular biology of pancreatic ductal adenocarcinoma progression: aberrant activation of developmental pathways. *Progress in molecular biology and translational science*, 97:41–78, 2010.
- [123] Elyne Backx, Katarina Coolens, Jan-Lars Van den Bossche, Isabelle Houbrecken, Elisa Espinet, and Ilse Rooman. On the origin of pancreatic cancer: molecular tumor subtypes in perspective of exocrine cell plasticity. *Cellular and molecular gastroenterology and hepatology*, 13(4):1243–1253, 2022.
- [124] Panagiotis Sarantis, Evangelos Koustas, Adriana Papadimitropoulou, Athanasios G Papavassiliou, and Michalis V Karamouzis. Pancreatic ductal adenocarcinoma: Treatment hurdles, tumor microenvironment and immunotherapy. *World journal of gastrointestinal oncology*, 12(2):173, 2020.
- [125] Christine G Simone, Tania Zuluaga Toro, Ellie Chan, Michael M Feely, Jose G Trevino, and Thomas J George Jr. Characteristics and outcomes of adenosquamous carcinoma of the pancreas. *Gastrointestinal cancer research: GCR*, 6(3):75, 2013.
- [126] Qunli Xiong, Zhiwei Zhang, Yongfeng Xu, and Qing Zhu. Pancreatic adenosquamous carcinoma: a rare pathological subtype of pancreatic cancer. *Journal of Clinical Medicine*, 11(24):7401, 2022.
- [127] Sonia T Orcutt, Domenico Coppola, and Pamela J Hodul. Colloid carcinoma of the pancreas: case report and review of the literature. *Case Reports in Pancreatic Cancer*, 2(1):40–45, 2016.
- [128] Yang Gao, Ya-Yun Zhu, and Zhou Yuan. Colloid (mucinous non-cystic) carcinoma of the pancreas: a case report. *Oncology letters*, 10(5):3195–3198, 2015.
- [129] Hilary A Brown, Jorge Dotto, Marie Robert, and Ronald R Salem. Squamous cell carcinoma of the pancreas. *Journal of clinical gastroenterology*, 39(10):915–919, 2005.
- [130] Seyed Hassan Abedi, Alireza Ahmadzadeh, and Amir Houshang Mohammad Alizadeh. Pancreatic squamous cell carcinoma. *Case reports in gastroenterology*, 11(1):219–224, 2017.
- [131] Stefano La Rosa, Fausto Sessa, and Carlo Capella. Acinar cell carcinoma of the pancreas: overview of clinicopathologic features and insights into the molecular pathology. *Frontiers in medicine*, 2:41, 2015.
- [132] Gabriel Benyomo Mpilla, Philip Agop Philip, Bassel El-Rayes, and Asfar Sohail Azmi. Pancreatic neuroendocrine tumors: Therapeutic challenges and research limitations. *World Journal of Gastroenterology*, 26(28):4036, 2020.
- [133] Teresa Starzyńska, Jakub Karczmarski, Agnieszka Paziowska, Maria Kulecka, Katarzyna Kuśnierz, Natalia Żeber-Lubecka, Filip Ambrożkiewicz, Michał

- Mikula, Beata Kos-Kudła, and Jerzy Ostrowski. Differences between well-differentiated neuroendocrine tumors and ductal adenocarcinomas of the pancreas assessed by multi-omics profiling. *International journal of molecular sciences*, 21(12):4470, 2020.
- [134] NCI/ National Cancer Institute. Pancreatic cancer treatment (pdq)–patient version, 2024/ 2024.
  - [135] NCI/ National Cancer Institute. Folfirinox, 2011/ 2023.
  - [136] Christoph Springfield, Dirk Jäger, Markus W Büchler, Oliver Strobel, Thilo Hackert, Daniel H Palmer, and John P Neoptolemos. Chemotherapy for pancreatic cancer. *La Presse Medicale*, 48(3):e159–e174, 2019.
  - [137] Evan Landau and Shalom Kalnicki. The evolving role of radiation in pancreatic cancer. *Surgical Clinics*, 98(1):113–125, 2018.
  - [138] Jeffrey Chi, Su Yun Chung, Shreya Prasad, and M Wasif Saif. The role of olaparib in metastatic pancreatic cancer. *Cancer medicine journal*, 4(3):89, 2021.
  - [139] Thomas P Slavin, Susan L Neuhausen, Bitu Nehoray, Mariana Niell-Swiler, Ilana Solomon, Christina Rybak, Kathleen Blazer, Aaron Adamson, Kai Yang, Sharon Sand, et al. The spectrum of genetic variants in hereditary pancreatic cancer includes fanconi anemia genes. *Familial cancer*, 17:235–245, 2018.
  - [140] Michiel S Van der Heijden, Charles J Yeo, Ralph H Hruban, and Scott E Kern. Fanconi anemia gene mutations in young-onset pancreatic cancer. *Cancer research*, 63(10):2585–2588, 2003.
  - [141] Carmelle D Rogers, Michiel S van der Heijden, Kieran Brune, Charles J Yeo, Ralph H Hruban, Scott E Kern, and Michael Goggins. The genetics of fancf and fancg in familial pancreatic cancer. *Cancer biology & therapy*, 3(2):167–169, 2004.
  - [142] Michiel S Van der Heijden, Jonathan R Brody, Eike Gallmeier, Steven C Cunningham, David A Dezentje, Dong Shen, Ralph H Hruban, and Scott E Kern. Functional defects in the fanconi anemia pathway in pancreatic cancer cells. *The American journal of pathology*, 165(2):651–657, 2004.
  - [143] Julie Earl, Cristina Galindo-Pumariño, Jessica Encinas, Emma Barreto, Maria E Castillo, Vanessa Pachón, Reyes Ferreiro, Mercedes Rodríguez-Garrote, Silvia González-Martínez, Teresa Ramon y Cajal, et al. A comprehensive analysis of candidate genes in familial pancreatic cancer families reveals a high frequency of potentially pathogenic germline variants. *EBioMedicine*, 53, 2020.
  - [144] Mathias Schwartz, Clement Korenbaum, Meriem Benfoda, Mickael Mary, Chrystelle Colas, Florence Coulet, Melissa Parrin, Philippe Jonveaux, Olivier Ingster, Sandra Granier, et al. Familial pancreatic adenocarcinoma: a retrospective analysis of germline genetic testing in a french multicentre cohort. *Clinical Genetics*, 96(6):579–584, 2019.

- [145] Elena Fountzilas, Alexia Eliades, Georgia-Angeliki Koliou, Achilleas Achilleos, Charalambos Loizides, Kyriakos Tsangaras, Dimitrios Pectasides, Joseph Sgouros, Pavlos Papakostas, Grigorios Rallis, et al. Clinical significance of germline cancer predisposing variants in unselected patients with pancreatic adenocarcinoma. *Cancers*, 13(2):198, 2021.
- [146] Xiaozhou Xie, Yulong Zhao, Fengying Du, Baoshan Cai, Zhen Fang, Yuan Liu, Yaodong Sang, Chenghao Ma, Zhaodong Liu, Xinshuai Yu, et al. Pan-cancer analysis of the tumorigenic role of fanconi anemia complementation group d2 (fancd2) in human tumors. *Genomics*, 116(1):110762, 2024.
- [147] Jacob P McCoy, Bernice Leung, and Bonnie W Lau. Inhibition of parp1 reduces cell viability and increases markers of dna damage in fanconi anemia-mutated acute myeloid leukemia. *Blood*, 138:4348, 2021.
- [148] Nuala McCabe, Nicholas C Turner, Christopher J Lord, Katarzyna Kluzek, Aneta Białkowska, Sally Swift, Sabrina Giavara, Mark J O'Connor, Andrew N Tutt, Małgorzata Z Zdzienicka, et al. Deficiency in the repair of dna damage by homologous recombination and sensitivity to poly (adp-ribose) polymerase inhibition. *Cancer research*, 66(16):8109–8115, 2006.
- [149] Wojciech Niedzwiedz, Georgina Mosedale, Mark Johnson, Chong Yi Ong, Paul Pace, and Ketan J Patel. The fanconi anaemia gene fancc promotes homologous recombination and error-prone dna repair. *Molecular cell*, 15(4):607–620, 2004.
- [150] Bing Qian, Wenshu Leng, Zhengqing Yan, Jin Lu, Shiqing Chen, Huan Yi, and Zhi Jiang. Clinical benefit with parp inhibitor for pathogenic germline fancj-mutated relapsed epithelial ovarian cancer: a case report. *Frontiers in Oncology*, 12:778545, 2022.
- [151] Ke Cong, Nathan MacGilvary, Silviana Lee, Shannon G MacLeod, Jennifer Calvo, Min Peng, Arne Nedergaard Kousholt, Tovah A Day, and Sharon B Cantor. Fancj promotes parp1 activity during dna replication that is essential in brca1 deficient cells. *Nature Communications*, 15(1):2599, 2024.
- [152] Bert van de Kooij, Fenna J van der Wal, Magdalena B Rother, Wouter W Wiegant, Pau Creixell, Merula Stout, Brian A Joughin, Julia Vornberger, Matthias Altmeyer, Marcel ATM van Vugt, et al. The fanconi anemia core complex promotes ctip-dependent end resection to drive homologous recombination at dna double-strand breaks. *Nature Communications*, 15(1):7076, 2024.
- [153] Chantal Stoepker, Atiq Faramarz, Martin A Rooimans, Saskia E van Mil, Jesper A Balk, Eunike Velleuer, Najim Ameziane, Hein Te Riele, and Johan P de Winter. Dna helicases fancm and ddx11 are determinants of parp inhibitor sensitivity. *DNA repair*, 26:54–64, 2015.
- [154] Takuya Tsujino, Tomoaki Takai, Kunihiro Hinohara, Fu Gui, Takeshi Tsutsumi, Xiao Bai, Chenkui Miao, Chao Feng, Bin Gui, Zsolt Sztupinszki, et al. Crispr screens reveal genetic determinants of parp inhibitor sensitivity and

- resistance in prostate cancer. *Nature Communications*, 14(1):252, 2023.
- [155] Christopher J Lord, Sarah McDonald, Sally Swift, Nicholas C Turner, and Alan Ashworth. A high-throughput rna interference screen for dna repair determinants of parp inhibitor sensitivity. *DNA repair*, 7(12):2010–2019, 2008.
- [156] Pingping Fang, Cristabelle De Souza, Kay Minn, and Jeremy Chien. Genome-scale crispr knockout screen identifies tigar as a modifier of parp inhibitor sensitivity. *Communications biology*, 2(1):335, 2019.
- [157] Michal Zimmermann, Olga Murina, Martin AM Reijns, Angelo Agathangelou, Rachel Challis, Žygimantė Tarnauskaitė, Morwenna Muir, Adeline Fluteau, Michael Aregger, Andrea McEwan, et al. Crispr screens identify genomic ribonucleotides as a source of parp-trapping lesions. *Nature*, 559(7713):285–289, 2018.
- [158] Luke A Gilbert, Max A Horlbeck, Britt Adamson, Jacqueline E Villalta, Yuwen Chen, Evan H Whitehead, Carla Guimaraes, Barbara Panning, Hidde L Ploegh, Michael C Bassik, et al. Genome-scale crispr-mediated control of gene repression and activation. *Cell*, 159(3):647–661, 2014.
- [159] Shane Crotty and Matthew E Pipkin. In vivo rnai screens: concepts and applications. *Trends in immunology*, 36(5):315–322, 2015.
- [160] Stephanie E Mohr, Jennifer A Smith, Caroline E Shamu, Ralph A Neumüller, and Norbert Perrimon. Rnai screening comes of age: improved techniques and complementary approaches. *Nature reviews Molecular cell biology*, 15(9):591–600, 2014.
- [161] David W Morgens, Richard M Deans, Amy Li, and Michael C Bassik. Systematic comparison of crispr/cas9 and rnai screens for essential genes. *Nature biotechnology*, 34(6):634–636, 2016.
- [162] Christoph Bock, Paul Datlinger, Florence Chardon, Matthew A Coelho, Matthew B Dong, Keith A Lawson, Tian Lu, Laetitia Maroc, Thomas M Norman, Bicna Song, et al. High-content crispr screening. *Nature Reviews Methods Primers*, 2(1):1–23, 2022.
- [163] Yau-Tuen Chan, Yuanjun Lu, Junyu Wu, Cheng Zhang, Hor-Yue Tan, Zhaoxiang Bian, Ning Wang, and Yibin Feng. Crispr-cas9 library screening approach for anti-cancer drug discovery: overview and perspectives. *Theranostics*, 12(7):3329, 2022.
- [164] Yiyuan Niu, Catarina A Ferreira Azevedo, Xin Li, Elahe Kamali, Ole Haagen Nielsen, Claus Storgaard Sørensen, and Morten Frödin. Multiparametric and accurate functional analysis of genetic sequence variants using crispr-select. *Nature Genetics*, 54(12):1983–1993, 2022.
- [165] Yoshizumi Ishino, Mart Krupovic, and Patrick Forterre. History of crispr-cas from encounter with a mysterious repeated sequence to genome editing technology. *Journal of bacteriology*, 200(7):10–1128, 2018.
- [166] Irina Gostimskaya. Crispr–cas9: A history of its discovery and ethical considerations of its use in genome editing. *Biochemistry (Moscow)*, 87(8):777–788,

- 2022.
- [167] Martin Jinek, Krzysztof Chylinski, Ines Fonfara, Michael Hauer, Jennifer A Doudna, and Emmanuelle Charpentier. A programmable dual-rna-guided dna endonuclease in adaptive bacterial immunity. *science*, 337(6096):816–821, 2012.
  - [168] F Uddin, CM Rudin, and T Sen. Crispr gene therapy: applications, limitations, and implications for the future. *front oncol.* 2020; 10: 1387, 2020.
  - [169] Yue Yang, Jin Xu, Shuyu Ge, and Liqin Lai. Crispr/cas: advances, limitations, and applications for precision cancer research. *Frontiers in medicine*, 8:649896, 2021.
  - [170] Nader Alerasool, Dmitri Segal, Hunsang Lee, and Mikko Taipale. An efficient krab domain for crispr applications in human cells. *Nature methods*, 17(11):1093–1096, 2020.
  - [171] Martin Kampmann. Crispr and crispra screens in mammalian cells for precision biology and medicine. *ACS chemical biology*, 13(2):406–416, 2018.
  - [172] Lei S Qi, Matthew H Larson, Luke A Gilbert, Jennifer A Doudna, Jonathan S Weissman, Adam P Arkin, and Wendell A Lim. Repurposing crispr as an rna-guided platform for sequence-specific control of gene expression. *Cell*, 152(5):1173–1183, 2013.
  - [173] Andrea MP Romani. Cisplatin in cancer treatment. *Biochemical pharmacology*, 206:115323, 2022.
  - [174] Barnett Rosenberg, Loretta Van Camp, Eugene B Grimley, and Andrew J Thomson. The inhibition of growth or cell division in escherichia coli by different ionic species of platinum (iv) complexes. *Journal of Biological Chemistry*, 242(6):1347–1352, 1967.
  - [175] NCI/ National Cancer Institute. The "accidental" cure—platinum-based treatment for cancer: The discovery of cisplatin, 2014/ 2014.
  - [176] Andrea Brown, Sanjay Kumar, and Paul B Tchounwou. Cisplatin-based chemotherapy of human cancers. *Journal of cancer science & therapy*, 11(4), 2019.
  - [177] Paul B Tchounwou, Shaloam Dasari, Felicite K Noubissi, Paresh Ray, and Sanjay Kumar. Advances in our understanding of the molecular mechanisms of action of cisplatin in cancer therapy. *Journal of experimental pharmacology*, pages 303–328, 2021.
  - [178] Shaloam Dasari and Paul Bernard Tchounwou. Cisplatin in cancer therapy: molecular mechanisms of action. *European journal of pharmacology*, 740:364–378, 2014.
  - [179] Yang Hu, Bin Sun, Bin Zhao, Dan Mei, Qing Gu, and Zhuang Tian. Cisplatin-induced cardiotoxicity with midrange ejection fraction: A case report and review of the literature. *Medicine*, 97(52):e13807, 2018.
  - [180] MK Kuhlmann, G Burkhardt, and H Köhler. Insights into potential cellular mechanisms of cisplatin nephrotoxicity and their clinical application.

- Nephrology, dialysis, transplantation: Official publication of the European dialysis and transplant association-european renal association*, 12(12):2478–2480, 1997.
- [181] Michael Jefford, Michael Michael, Mark A Rosenthal, Ian D Davis, Michael Green, Bev McClure, Jennifer Smith, Brigid Waite, and John Zalcborg. A novel combination of cisplatin, irinotecan, and capecitabine in patients with advanced cancer. *Investigational new drugs*, 22:185–192, 2004.
  - [182] Zufan Zazuli, Renate Kos, Joris D Veltman, Wilma Uytterlinde, Cristina Longo, Paul Baas, Rosalinde Masereeuw, Susanne JH Vijverberg, and Anke-Hilse Maitland-van der Zee. Comparison of myelotoxicity and nephrotoxicity between daily low-dose cisplatin with concurrent radiation and cyclic high-dose cisplatin in non-small cell lung cancer patients. *Frontiers in Pharmacology*, 11:975, 2020.
  - [183] Jonathan Bramson and Lawrence C Panasci. Effect of ercc-1 overexpression on sensitivity of chinese hamster ovary cells to dna damaging agents. *Cancer research*, 53(14):3237–3240, 1993.
  - [184] Vasiliy Koshkin, Mariana Bleker De Oliveira, Chun Peng, Laurie E Ailles, Geoffrey Liu, Allan Covens, and Sergey N Krylov. Multi-drug-resistance efflux in cisplatin-naive and cisplatin-exposed a2780 ovarian cancer cells responds differently to cell culture dimensionality. *Molecular and Clinical Oncology*, 15(2):1–8, 2021.
  - [185] Ding-Wu Shen, Lynn M Pouliot, Matthew D Hall, and Michael M Gottesman. Cisplatin resistance: a cellular self-defense mechanism resulting from multiple epigenetic and genetic changes. *Pharmacological reviews*, 64(3):706–721, 2012.
  - [186] Jaber Zafari, Nima Rastegar-Pouyani, Fatemeh Javani Jouni, Nabaa Najjar, Seyedeh Zohreh Azarshin, Emad Jafarzadeh, Parviz Abdolmaleki, and Farshad Hoseini Shirazi. Static magnetic field reduces cisplatin resistance via increasing apoptosis pathways and genotoxicity in cancer cell lines. *Scientific Reports*, 14(1):5792, 2024.
  - [187] V Heinemann, H Wilke, H-G Mergenthaler, M Clemens, H König, HJ Illiger, M Arning, A Schalhorn, K Possinger, and U Fink. Gemcitabine and cisplatin in the treatment of advanced or metastatic pancreatic cancer. *Annals of Oncology*, 11(11):1399–1403, 2000.
  - [188] JA Wils, T Kok, DJ Th Wagener, J Selleslags, N Duez, Gastrointestinal GI Tract Group of the European, and Organization for Research. Activity of cisplatin in adenocarcinoma of the pancreas. *European Journal of Cancer*, 29(2):203–204, 1993.
  - [189] Guoqing Ouyang, Zhipeng Liu, Shengfu Huang, Qianglong Li, Li Xiong, Xiongying Miao, and Yu Wen. Gemcitabine plus cisplatin versus gemcitabine alone in the treatment of pancreatic cancer: a meta-analysis. *World journal of surgical oncology*, 14:1–9, 2016.

- [190] FDA/ Food and Drug Administration. The "accidental" cure—platinum-based treatment for cancer: The discovery of cisplatin, 2020/ 2020.
- [191] Halley B Rycenga and David T Long. The evolving role of dna inter-strand crosslinks in chemotherapy. *Current opinion in pharmacology*, 41:20–26, 2018.
- [192] David Lopez-Martinez, Chih-Chao Liang, and Martin A Cohn. Cellular response to dna interstrand crosslinks: the fanconi anemia pathway. *Cellular and molecular life sciences*, 73:3097–3114, 2016.
- [193] Amy J Warren, Alexander E Maccubbin, and Joshua W Hamilton. Detection of mitomycin c-dna adducts in vivo by 32p-postlabeling: time course for formation and removal of adducts and biochemical modulation. *Cancer research*, 58(3):453–461, 1998.
- [194] Phillip D Bass, Daniel A Gubler, Ted C Judd, and Robert M Williams. Mitomycinoid alkaloids: mechanism of action, biosynthesis, total syntheses, and synthetic approaches. *Chemical reviews*, 113(8):6816–6863, 2013.
- [195] David Norman, David Live, Mallika Sastry, Roselyn Lipman, Brian E Hingerty, Maria Tomasz, Suse Broyde, and Dinshaw J Patel. Nmr and computational characterization of mitomycin cross-linked to adjacent deoxyguanosines in the minor groove of the d (tacgta). cntdot. d (tacgta) duplex. *Biochemistry*, 29(11):2861–2875, 1990.
- [196] Stacia M Rink, Roselyn Lipman, Stephen C Alley, Paul B Hopkins, and Maria Tomasz. Bending of dna by the mitomycin c-induced, gpg intrastrand cross-link. *Chemical research in toxicology*, 9(2):382–389, 1996.
- [197] Wilfried Budach, F Paulsen, S Welz, J Classen, H Scheithauer, P Marini, C Belka, and M Bamberg. Mitomycin c in combination with radiotherapy as a potent inhibitor of tumour cell repopulation in a human squamous cell carcinoma. *British journal of cancer*, 86(3):470–476, 2002.
- [198] Gehan Botrus, Denise Roe, Gayle S Jameson, Pedro Luiz Serrano Uson Junior, Ronald Lee Korn, Lana Caldwell, Taylor Bargenquast, Max Miller, and Erkut Hasan Borazanci. Mitomycin c in homologous recombination deficient metastatic pancreatic cancer after disease progression on platinum-based chemotherapy and olaparib. *Biomedicines*, 10(11):2705, 2022.
- [199] Liguoxie, Lifangyu Cheng, and Yunlin Wei. Mitomycin c enhanced the antitumor efficacy of rocaglamide in colorectal cancer. *Pathology-Research and Practice*, 243:154350, 2023.
- [200] A Volpe, M Racioppi, D D'Agostino, E Cappa, A Filianoti, and PF Bassi. Mitomycin c for the treatment of bladder cancer. *Minerva urologica e nefrologica= The Italian journal of urology and nephrology*, 62(2):133–144, 2010.
- [201] NCI/ National Cancer Institute. Mitomycin, 2011/ 2023.
- [202] Gemma Molyneux, Frances M Gibson, Edward C Gordon-Smith, Andrew M Pilling, Kai Chiu Liu, Sian Rizzo, Susan Sulsh, and John A Turton. The haemotoxicity of mitomycin in a repeat dose study in the female cd-1 mouse. *International journal of experimental pathology*, 86(6):415–430, 2005.

- [203] Suk Jun Lee, Youngbae Jeon, Hae Won Lee, Jeonghyun Kang, Seung Hyuk Baik, and Eun Jung Park. Impact of mitomycin-c-induced neutropenia after hyperthermic intraperitoneal chemotherapy with cytoreductive surgery in colorectal cancer patients with peritoneal carcinomatosis. *Annals of Surgical Oncology*, pages 1–10, 2022.
- [204] Scott H Okuno and Stephen Frytak. Mitomycin lung toxicity: Acute and chronic phases. *American journal of clinical oncology*, 20(3):282–284, 1997.
- [205] Bing H Xu, Vicram Gupta, and Shivendra V Singh. Mitomycin c sensitivity in human bladder cancer cells: possible role of glutathione and glutathione transferase in resistance. *Archives of biochemistry and biophysics*, 308(1):164–170, 1994.
- [206] Jingyu Zhao, Yixin Zhang, Wenbo Li, Mengmeng Yao, Chuqi Liu, Zihan Zhang, Caiqin Wang, Xiaomei Wang, and Kai Meng. Research progress of the fanconi anemia pathway and premature ovarian insufficiency. *Biology of Reproduction*, 109(5):570–585, 2023.
- [207] Anne M van Harten, Ronak Shah, D Vicky de Boer, Marijke Buijze, Maaïke Kreft, Ji-Ying Song, Lisa M Zürcher, Heinz Jacobs, and Ruud H Brakenhoff. Gemcitabine as chemotherapy of head and neck cancer in fanconi anemia patients. *Oncogenesis*, 13(1):26, 2024.
- [208] Chenhui Ma and Evren Gurkan-Cavusoglu. A comprehensive review of computational cell cycle models in guiding cancer treatment strategies. *NPJ Systems Biology and Applications*, 10(1):71, 2024.
- [209] Anna Palovcak, Fenghua Yuan, Ramiro Verdun, Liang Luo, and Yanbin Zhang. Fanconi anemia associated protein 20 (faap20) plays an essential role in homology-directed repair of dna double-strand breaks. *Communications Biology*, 6(1):873, 2023.
- [210] Ryan L Setten, John J Rossi, and Si-ping Han. The current state and future directions of rnai-based therapeutics. *Nature reviews Drug discovery*, 18(6):421–446, 2019.
- [211] Tianxiang Li, Yanyan Yang, Hongzhao Qi, Weigang Cui, Lin Zhang, Xiuxiu Fu, Xiangqin He, Meixin Liu, Pei-feng Li, and Tao Yu. Crispr/cas9 therapeutics: progress and prospects. *Signal Transduction and Targeted Therapy*, 8(1):36, 2023.
- [212] Arafat Siddiqui, Manuela Tumiati, Alia Joko, Jouko Sandholm, Pia Roering, Sofia Aakko, Reetta Vainionpää, Katja Kaipio, Kaisa Huhtinen, Liisa Kauppi, et al. Targeting dna homologous repair proficiency with concomitant topoisomerase ii and c-abl inhibition. *Frontiers in oncology*, 11:733700, 2021.
- [213] Kung-Wen Lu, Mei-Due Yang, Shu-Fen Peng, Jaw-Chyun Chen, Po-Yuan Chen, Hung-Yi Chen, Tai-Jung Lu, Fu-Shin Chueh, Jin-Cherng Lien, Kuang-Chi Lai, et al. Maslinic acid induces dna damage and impairs dna repair in human cervical cancer hela cells. *Anticancer Research*, 40(12):6869–6877,

- 2020.
- [214] Jude B Khatib, Ashna Dhoonmoon, George-Lucian Moldovan, and Claudia M Nicolae. Parp10 promotes the repair of nascent strand dna gaps through rad18 mediated translesion synthesis. *Nature communications*, 15(1):6197, 2024.
- [215] Yasuyoshi Oka, Yuka Nakazawa, Mayuko Shimada, and Tomoo Ogi. Endogenous aldehyde-induced dna–protein crosslinks are resolved by transcription-coupled repair. *Nature Cell Biology*, pages 1–13, 2024.
- [216] Daniel Gómez-Cabello, George Pappas, Diana Aguilar-Morante, Christoffel Dinant, and Jiri Bartek. Ctip-dependent nascent rna expression flanking dna breaks guides the choice of dna repair pathway. *Nature Communications*, 13(1):5303, 2022.
- [217] Anne Olazabal-Herrero, Boxue He, Youngho Kwon, Abhishek K Gupta, Arijit Dutta, Yuxin Huang, Prajwal Boddu, Zhuobin Liang, Fengshan Liang, Yaqun Teng, et al. The fanci/fancd2 complex links dna damage response to r-loop regulation through srsf1-mediated mrna export. *Cell reports*, 43(1), 2024.
- [218] Hui Xing and Ling-hua Meng. Crispr-cas9: a powerful tool towards precision medicine in cancer treatment. *Acta Pharmacologica Sinica*, 41(5):583–587, 2020.
- [219] Lukas Villiger, Julia Joung, Luke Koblan, Jonathan Weissman, Omar O Abudayyeh, and Jonathan S Gootenberg. Crispr technologies for genome, epigenome and transcriptome editing. *Nature Reviews Molecular Cell Biology*, pages 1–24, 2024.
- [220] V Edwin Hillary and S Antony Ceasar. A review on the mechanism and applications of crispr/cas9/cas12/cas13/cas14 proteins utilized for genome engineering. *Molecular Biotechnology*, 65(3):311–325, 2023.
- [221] Diana Raquel Rodríguez-Rodríguez, Ramiro Ramirez-Solis, Mario Alberto Garza-Elizondo, Maria de Lourdes Garza-Rodriguez, and Hugo Alberto Barrera-Saldana. Genome editing: A perspective on the application of crispr/cas9 to study human diseases. *International journal of molecular medicine*, 43(4):1559–1574, 2019.
- [222] David Fox, Zhijiang Yan, Chen Ling, Ye Zhao, Duck-Yeon Lee, Tatsuo Fukagawa, Wei Yang, and Weidong Wang. The histone-fold complex mhf is remodeled by fancm to recognize branched dna and protect genome stability. *Cell research*, 24(5):560–575, 2014.
- [223] Valentina Gandin, James D Hoeschele, and Nicola Margiotta. Special issue “cisplatin in cancer therapy: Molecular mechanisms of action 3.0”, 2023.
- [224] Askar Yimit, Ogun Adebali, Aziz Sancar, and Yuchao Jiang. Differential damage and repair of dna-adducts induced by anti-cancer drug cisplatin across mouse organs. *Nature communications*, 10(1):309, 2019.
- [225] Zeyuan Liu, Huadong Jiang, Sze Yuen Lee, Nannan Kong, and Ying Wai Chan. Fancm promotes parp inhibitor resistance by minimizing ssdna gap

- formation and counteracting resection inhibition. *Cell Reports*, 43(7), 2024.
- [226] LJ Mah, A El-Osta, and TC Karagiannis.  $\gamma$ h2ax: a sensitive molecular marker of dna damage and repair. *Leukemia*, 24(4):679–686, 2010.
- [227] Timothy J Brown and Kim A Reiss. Parp inhibitors in pancreatic cancer. *The Cancer Journal*, 27(6):465–475, 2021.
- [228] Hong Zhao, Yafei Zhuang, Ruibin Li, Yinyin Liu, Zijie Mei, Zhongshi He, Fuxiang Zhou, and Yunfeng Zhou. Effects of different doses of x-ray irradiation on cell apoptosis, cell cycle, dna damage repair and glycolysis in hela cells. *Oncology letters*, 17(1):42–54, 2019.
- [229] JL Roti Roti and WD Wright. Visualization of dna loops in nucleoids from hela cells: assays for dna damage and repair. *Cytometry: The Journal of the International Society for Analytical Cytology*, 8(5):461–467, 1987.
- [230] Zhaohui Xue, Zhiwei Liu, Moucheng Wu, Shiwen Zhuang, and Wancong Yu. Effect of rapeseed peptide on dna damage and apoptosis in hela cells. *Experimental and Toxicologic Pathology*, 62(5):519–523, 2010.
- [231] Max A Horlbeck, Luke A Gilbert, Jacqueline E Villalta, Britt Adamson, Ryan A Pak, Yuwen Chen, Alexander P Fields, Chong Yon Park, Jacob E Corn, Martin Kampmann, et al. Compact and highly active next-generation libraries for crispr-mediated gene repression and activation. *elife*, 5:e19760, 2016.
- [232] Guotai Xu, J Ross Chapman, Inger Brandsma, Jingsong Yuan, Martin Mistrik, Peter Bouwman, Jirina Bartkova, Ewa Gogola, Daniël Warmerdam, Marco Barazas, et al. Rev7 counteracts dna double-strand break resection and affects parp inhibition. *Nature*, 521(7553):541–544, 2015.
- [233] David C Wilkes, Verena Sailer, Hui Xue, Hongwei Cheng, Colin C Collins, Martin Gleave, Yuzhuo Wang, Francesca Demichelis, Himisha Beltran, Mark A Rubin, et al. A germline fanca alteration that is associated with increased sensitivity to dna damaging agents. *Molecular Case Studies*, 3(5):a001487, 2017.
- [234] Brian W Freie, Samantha LM Ciccone, Xiaxin Li, P Artur Plett, Christie M Orschell, Edward F Srouf, Helmut Hanenberg, Detlev Schindler, Suk-Hee Lee, and D Wade Clapp. A role for the fanconi anemia c protein in maintaining the dna damage-induced g2 checkpoint. *Journal of Biological Chemistry*, 279(49):50986–50993, 2004.
- [235] Yu-Zhou Huang, Ming-Yi Sang, Pei-Wen Xi, Ruo-Xi Xu, Meng-Yuan Cai, Zi-Wen Wang, Jian-Yi Zhao, Yi-Han Li, Ji-Fu Wei, and Qiang Ding. Fanci inhibition induces parp1 redistribution to enhance the efficacy of parp inhibitors in breast cancer. *Cancer Research*, 84(20):3447–3463, 2024.
- [236] Laura Kruper, Kevin McDonnell, Joseph Bonner, Kevin K Tsang, Veronica Jones, Joanne Mortimer, Sidney S Lindsey, Ilana Solomon, Heather Hampel, Wai Park, et al. Abstract pd14-03: Pd14-03 reappraising the fanconi anemia dna repair pathway in breast cancer risk and precision intervention: Insights

- and opportunities from the city of hope inspire study. *Cancer Research*, 83(5-Supplement):PD14–03, 2023.
- [237] Haiwei Mou, Jordan L Smith, Lingtao Peng, Hao Yin, Jill Moore, Xiao-Ou Zhang, Chun-Qing Song, Ankur Sheel, Qiongqiong Wu, Deniz M Ozata, et al. Crispr/cas9-mediated genome editing induces exon skipping by alternative splicing or exon deletion. *Genome biology*, 18:1–8, 2017.
- [238] Jakub Liu, Magdalena Mroczek, Anna Mach, Maria Stepień, Angelika Apłás, Bartosz Pronobis-Szczylik, Szymon Bukowski, Magda Mielczarek, Ewelina Gajewska, Piotr Topolski, et al. Genetics, genomics and emerging molecular therapies of pancreatic cancer. *Cancers*, 15(3):779, 2023.
- [239] Elizabeth D Thompson, Nicholas J Roberts, Laura D Wood, James R Eshleman, Michael G Goggins, Scott E Kern, Alison P Klein, and Ralph H Hruban. The genetics of ductal adenocarcinoma of the pancreas in the year 2020: dramatic progress, but far to go. *Modern Pathology*, 33(12):2544–2563, 2020.

# Acknowledgements

Sono tante le persone che vorrei ringraziare per diversi motivi.

Voglio ringraziare il mio supervisor, il prof. Andrea Cavalli, per aver avuto fiducia in me in questi anni, supportando un progetto ed un'idea che spero abbia avuto i risvolti attesi. Lo ringrazio anche per l'opportunità di lavorare in un ottimo centro di ricerca dove ho imparato molto.

Ringrazio la mia co-supervisor, la Prof.ssa Fulvia Farabegoli. Una scienziata incredibile, una persona onesta, sincera e buona. Con lei abbiamo navigato insieme in questo mondo di pazzi che è quello della ricerca, e insieme siamo arrivate alla fine di questo percorso. Infiniti sono stati i nostri primi incontri e a seguire le chiamate date dalla distanza Bologna-Milano. In tutto questo tempo ed in tutti i modi possibili, Fulvia è sempre stata una guida e un'ancora fondamentale. Senza di lei, la sua gentilezza e la sua infinita pazienza, non avrei saputo come affrontare molti ostacoli. A lei, va quindi un ringraziamento particolare. Ti porterò sempre nel mio cuore.

Ringrazio anche le persone che, lavorando in amministrazione, mi hanno seguita in questi anni. Lavorare anche con loro è stato piacevole, in particolare con la grande Iota, Cristina Masetti, Alessandra Bisi, Angela Tomasini ed Enrica Vaccarezza.

Il mio dottorato si è svolto per la maggior parte nella sede IIT di Milano (CGS@SEMM). Qui, sono stata ospitata dal laboratorio di Francesco Nicassio che ringrazio per avermi dato l'opportunità di lavorare in centro di ricerca avanzato. Del suo laboratorio, ringrazio anche Matteo, Chiara, Sara e Alessandro. Ringrazio in particolar modo Virginia per avermi guidata nei primi mesi e avermi insegnato molte tecniche, insieme anche a Bianca e Carmela. Ringrazio anche Maria per i momenti di leggerezza che ogni tanto ci concedevamo in lab.

A Milano, ho avuto la possibilità di conoscere validi/e scienziati/e, ed amici indimenticabili. Il mio bro, Francesco detto Fra, compaesano per 2 mesi ma amico da anni. Avrò sempre nel cuore i nostri caffè per inaugurare l'inizio della giornata

(con annesse storie da 1h) o per rimediare ad un mal di testa durante la giornata. Ricorderò anche con molto affetto gli ultimi mesi del dottorato, dove da buona compagna di banco rendevo “imprevedibili” le tue giornate.

Lucy e Gio, pazze come il pollo di Moana. La nostra giornata tipo iniziava con domande scientifiche a Lucy che si accollava tutti i miei dubbi sugli esperimenti. A seguire, dei discorsi prolissi che con la scienza c’entravano ben poco. A voi ringrazio per essere delle amiche spontanee e sincere e per avermi regalato delle giornate che hanno reso questo dottorato più leggero e felice.

Simone e Mattia, menti eccezionali e persone gentili protagoniste di tanti bei momenti passati insieme. Ringrazio ovviamente anche Paola e Valeria per aver condiviso le gioie (e sofferenze) legate al mondo della ricerca. Ringrazio anche Ari e Sara per i nostri appuntamenti nei corridoi IIT per dare soluzione a vari dubbi e scoprire le nuove collocazioni dei reagenti.

Ringrazio infine Diego, Giuseppe, Martina, Raffaele e Marianna per aver condiviso con me il nascondiglio dei cioccolatini da aprire nei momenti di maggior necessità.

Nei 7 mesi trascorsi all’estero, sono stata ospitata dal prof. Claus Storgaard Sorensen che ringrazio per avermi concesso la possibilità di imparare tecniche avanzate in un laboratorio colmo di scienziati incredibili.

Tra questi ringrazio Thorkell che mi ha seguita soprattutto nei primi mesi e a cui mi vanto aver fatto lo scherzo più geniale della storia degli scherzi. Simon, per le miliardi di domande a cui ha risposto e per aver sempre creato e mantenuto un ambiente di lavoro leggero e divertente insieme a Jan. Le nostre battaglie con le pistole ad acqua durante il Summer Party saranno ricordate dalle generazioni future. Ringrazio anche Jay per la gentilezza mostrata durante quei mesi. Enrique, miglior lab manager di sempre, voglio ringraziarlo per avermi dato un amico e un confidente che terrò sempre nel mio cuore. Ringrazio anche Zijiun, Miao, Pei, Diya, Filippo e Judith per esserci sempre stati e per tutte le mangiate interculturali fatte insieme. In definitiva, ringrazio un lab di scappati di casa con tanta voglia di mangiare e scherzare tra un esperimento e l’altro.

Ringrazio anche una stimata collega e sincera amica: Lalla. A te ringrazio per esserci stata sin dal primo giorno in cui ho varcato le soglie di San Donato 15. Dai primi mesi di confronto in lab, a tutti gli altri anni con le nostre interminabili chiacchiate tre Bologna e Milano. Grazie per la tua capacità di comprendere e supportare, e per la tua naturale gentilezza che mi ha sostenuta per tutto questo tempo. Non vedo l’ora di raccontarci nuove avventure in una delle nostre chiamate.

Un’altra persona che porto nel cuore è la mia Mary. Come trovare le parole

giuste per ringraziare un'amica con cui hai praticamente condiviso tutto? Non è mai importata la distanza, quasi ogni giorno tra i messaggi in arrivo c'erano e ci sono sempre i tuoi vocali con risposte, commenti e consigli per tutte le vicende che mi sono successe in tutti questi anni. Con ferocia ho ascoltato le tue attesissime parole perché ho sempre saputo e so che, con estrema cura, mi faranno andare sempre avanti, più consapevole, più felice e più grata per averti accanto. Sempre con ferocia, abbiamo divorato tonnellate di sushi in giornate che custodisco con gelosia. Ti voglio un bene dell'anima. Ci vediamo per il prossimo sushi.

La strada verso il dottorato è iniziata a Torino. Qui ho sempre avuto il supporto delle mie amiche storiche, Renata (Pif), Roberta (Nana) e Simona. Non esagero se dico che ci conosciamo da una vita. Aver condiviso con voi questi anni è stato importante e mi ha fatto ancora di più apprezzare il valore dell'amicizia vissuta a distanza. Con voi spero di condividere tutti gli altri passi che farò dopo questo (sudato) traguardo.

Sempre a Torino, ho conosciuto degli amici preziosi, protagonisti di tante serate al Derkeller, giochi di società e scampagnate. Ringrazio Chiara per avermi fatto capire che esistono persone più freddolose di me che necessitano di 3 giubotti e 4 maglioni in una giornata con 15°C. Oltre per questo, anche per le interminabili chiacchiere che sono sempre stato momento di conforto, crescita e gioia. Ringrazio anche Carletto, Mili detto Emilio e Matteo. Grazie per avermi regalato tanti momenti di spensieratezza e degli amici strambi quasi quanto me.

Siamo quasi alla fine, resistete ancora un po'.

Voglio ringraziare la mia nuova famiglia seguendo l'ordine dettato dalla regola dei  $\frac{3}{4}$ , dove il primo dittongo segue alla terza sillaba in ordine crescente. Ringrazio quindi Deborah, Yvonne, Marcolino, Christian e Matteo per aver condiviso con me tutti questi anni (1 per Christian) e che mi hanno sempre supportata durante il dottorato e non solo. Ringrazio anche Dino e Laura che con pazienza hanno ascoltato i racconti di questo mondo strano, dandomi conforto e sostegno.

Ringrazio anche i 3 pazzi della famiglia, Fabio, Mauro e Mattia. Mi avete regalato momenti di gioia puri, divertimento e a volte anche riflessione. Da veneti puri, mi avete anche insegnato la nobile arte del bere lo Spritz alle 10 del mattino e, tra un non complimento e un paragone ad un animale di qualche tipo (e.g. scimmietta), mi avete sempre fatta sentire bene. Un toccasana per staccare la presa dagli esperimenti e ricordare l'importanza di ritagliarsi del tempo per assaporare questi momenti semplici. Siete preziosi e vi voglio tanto bene.

Infine ringrazio la mia famiglia, a partire da mio fratello Andrea, per i momenti

di leggerezza passati insieme durante questi anni. Ai miei genitori, il mio faro e la mia forza. Mi avete sempre sostenuta durante questi anni, nonostante i continui ostacoli affrontati. Capire e supportare delle scelte non è semplice, soprattutto quando queste richiedono tanti sacrifici, a volte troppi. Vi ringrazio per la luce che mi avete dato ogni giorno e per aver reso questo traguardo speciale. Spero un giorno di poter raggiungere quello che cerco e finalmente di rendervi orgogliosi, come io lo sono di voi.

Per concludere, ringrazio Luca, partner e compagno di tutte le avventure che la vita ci ha proposto. Una di queste, essere una coppia dove entrambi fanno un dottorato, quasi come una sfida a chi accumula più stress (di cui ancora dobbiamo decretare il vincitore). Grazie per esserci sempre, per avermi aiutata ad affrontare a testa alta questo percorso e ascoltata tutti i giorni. Grazie anche per tutti i momenti di serenità, felicità e tranquillità che ci hai dato, creando un posto sicuro dove rifugiarsi da questo mondo un po' matto. Anche a te dedico questo traguardo, con la speranza che possa contribuire a costruirci un futuro roseo insieme. Direi che ce lo meritiamo, eh che cavolo. In attesa del prossimo passo, sorrido e respiro la fortuna di averti accanto.